Nitrous Oxide Emissions from Wastewater Treatment and Process Parameters Affecting Emissions

Shannon K. Cavanaugh

A thesis
submitted in partial fulfillment of the
requirements for the degree of

Master of Science

University of Washington
2021

Committee:
Mari-Karoliina H. Winkler, Chair
Rebecca B. Neumann

Program Authorized to Offer Degree:
Civil and Environmental Engineering

University of Washington

Abstract

Nitrous Oxide Emissions from Wastewater Treatment Processes and

Process Parameters Affecting Emissions

Shannon K. Cavanaugh

Chair of the Supervisory Committee:

Professor Mari-Karoliina H. Winkler

Department of Civil and Environmental Engineering

Most wastewater treatment plants in the United States must be upgraded to reduce nutrient discharges. These improvements are needed to meet upcoming permit requirements and to prevent negative environmental impacts like eutrophication of receiving water bodies. However, one of the potential side-effects of increased nitrogen removal in wastewater treatment processes is increased nitrous oxide (N_2O) emissions from biological nitrification and denitrification. N_2O is a greenhouse gas (GHG) approximately 300 times stronger than an equivalent amount of CO_2; thus, it is imperative to (1) establish comprehensive methodologies to accurately quantify N_2O emissions from full-scale treatment processes and (2) understand the relevant process parameters and microbiology involved in emissions from wastewater treatment. This serves to ultimately

minimize emissions (and therefore the carbon footprint) of wastewater treatment plants (WWTPs).

To address this, emissions from two wastewater treatment processes were quantified, and relevant process parameters and microbial emission pathways were investigated. While the two treatment systems differ in terms of scale and processes utilized, both are innovative wastewater treatment technologies designed for efficient use of space and nutrient removal.

(1) At Brightwater Treatment Plant (Woodinville, WA), aqueous and gaseous N_2O monitoring techniques were employed at a full-scale membrane bioreactor (MBR) for 5.5 months. To the knowledge of the investigators, this campaign was the most comprehensive study of a fully covered MBR to date. Emission estimates from both aqueous and gaseous analyzers were compared to determine their reliability, and the average emission factor (using data from both analyzers) was 0.58% of plant influent total Kjeldahl nitrogen (TKN) emitted as N_2O-N. Emissions were positively correlated with influent pH, nitrification efficiency, and aeration basin/effluent NH_4^+ and NO_3^-. They correlated negatively with primary effluent COD:N ratio and effluent pH, signifying that nitrification was likely the dominant N_2O-production pathway.

(2) A laboratory-scale, aerobic granular sludge (AGS) sequencing batch reactor (SBR) was operated for 11 months to measure N_2O emissions with full phosphate removal and simultaneous nitrification-denitrification (SND). The reactor was operated at varying dissolved oxygen (DO) concentrations and with nitrite (NO_2^-) spikes to investigate the impact of these process parameters on emissions. Increased DO and NO_2^- concentrations were associated with increased emissions. N_2O was minimized at

a dissolved oxygen concentration of 1 mg O_2 L^{-1}, with an emission factor of 0.18% of oxidized NH_3-N emitted as N_2O-N. This emission factor is lower than many previously reported factors from AGS reactors. Molecular analyses revealed a population of microbes capable of shortcut nitrogen removal, which is advantageous for wastewater treatment because of decreased oxygen and carbon requirements.

TABLE OF CONTENTS

LIST OF FIGURES

LIST OF TABLES

ACKNOWLEDGEMENTS

I am profoundly grateful to those who have supported me during my time at UW. I would like to thank my advisor, Professor Mari Winkler, for her guidance, support, and encouragement throughout my Master's studies. Her inspiring leadership and determination consistently pushed me to be my best and I am proud of the researcher I have become with her mentorship. I would also like to extend gratitude to my committee member Professor Rebecca Neumann.

This research was funded by the King County Wastewater Treatment Division Graduate Student Research Fellowship, and I am extremely grateful for the opportunity to perform this work and for the support of my graduate education. I received invaluable mentorship and insight from the WTD Tech Assessment team: Bob Bucher, Pardi Sukapanpotharam, and Eron Jacobson. I would especially like to thank Eron for all of his guidance and collaboration on the Brightwater project. I extend my gratitude to King County staff who supported our work at Brightwater and provided data that was essential to the project.

I would like to thank all members of the Stahl/Winkler lab for their insights, expertise, and friendship over the past two years. I am especially grateful to Bao Nguyen Quoc for his integral role in the lab reactor project. Much of my research would not have been possible without his support, and I was very lucky to have his advice every step of the way.

Thank you to my family and friends who have supported me through it all, especially my parents Matt Cavanaugh and Annie Kusaka who inspire me every day.

Finally, I would like to acknowledge that this research was performed on Coast Salish land, which touches shared waters of all tribes and bands within the Duwamish, Puyallup, Suquamish, Tulalip, and Muckleshoot nations, whose people have been the stewards of these waters since time immemorial.

Chapter 1. INTRODUCTION

Nitrous oxide (N_2O) is a potent greenhouse gas with a Global Warming Potential 298 times greater than an equivalent amount of carbon dioxide (CO_2) over a 100 year horizon[1]. Although net global CO_2 and methane (CH_4) emissions are much greater than N_2O emissions, the substantial warming potential of N_2O makes it a significant greenhouse gas that must be closely monitored and regulated in order to comprehensively address climate change[2]. When reported as CO_2 equivalents, with CH_4 and N_2O equal to 84 and 298 CO_2 equivalents each, global GHG emissions are 76% CO_2, 16% CH_4 and 6% N_2O[3]. N_2O is naturally emitted in various chemical and biological processes to the atmosphere, soil, and oceans. However, post-industrialization, anthropogenic emissions of these gases have led to an imbalanced nitrogen cycle with significant environmental and public health effects. Anthropogenic N_2O emissions now account for approximately 40% of total emissions, primarily from fertilizing agricultural soils, operating cattle feedlots, wastewater treatment, burning fossil fuels, and industrial processes like producing nitric acid[1]. In the US, about 74% of N_2O emissions are attributed to agricultural soil management, and 1.9% are attributed to wastewater treatment and composting combined. However, literature reveals that emissions from different wastewater treatment plants (WWTPs) are highly variable, with the IPCC's reported emission factors for centralized, aerobic treatment plants ranging from 0.016% to 4.5% of influent total nitrogen emitted as N_2O-N[4]. This wide range indicates uncertainty about the contribution of WWTPs to total N_2O emissions, especially as nitrogen removal processes become more widespread. Wastewater treatment systems are one of the few nitrogen cycling systems that are inherently engineered, meaning that they are a source of emissions that can be more readily controlled than other sources.

The greenhouse gases CO_2, CH_4, and N_2O are emitted during wastewater treatment processes, contributing to the carbon footprint of a treatment plant. CO_2 emissions are estimated based on the electricity demand of a plant, since direct emissions from treatment of organic matter are considered "short cycle CO_2" which are not considered in GHG emission estimates. N_2O and CH_4 are the main contributors to greenhouse gas emissions from wastewater treatment systems, with emissions of approximately 5 and 14 million metric tons of CO_2 equivalents per year in the US respectively[5]. However, a significant amount of CH_4 is emitted in the sewer system prior to treatment and in sludge handling. There is ongoing research attempting to minimize these emissions, but when focusing on processes that can be controlled within the wastewater treatment plant itself, minimizing N_2O emissions has the potential to significantly reduce the carbon footprint of wastewater treatment. There is therefore a pressing need to control emissions in this field, and this will be aided by better comprehension about how treatment process parameters affect emissions and which microbial processes are most relevant in wastewater systems. Researching these processes may also provide insight about N_2O emissions in other systems like agricultural or industrial processes.

In conventional biological nitrogen removal in wastewater treatment, nitrification ($NH_4^+ \rightarrow NO_3^-$) is followed by denitrification ($NO_3^- \rightarrow N_2$). The produced N_2 minimizes the fixed N in discharge waters and subsequent eutrophication that can be triggered by nitrate fluxes. If a plant is required to remove nitrogen, a conventional process involves sequentially alternating between oxic and anoxic conditions, or creating separate zones for nitrification and denitrification, respectively. In alternative approaches, high rates of simultaneous nitrification and denitrification are possible in biofilm-like systems such as granular sludge. In these systems, nitrification occurs at the liquid/biomass interface and denitrification occurs in subsurface areas[6]. Proper operation

of these systems is vital to ensure adequate removal efficiencies, with key design parameters including influent carbon, nitrogen, and phosphorus ratios, the chemical oxygen demand to nitrogen ratio (COD:N), and control of the dissolved oxygen concentration (DO)[6]. While nitrogen removal systems are well established, there are few guidelines on how to minimize their GHG emissions. Research suggests that reactor configuration and certain operational parameters affect the N_2O emissions from wastewater treatment processes, however there is not yet a consensus about how to operate reactors to minimize emissions. Kampschreur et al. (2009) reviewed N_2O emission values from both lab-scale and full-scale wastewater reactors and found that there is significant variation in emission values from different processes. The majority of treatment processes reviewed were activated sludge processes, with elevated N_2O emissions generally associated with lower DO concentrations, higher nitrite concentrations, decreased COD:N ratio during denitrification, rapidly changing process conditions (shocks to the system), and consumption of internal storage compounds like polyhydroxyalcanoates (PHB) that are used as electron donor for denitrification by GAO and PAO. Additional factors that may indirectly influence N_2O emissions include short solids retention time (SRT), toxic compounds like sulfide, low temperature, high salinity, and increased ammonium concentrations[7].

The quantification of emissions from full-scale treatment plants is difficult and varies greatly among varying treatment processes, and the major contributors to emissions at full-scale are not well understood. In contrast with lab-scale reactors, it is much more difficult to accurately quantify GHG emissions from full-scale processes because emission fluxes vary between different locations in a plant, the majority of plants are open to the atmosphere (making gaseous mass balances complicated), and there are more uncertain variables like process upsets and significant diurnal variations that may trigger emissions. In a review of N_2O emissions from full-

scale treatment processes, Vasilaki et al. (2019) found that emission factors from literature varied significantly, even from similar process types. They determined that the length of monitoring campaign influenced the reported emission factor, with shorter studies (less than one month) presumably underestimating emissions, signifying that seasonality likely also plays a role in N_2O emissions[8]. In some wastewater treatment plants, greenhouse gas emissions from N_2O outweigh emissions from the electricity needed to operate the plant[9], supporting the need for more research surrounding N_2O in order to fully understand and minimize total greenhouse gas emissions from these facilities.

To estimate N_2O emissions from full-scale WWTPs, the current standard protocol is to follow the Intergovernmental Panel on Climate Change (IPCC) guideline, which assigns a treatment process an emission factor, which is a set amount of N_2O-N assumed to be emitted based on factors like population size, process type, and influent and/or effluent nitrogen concentrations if the data is available. However, studies have concluded that using a single emission factor to estimate N_2O emissions is not sufficient, as predicted and measured N_2O emissions vary significantly[10,11]. Historically, the IPCC methodology has assumed that N_2O emissions directly from WWTPs are relatively insignificant compared to emissions from nitrification and denitrification in water bodies that receive WWTP effluent, assigning an emission factor of 0.5% of effluent nitrogen concentration (assumed to be emitted in receiving water bodies as N_2O-N)[4]. However, this assumption did not account for emissions within plants from biological treatment processes. In 2019, a refinement to the guideline was published, with a default emission factor of 1.6% of influent N emitted as N_2O-N for centralized, aerobic treatment plants, however the literature values used to determine this factor ranged from .016 % to 4.5%, and did not differentiate between different centralized process types (e.g. nitrifying or BNR processes)[12].

Future research will determine the reliability of this default factor. As regulations become stricter concerning nitrogen entering surface waters and resource recovery of N becomes more attractive, nitrogen removal in WWTPs will become more widespread and N_2O emissions estimates will need to address the potential N_2O emissions from these process improvements.

1.1 SUMMARY

As the global nitrogen cycle operates out of balance due to anthropogenic activities, it is imperative to understand the significance and impact of elevated nitrogen levels in the environment. **Chapter 1** *Introduction* introduces and summarizes the work of this thesis. **Chapter 2** *Nitrous Oxide Emissions from Biological Nitrogen Cycling* provides background about the nitrogen cycle, anthropogenic impacts on it, and the microbes involved in its major processes. N_2O-emitting pathways, microbes involved, and their presence in wastewater treatment are discussed. This background information gives context for the projects discussed throughout the thesis and provides insight about the motivations behind the research.

Different treatment processes have been shown to emit very different amounts of N_2O. Thus, studies from various types of plants are needed to bolster knowledge about emission levels from different types of processes. **Chapter 3** *Nitrous Oxide Emissions from a Full-Scale Membrane Bioreactor Treatment Plant Using Aqueous and Gaseous Monitoring Techniques* discusses a N_2O monitoring study at Brightwater Treatment Plant. This project served to quantify emissions from the plant and to develop a methodology for N_2O emissions monitoring at other King County WWTPs. Beginning this series of monitoring campaigns at Brightwater was beneficial because the plant has a fully-covered odor control system, which allowed for very accurate emissions quantification and development of a method to adjust emissions estimates from

aqueous probes using data from a gaseous analyzer. Additionally, this project served to quantify baseline N_2O emissions before aeration basin upgrades planned at the plant. It is unknown how the planned improvements will impact N_2O emissions, so a second N_2O monitoring campaign is planned to take place after the capital project, which is described in more detail in Chapter 5 *Conclusions*.

Chapter 4 *Sustainable Nitrogen and Phosphorus Removal: Limiting Nitrous Oxide Emissions From a Granular Sludge Sequencing Batch Reactor* investigates N_2O emissions from a lab-scale aerobic granular sludge (AGS) sequencing batch reactor (SBR). AGS is capable of simultaneous nitrification, denitrification, and phosphorus removal while minimizing plant footprint and allowing for efficient sludge handling. This technology is very promising for the future of wastewater treatment and is especially attractive for its nutrient removal capabilities as effluent discharge limits become stricter. AGS SBRs are rapidly being established at full-scale, however little is known about their N_2O emission dynamics. The reactor was run for 11 months and N_2O emissions under different dissolved oxygen and nitrite concentrations were tested.

Chapter 3 has been accepted for WEFTEC 2021 conference proceedings, and Chapter 4 is a manuscript currently in preparation for journal submission. The key conclusions and future outlooks of this research are summarized in the concluding **Chapter 5**. Supplemental information for the research presented in Chapters 3 and 4 is listed in **Appendices A and B** respectively.

Chapter 2: NITROUS OXIDE EMISSIONS FROM BIOLOGICAL NITROGEN CYCLING

2.1 THE NITROGEN CYCLE

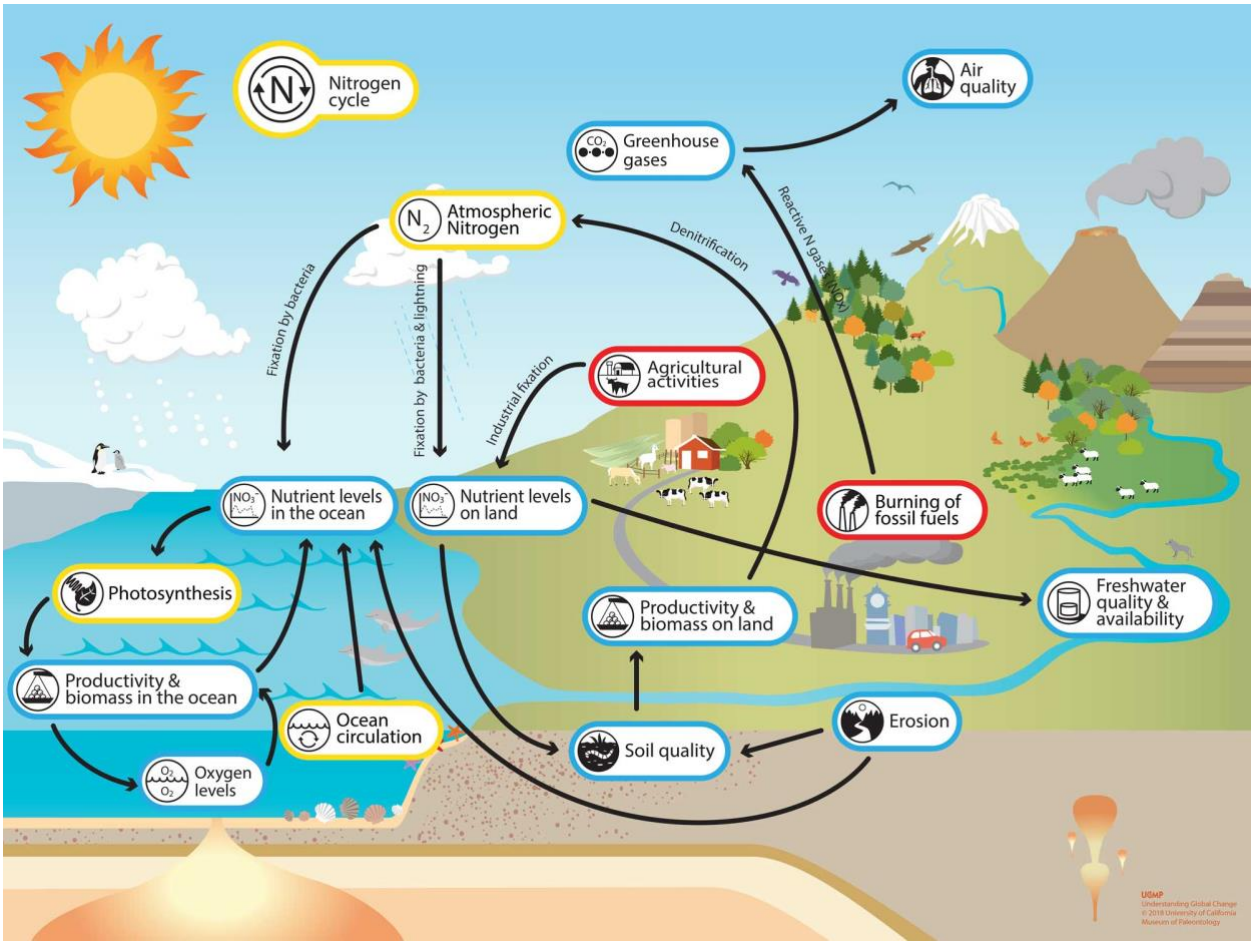

Figure 2-1. Earth system model of the nitrogen cycle (University of California Museum of Paleontology)[13].

The nitrogen cycle is a *biogeochemical* cycle, meaning that nitrogen moves through both biotic (biological) and abiotic (geologic, atmospheric, and hydrological) systems. The biological nitrogen cycle consists of five main transformations. (1) nitrogen fixation, (2) assimilation, (3)

nitrification, (4) denitrification, and (5) mineralization. (1) Nitrogen fixation is the conversion of nitrogen gas (N_2) in the atmosphere, sometimes referred to as *free nitrogen*, to ammonia (NH_3), or *fixed nitrogen* ($N_2 + 8H \rightarrow 2NH_3 + H_2$). (2) Assimilation is the formation of organic nitrogen from environmental NH_3 or NO_3^- by plants, fungi, and bacteria that cannot perform nitrogen fixation. (3) Nitrification is the oxidation of NH_3 to nitrate (NO_3^-), and (4) denitrification is the reduction of NO_3^- to gaseous nitrogen compounds ($NO_3^- \rightarrow NO_2^- \rightarrow NO \rightarrow N_2O \rightarrow N_2$). (5) Ammonification, or *mineralization*, is the release of NH_3 during the decomposition of organic nitrogen (NH_2 groups such as amino acids and nucleotides). These processes are displayed in Figure 2-2. Additional biological N transformations are discussed in *2.2 Biological Nitrogen Cycling.* In addition to these transformations, nitrogen is subject to abiotic processes such as erosion and lightning. The processes driving the nitrogen cycle evolved about 2.7 billion years ago with these atmospheric, geological, and microbial processes, however in the past century agricultural practices, the growing global demand for food, and the burning of fossil fuels have drastically disrupted this cycle. This has resulted in several negative environmental consequences including the eutrophication of surface waters, ozone depletion, and increased N_2O emissions. Figure 2-1 illustrates an Earth system model of the nitrogen cycle, highlighting many of the relevant anthropogenic components. To address the issue of excessive N_2O emissions from an imbalanced nitrogen cycle, it is important to thoroughly understand the pathways in the biological nitrogen cycle and microbes responsible for these transformations.

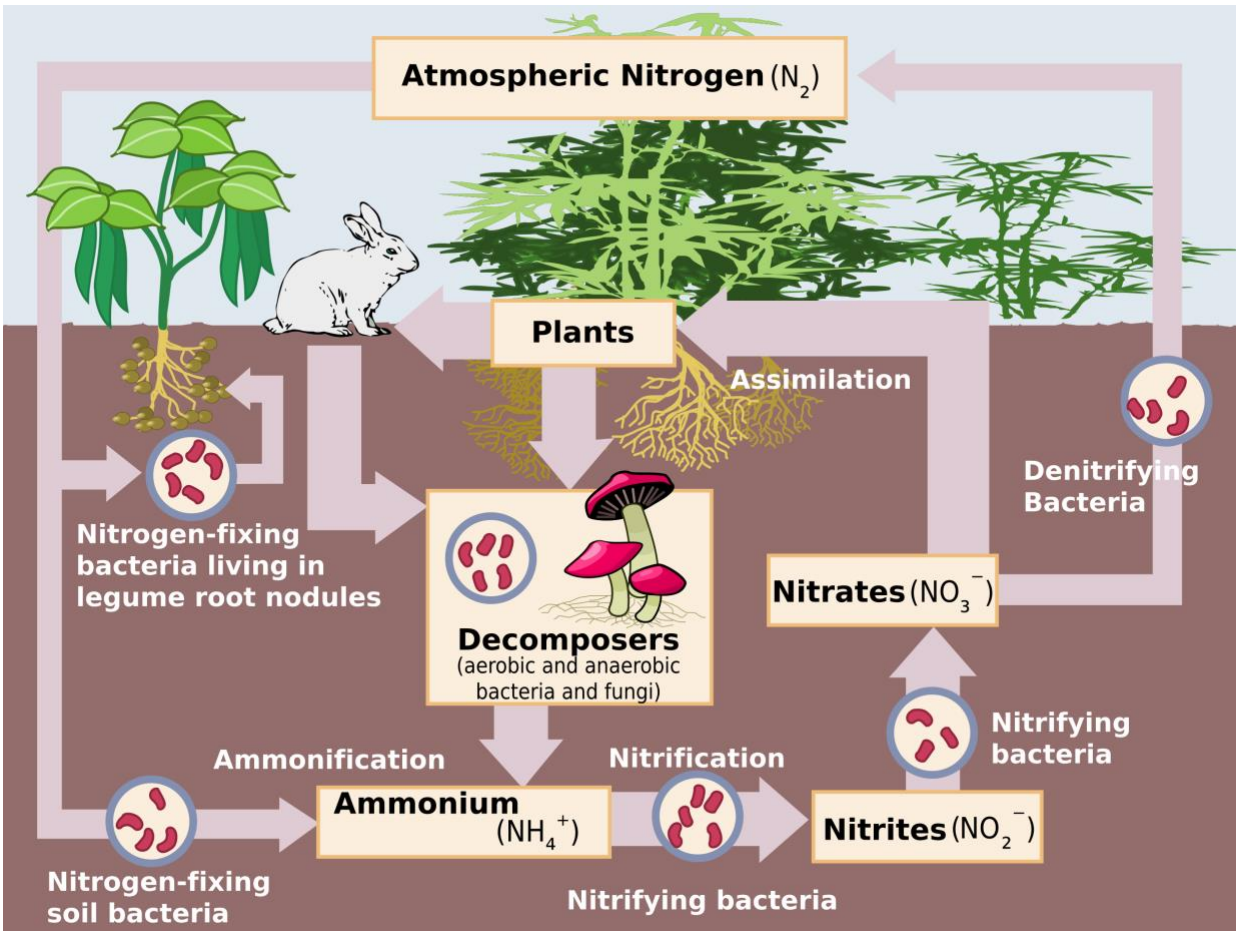

Figure 2-2. Major biological processes in the nitrogen cycle (USEPA, 2003)[14]

Before the anthropogenic disturbance of the nitrogen cycle, nitrogen fixation occurred primarily through lightning and biological nitrogen fixation. Nitrogen did not accumulate in environmental reservoirs because fixation and denitrification processes were approximately equivalent. In recent years, nitrogen fixation by humans has exceeded the fixation from all natural and terrestrial systems. As a result, nitrogen accumulates in the environment at local, regional, and global scales. This is largely attributed to the widespread cultivation of legumes, rice, and other crops that promote biological nitrogen fixation, the combustion of fossil fuels (which converts both atmospheric N_2 and fossil N to reactive NO_x), and the Haber-Bosch process (which chemically converts N_2 to NH_3). Anthropogenic nitrogen creation increased from 15 teragrams

(Tg) per year in 1860 to 165 Tg per year in 2000, with 100 of these Tg coming from the Haber-Bosch process alone[15]. Since a large proportion of the human population is supported by food production dependent on this process, it is a major challenge to mitigate the negative environmental consequences caused by a drastically imbalanced global nitrogen cycle.

The Haber-Bosch process combines N_2 and H_2 under high temperature and pressure to form NH_3. Most of the industrially produced nitrogen is used in agriculture, but a significant amount applied to farmland runs off into water bodies. This is a significant nonpoint source of nitrogen pollution[16]. A significant point source of nitrogen pollution in surface waters is effluent from wastewater treatment plants, with humans' consumption of food resulting in N-rich waste and wastewater (if there is no nitrogen removal in treatment plants)[17]. Excessive runoff or leaching of nitrogen can lead to excessive algal growth (eutrophication). In the US, nitrogen pollution is considered the most serious coastal pollution problem[18,19]. Other effects are the loss of seagrass and macroalgal beds, changes in coral reefs, and anoxic or hypoxic (dead) zones[18,20,21]. Nearly all of the nitrogen entering surface waters is denitrified as it travels along streams, rivers, and estuaries, and some of this is converted to N_2O[22]. It is estimated that 30% of total anthropogenic N_2O emissions are from rivers, estuaries, and continental shelves[23].

Reactive nitrogen is widely dispersed by hydrologic and atmospheric transport, then accumulates in the environment because creation rates are greater than the rates of removal through denitrification. This accumulation is expected to continue to increase as the human population and per capita resource use increase. Nitrogen accumulation contributes to the production of tropospheric ozone and illness-inducing aerosols[24], forest and grassland productivity increase then decrease[25], and likely decreased biodiversity of many natural habitats[26]. It also contributes to acidification in lakes and streams and eutrophication, hypoxia, loss of biodiversity, and habitat

degradation in coastal ecosystems[19]. Finally, nitrogen accumulation contributes to global climate change and stratospheric ozone depletion because of increased N_2O and NO emissions[27].

2.2 BIOLOGICAL NITROGEN CYCLING

The global nitrogen cycle consists of geological, atmospheric, and biological processes, however the major fluxes between reservoirs are biologically driven, meaning the biological nitrogen cycle is of significant interest for understanding excessive N_2O emissions into the atmosphere. The major steps of the biological nitrogen cycle, the microbes involved, and their relevance to N_2O emissions are detailed below.

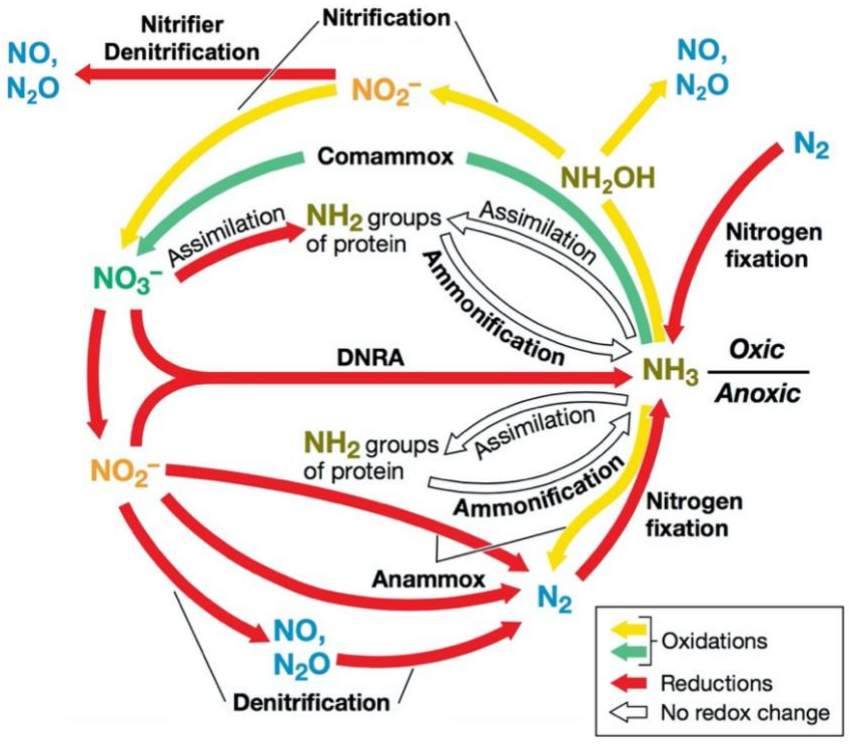

Figure 2-3. Biological nitrogen cycling with relevant N_2O emission pathways. (Adapted from Brock Biology of Microorganisms[28]).

2.2.1 Nitrogen Fixation and Assimilation

Nitrogen is the fifth most abundant element in the solar system and accounts for 78% of Earth's atmosphere as N_2, and cells need a significant amount of nitrogen for fundamental processes such as synthesizing proteins, nucleic acids, and other organic molecules. However, N_2 is "virtually inert" and must be fixed into nitrogen that can be used by primary producers in both marine and terrestrial ecosystems[29]. Most microbes use fixed forms of nitrogen such as ammonia or nitrate (NO_3^-). Only a small number of bacteria and archaea are able to use abundantly available gaseous N_2 as a cellular nitrogen source through the process of nitrogen fixation, in which N_2 is reduced to NH_3 using the nitrogenase metalloenzyme[30]. Ammonia produced is then assimilated into organic form, which then becomes available to organisms that cannot fix nitrogen[28]. Some nitrogen-fixing bacteria are free-living, and carry out the process independently, whereas some are symbiotic and fix nitrogen with certain eukaryotes such as legumes and termites[29]. To detect nitrogen-fixing microorganisms in the environment, the gene marker *nif*H is used[31]. Atmospheric nitrogen can also be fixed when the high energy of lightning breaks the bonds in N_2, allowing N to combine with oxygen and form nitrogen oxides, which dissolve in rain and form nitrates that are precipitated to the Earth[28].

2.2.2 Ammonification

Ammonification (also known as mineralization) occurs when organic nitrogen (from waste or a dead organism) is decomposed by heterotrophic bacteria or fungi into ammonium (NH_4^+). Enzymes involved are glutamine synthetase, glutamate 2-oxoglutarate aminotransferase, and glutamate dehydrogenase[32].

2.2.3 Nitrification

Canonical Ammonium and Nitrite Oxidation

Nitrification consists of two sets of reactions that aerobically oxidize the reduced inorganic nitrogen compounds NH_3 and NO_2^-. These reactions are performed by two chemolithotrophic nitrifying bacteria, which are widely distributed in soil, water, wastewater, and in the ocean. The first set of reactions are performed by ammonia oxidizing bacteria (AOB) and archaea (AOA), which catalyze the oxidation of ammonia to nitrite. Most AOB belong to the Betaproteobacteria and Gammaproteobacteria classes, and are found in nearly all environments, including WWTPs and fertilized soils[33]. AOA belong to the phylum Thaumarchaeota, and have been found to dominate soil and marine environments[34–36]. The oxidation of ammonia to nitrite has hydroxylamine (NH_2OH) as an intermediate, which reacts with NO_2^- to form NO and N_2O. While this is usually a chemical oxidation reaction, recent research has shown that the reaction may proceed biologically by cytochrome P460 in N. *europaea* under anaerobic conditions[37] or mediated by the hydroxylamine oxioreductase (HAO) enzyme under aerobic conditions[38]. Nonetheless, in this reaction NH_2OH is produced by AOB, so the distinction between chemical and biological processes is complicated[39].

The second set of reactions are performed by nitrite oxidizing bacteria (NOB), which oxidize nitrite to nitrate. This reaction is catalyzed by nitrite oxidoreductase (*nxr*). NOB are present in a variety of terrestrial, marine, and freshwater ecosystems[40].

Complete Ammonia Oxidation

Comammox bacteria are a recently discovered novel NOB of the genus *Nitrospira* that have the capacity to completely oxidize ammonia to nitrate, first converting ammonia into nitrite and then into nitrate[41]. Comammox are identified by ammonia monooxygenase and target gene *amo*A[42]. Prevalent in wastewater treatment environments, there is some evidence that comammox can reduce nitrate to nitrite and could be beneficial in systems that depend on denitrification via nitrite (like anaerobic ammonium oxidation), however the conditions that select for full nitrification are still unknown, and it is unknown if comammox are detrimental to nitritation processes[40,43].

2.2.4 Denitrification

Heterotrophic Denitrification

Denitrification is the reduction of nitrate to N_2. It is performed by a metabolically diverse group of bacteria and archaea, and NO and N_2O are intermediates in the denitrification process, so incomplete denitrification can lead to NO and N_2O emissions. Facultative anaerobic bacteria perform denitrification with nitrogen electron acceptors NO_3^-, NO_2^-, NO, N_2O, and N_2 (from most to least thermodynamically favorable)[44]. The enzymes used to catalyze these reactions are nitrate reductase[45], nitrite reductase[46], nitric oxide reductase[47], and nitrous oxide reductase[48], respectively.

Nitrifier Denitrification

Nitrifier denitrification is the pathway by which ammonia is oxidized to nitrite, followed by the reduction of nitrite to nitric oxide, nitrous oxide, and N_2. This process is performed by autotrophic nitrifiers, and is a potentially significant source of N_2O emissions, especially in

fertilized soils, so current research focuses on quantification of this emissions pathway with different soils under different conditions. The enzyme required by ammonia-oxidizers, nitrite reductase, is believed to be the same as for ammonia oxidation and denitrification[49].

Denitrification by PAO and GAO

Heterotrophic denitrifiers relevant to wastewater treatment processes include ordinary heterotrophs (directly oxidizing organic carbon to CO_2) as well as phosphorus accumulating organisms (PAO) and glycogen accumulating organisms (GAO) that anaerobically store organic carbon and oxidize it once an external electron acceptor is available. Excess phosphorus in effluent from WWTPs can contribute to eutrophication of surface waters, so PAOs are used to remove phosphate. PAOs remove phosphate biologically rather than chemically, which circumvents the production of hazardous excess sludge[50]. The metabolism of GAOs is similar to PAOs except that PAOs lack genes for phosphate uptake and release. PAOs and GAOs most typically utilize oxygen for cell respiration, however they are capable of utilizing NO_3^-/NO_2^- as an electron acceptor in the absence of oxygen and are then termed denitrifying-PAO (DPAO) or denitrifying-GAO (DGAO), as both N and P are removed in the same process[51]. DPAOs are able to take up P under anoxic (denitrifying) conditions, which is advantageous compared to aerobic oxic P removal, which requires more oxygen and organic carbon[52]. During anaerobic conditions PAO and DPAOs excrete intracellularly stored polyphosphate as orthophosphate extracellularly and utilize the gained energy to accumulate polyhydroxyalkanoates (PHA) from volatile fatty acids (VFAs) present in the bulk liquid. Under aerobic or anoxic conditions the reduction of these electron acceptors leads to the removal of nitrogen (in case of NO_3^-) from the bulk liquid. The co-occurring oxidation of internally stored PHB provides energy for the replenishment of polyP reserves, resulting in phosphate removal from the effluent[53]. DPAOs have been shown to

generate high levels of N_2O in a DPAO-enriched bioprocess[54], and in this work it was hypothesized that emissions could be linked to selection for organisms with truncated denitrification pathways that lack the genomic capacity for N_2O production (DPAOs or non-PAO denitrifiers)[55]. High free nitrous acid (FNA) concentrations likely inhibit N_2O production and may hence be used to mitigate this potent GHG[56]. However, a study using mass balance calculations did not find significant N_2O emissions from a denitrifying biological phosphorus removal reactor[57], so further investigation is required to determine the contribution of DPAO to N_2O emissions. Biological phosphate removal selects for PAO, however at higher temperatures GAO form[58]. Very little is known about GAO, apart from their phenotype[59], but GAO have also demonstrated denitrifying capabilities (DGAO) with similar mechanisms to DPAO[60], and DGAOs have been observed to emit N_2O during denitrification[61–63], possibly because PHB consumption is the rate-limiting step for organisms growing on storage compounds[64].

2.2.5 Anaerobic Ammonia Oxidation

Ammonia can be oxidized anoxically by anaerobic ammonium oxidizing (anammox) bacteria, which anaerobically oxidize ammonia with NO_2^- as the electron acceptor and N_2 as the final product[65]. Anammox is a major process in anoxic marine basins and sediments[28] and is successfully implemented to treat reject water from anaerobic digesters in full-scale sewage treatment. Although anammox denitrify, they are not expected to emit N_2O because they do not possess nitric oxide reductase (NOR) genes responsible for N_2O emissions. As a result no N_2O is formed as an intermediate in this autotrophic denitrification process[66]. This allows a nitrogen removal technology with fewer greenhouse gas emissions than a conventional denitrification process. However, Anammox rely on the nitrite that must be produced by AOB, which can emit N_2O via nitrification or nitrifier denitrification. Catabolic enzymes of anammox bacteria are

hydrazine dehydrogenase, hydrazine synthase, nitrite reductase, hydroxylamine oxidase, and nitrite oxidoreductase[67].

2.2.6 Dissimilatory Nitrate or Nitrite Reduction to Ammonia

In dissimilatory nitrate or nitrite reduction to ammonia (DNRA), nitrite and nitrate can be reduced to ammonia. It is difficult to tell which organisms are performing DNRA or denitrification since the processes can co-occur[68]. The environmental importance of DNRA is not yet known, but in marine and lake sediments it appears to be favored over denitrification when there is an excess of the electron donor relative to nitrate[69]. In wastewater treatment this process would be highly unfavorable as nitrate would be converted back to ammonium by which aeration requirements would be significantly increased[70].

2.3 N_2O EMISSION PATHWAYS IN WASTEWATER TREATMENT

N_2O emissions in wastewater treatment are heavily influenced by the structure and function of the microbial community, however there is significant uncertainty surrounding this community, so it is difficult to determine the optimal design and operation of wastewater treatment plants to reduce emissions without an improved understanding of these biological processes. Both autotrophic nitrification and heterotrophic denitrification processes contribute to N_2O emissions in wastewater treatment processes[43].

In wastewater treatment, nitrification is predominantly performed by autotrophic AOB and NOB. Ammonia-oxidizing archaea (AOA) were also found in WWTPs operating at low DO levels with long solids retention time, and ammonia oxidation can be performed by heterotrophic bacteria, but the reaction proceeds very slowly, and may only dominate at relatively high organic loading

rates (COD:N>10) and low DO[71]. Overall, in conventional wastewater treatment processes, there is no indication that heterotrophic ammonia oxidizers or AOA have a significant role in activated sludge processes, however they may be significant in N_2O production[72]. Although N_2O is not an intermediate in the main catabolic pathway of nitrification, AOB can denitrify from nitrite to form N_2O, using ammonium or hydrogen as the electron donor, and chemical reactions of unstable biological intermediates could also contribute to N_2O emissions[7,73].

Because N_2O is an intermediate of heterotrophic denitrification (and not an intermediate in the main nitrification pathway) it would be expected that denitrification would be the main pathway for emissions, however in wastewater treatment there is still uncertainty about which process contributes the most emissions. Aerobic denitrification and nitrifier denitrification may yield greater N_2O emissions than heterotrophic denitrification, although it is unclear exactly what emissions each group contributes[74]. Kampschreur et al. (2008) determined that the denitrification pathway of AOB with ammonium as its electron donor was the main N_2O production pathway in a lab-scale nitrifying reactor system, though current research continues to test this hypothesis[75].

Most research investigating N_2O emissions from wastewater treatment focuses on process-related emission triggers. This research is vital because a leading question for process engineers is how to minimize emissions using mechanisms within the control of a given wastewater treatment plant. However, by studying the microbiology involved more insight can be gained about *why* certain operational parameters trigger emissions and others do not. This will help address the overarching question of how to minimize emissions while still meeting a treatment plant's immediate goals.

Chapter 3. NITROUS OXIDE EMISSIONS FROM A FULL-SCALE MEMBRANE BIOREACTOR TREATMENT PLANT USING AQUEOUS AND GASEOUS MONITORING TECHNIQUES

This work has been accepted as:

S. K. Cavanaugh, E. Jacobson, P. Sukapanpotharam, M. K. H. Winkler, N_2O emissions from a full-scale membrane bioreactor treatment plant using aqueous and gaseous monitoring techniques, Proceedings of the Water Environment Federation 2021 (2021).

3.1 ABSTRACT

N_2O from a full-scale MBR treatment plant was measured on-line for 5.5 months using gas-phase and liquid-phase analyzers. Both gaseous and aqueous measurements showed similar emission trends, but the aqueous analyzer overestimated emissions and therefore an adjustment factor of 0.66 was applied to the emissions estimate of the aqueous analyzer to match results of the gaseous analyzer. The average emission factor was 0.58% of plant influent TKN emitted as N_2O-N—lower than many of the reported emission factors from similar processes. It was determined that 39% of plant emissions were from the aerated membrane basins. N_2O emissions correlated positively with influent pH, nitrification efficiency, and aeration basin/effluent NH_4^+ and NO_3^-. It correlated negatively with primary effluent COD:N ratio and effluent pH. These trends signify that nitrification was likely the dominant N_2O-production pathway.

3.2 INTRODUCTION

Nitrous oxide (N_2O) is a strong greenhouse gas (GHG) with a global warming potential approximately 300 times that of carbon dioxide (CO_2) over a 100 year horizon[1]. Quantification of N_2O emissions from water reclamation facilities (WRFs) is becoming increasingly important as greenhouse gases become more closely monitored and regulated as part of the climate change crisis. In the US, 1.9% of N_2O emissions are attributed to wastewater treatment and composting combined. However, literature reports that emissions from different WRFs are highly variable[4], indicating uncertainty about their net contribution to total N_2O emissions, even as nitrogen removal becomes more mandated. N_2O is one of the main contributors to total greenhouse gas emissions from wastewater treatment systems (approximately 5 million metric tons of CO_2 equivalents per year in the US), meaning that minimizing N_2O emissions could significantly reduce the carbon footprint of wastewater treatment systems as a whole[5]. Additionally, tracking and reducing GHG emissions from WRFs may be mandated in the future. As regulations managing nutrient discharge into surface streams become more stringent and resource recovery becomes more attractive, nitrogen removal in WRFs will become more widespread and N_2O emission estimates will need to be more accurate. Studies have concluded that using a single emission factor to estimate N_2O emissions from different WRFs is not sufficient, as predicted and measured N_2O emissions vary significantly[10,11]. The Intergovernmental Panel on Climate Change (IPCC) range of potential emission factors for centralized, aerobic treatment plants is 0.016% to 4.5% of influent total nitrogen[12] and future research will determine the reliability of these factors. N_2O emission rates have been observed to vary dramatically between different types of WRFs, making it difficult to estimate a plant's N_2O emissions based on literature alone. Of the limited studies monitoring N_2O from full-scale treatment plants, there is a wide range of

emission rates observed even among plants with similar biological processes. There is therefore a pressing need to develop easily implementable methods allowing any treatment plant to determine their emission factor, and our study provides a method for N_2O measurements at scale.

3.2.1 Monitoring N_2O Emissions at Full-Scale

Previous studies have monitored N_2O emissions using both gaseous and aqueous methods at full-scale WRFs, but very few have monitored emissions on-line for long periods of time, capturing the scope of diurnal and seasonal variations that affect N_2O emissions[76]. Even fewer studies have compared gaseous and aqueous emission monitoring methods, and had the benefit of a fully-covered process[77,78]. It is of interest to compare the two methods since liquid analyzers are more practical for most plants to install, but converting from aqueous concentrations to gaseous emissions relies on several assumptions which impact their accuracy. Off-gas measurements from floating hoods are common in the field since most plants do not have fully-covered off-gas systems. However, the mass balance for measurements from floating hoods relies on several assumptions that introduce uncertainty to their emission estimates. It is therefore beneficial to measure N_2O in the liquid phase; this study provides a comprehensive comparison of gas and liquid phase measurements to determine the reliability of the liquid phase measurement method. Additionally, few studies have investigated N_2O emissions from membrane bioreactors (MBRs). It is generally assumed that the majority of N_2O emissions from WRFs are from aeration basins, since aeration strips out dissolved N_2O with the off-gas[7]. However, features of MBRs that may impact their N_2O emissions include the absence of secondary clarifiers, increased aeration for membrane fouling mitigation, and biomass selection in the membrane basins. Foley et al. (2015)[79] studied a full-scale MBR (activated sludge with sequenced aeration, followed by MBR) in France using floating hoods and reported an emission factor of 0.11% of influent Total

Kjeldahl Nitrogen (TKN) emitted as N_2O-N. These findings were part of a large technical report, so information about the duration of sampling is unavailable. To the knowledge of the authors, the present study is the most comprehensive monitoring of N_2O emissions from a full-scale MBR to date.

3.2.2 Involved Microbiology

There are three main N_2O emission pathways from wastewater treatment processes. (1) During the first step of *nitrification* ammonia oxidizing bacteria (AOB) produce NH_2OH, which reacts with NO_2^- to form NO and N_2O. (2) Under anoxic conditions, AOB can also denitrify from NO_2^- to N_2O[80]. This process is known as *nitrifier denitrification*. (3) During *heterotrophic denitrification*, NO_3^- is reduced to N_2 gas, with N_2O as one of the intermediates. It is uncertain which process is the dominant N_2O emitter in WRFs, but it is likely that all three play a role, and process-specific conditions (such as N-removal via denitrification in the plant) impact the contribution of each pathway to plant emissions[7].

3.2.3 Relevant Process Parameters

Several studies, mostly at lab-scale, have investigated how wastewater treatment process parameters impact N_2O emissions. In full-scale activated sludge plants, N_2O emissions have been observed to increase with the following parameters: high nitrite, ammonium, and dissolved oxygen concentrations in aerobic zones[10], low COD:N, high aeration flow-rates[81], and the presence of biological nitrogen removal (BNR)[82]. Few full-scale WRF studies have investigated the impact of varying process parameters at high temporal resolution and over extended periods of time. In this study, statistical analysis was performed on the plant's routinely collected process data to determine if any parameters were correlated with elevated N_2O emissions.

This study quantified N_2O emissions from a full-scale MBR with covered basins and an off-gas control system using continuous, on-line aqueous and gaseous monitoring techniques. Detailed N_2O emission data was collected simultaneously with both techniques over a period of 5.5 months. The direct comparison of the two methods can guide method selection for other N_2O emission studies. Additionally, process parameters demonstrating correlation with elevated N_2O emissions are discussed.

3.3 METHODS

3.3.1 Selection of Study Site

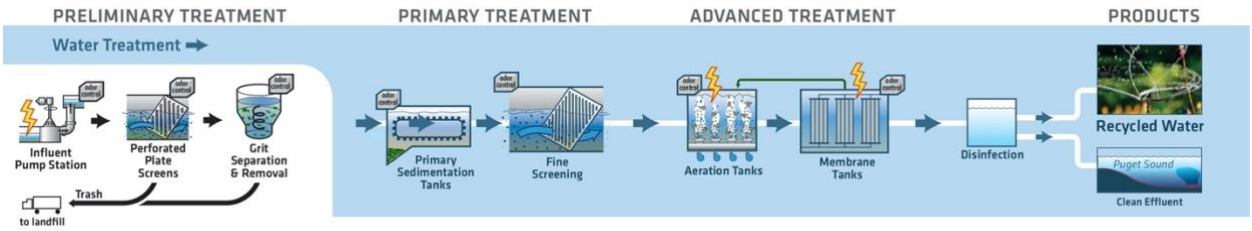

Figure 3-1. Brightwater liquid stream treatment process (King County, 2018)[83].

N_2O emissions from the MBR secondary process at King County's Brightwater Treatment Plant (Woodinville, Washington) were monitored for 5.5 months. Brightwater treats municipal wastewater for a population equivalent of 250,000. During winter months, flow into the plant is 63% residential, 10% commercial, and 4% industrial wastewater, with 23% from stormwater inflow and groundwater infiltration. The annual average flow in 2019 was approximately 62,000 cubic meters per day (16.3 mgd), with an influent total nitrogen concentration of 61.2 mg N L^{-1}. Wastewater characteristics during the monitoring period are detailed in Table 3-1. The study took place predominately during the wet season in the Pacific Northwest, when influent nitrogen concentrations are generally lower than annual averages. Brightwater is an activated sludge

MBR secondary treatment facility equipped with Suez's ZeeWeed® MBR technology with LEAP™ aeration. The full liquid stream treatment process is shown in Figure 3-1. Biological treatment consists of three aeration basins that operate in a Modified Ludzack-Ettinger (MLE) configuration. Each basin consists of a mixed anoxic zone and four aerobic zones. Both carbonaceous biochemical oxygen demand removal and nitrification occur in the aeration basins, with internal mixed liquor recycle to the anoxic zone. Brightwater achieves full nitrification and partial denitrification to meet membrane influent requirements. Each aeration basin is 7.6 meters (25 feet) deep with a total capacity of 17,700 cubic meters (4.67 million gallons), with fine bubble diffusers for aeration. The dissolved oxygen concentration (DO) setpoint, which is controlled in the second of four aerobic zones in each aeration basin, typically operates between 1.5 and 2.1 mg L^{-1}. DO is quite variable across the four aerobic zones (generally, lower than the setpoint in zone one and higher in zones three and four), and inconsistent DO has been found to cause elevated N_2O emissions at other plants[84,85]. Design hydraulic retention time (HRT) and solids retention time (SRT) are 4.2 hours and 10 days respectively, but normally the plant operates with an SRT closer to 20-25 days to fully nitrify and create a mixed liquor that is conducive to good membrane filterability. The temperature range of influent during the monitoring period was 9.4 – 20 °C (49 – 67 °F). After aeration, mixed liquor is pumped to eight membrane basins, each containing 20 cassettes of hollow-fiber membranes. The aeration and membrane basins are completely covered for odor control, with foul air routed to an odor control system consisting of four, two-stage, odor control trains. This odor control system makes Brightwater ideal for gaseous analysis of N_2O emissions, with all gases from biological and membrane processes passing through a closed system before being emitted from the plant.

Table 3-1. Daily wastewater characteristics (mean concentrations and standard deviations (SD)) at Brightwater during the monitoring campaign (10/13/2020 – 3/30/2021).

Parameters	Influent [mean (SD)]	Primary Effluent [mean (SD)]	Mixed Liquor Feed [mean (SD)]	Membrane Effluent [mean (SD)]	Final Effluent [mean (SD)]
COD (mg L^{-1})		283 (40)	58 (20)	20 (2.5)	
BOD (mg L^{-1})		138 (23)		1.5 (0.4)	
TKN (mg N L^{-1})	49 (10)	52 (7.9)		1.6 (0.5)	1.5 (0.5)
NH_4^+ (mg N L^{-1})	30 (6.5)	37 (6.7)	1.4 (0.8)	0.1 (0.1)	0.1 (0.1)
NO_2^-+NO_3^- (mg N L^{-1})	1.6 (0.8)	4 (1.1)		35 (4.4)	35 (5)
TSS (mg L^{-1})		64 (8.9)			
Alkalinity (mg L^{-1})		221 (29)		122 (32)	
SCOD (mg L^{-1})			48 (15)		

Figure 3-2. Brightwater Treatment Plant with N_2O monitoring configuration.

3.3.2 N_2O Measurement and Monitoring

The N_2O monitoring study at Brightwater began on October 13, 2020 and ended on March 30, 2021. Aqueous and gaseous monitoring of N_2O emissions took place nearly continuously during the 5.5-month campaign.

3.3.3 Aqueous Analyzer

Aqueous N_2O concentrations were measured on-line with the Unisense Environment A/S N_2O Wastewater System (Aarhus, Denmark), which consists of two N_2O wastewater sensors (probes) and an N_2O wastewater controller. The sensor head is a Clark-type Sensor, and the sensor body contains a temperature sensor. The wastewater controller was used to log measurements from the connected sensors, and data was downloaded from the controller's USB port. The system was calibrated every two months using Unisense Environment's N_2O calibration kit according to the manufacturer's protocol. Calibration procedures are detailed in Appendix A1. The first probe was placed directly downstream of the anoxic zone and the second in aerated zone two of aeration basin 1 (Figure 3-3). Ideally, the anoxic probe would be placed directly in the anoxic zone, however access to the basin was limited because of the covers, thus the chosen location was assumed to adequately represent anoxic zone conditions, directly downstream of the weir separating the anoxic and aerated zones. The aqueous N_2O concentration was assumed to be consistent between the three aeration basins, with the reading from basin one representing the concentration for all three basins. The calculation to convert aqueous concentrations to emissions accounted for the distinct liquid and gas flows to the three basins. Dissolved N_2O concentrations were reported as mg N_2O-N L^{-1}, and were used to calculate mass emissions following methods reported in literature[86,87]. Equations used for this method are in Appendix A1.

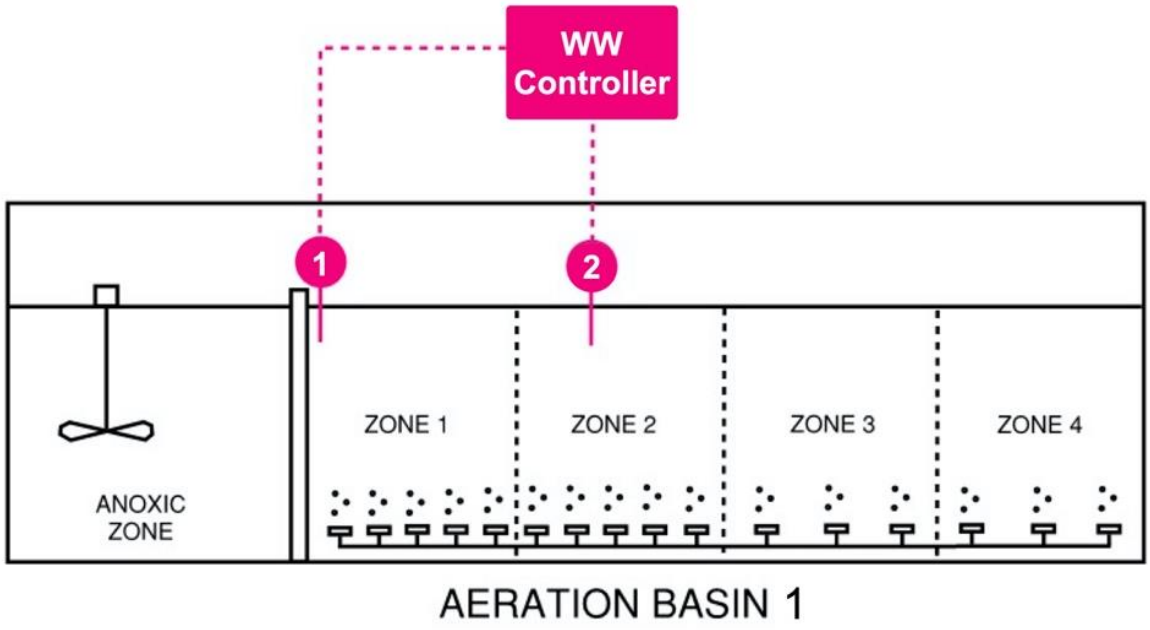

Figure 3-3. Aqueous N_2O measurement setup. N_2O sensors are labeled 1 and 2.

3.3.4 Gaseous Analyzer

Brightwater is an ideal study site for gaseous N_2O monitoring because all secondary processes (aeration and membrane basins) are completely covered and their off-gas is routed and treated through an odor control system consisting of four, two-stage odor control trains. Gaseous N_2O concentrations were measured from a foul air duct (downstream of liquid treatment processes, prior to odor treatment processes) using a Teledyne AI GFC 7002T N_2O Analyzer (San Diego, California) and a sampling train configured for outdoor field measurement. The gaseous analyzer uses Gas Filter Correlation (GFC) and Infrared Radiation (IR) to determine the concentration of N_2O in sample gas drawn through the instrument. The analyzer was calibrated using span gas (25 ppm_V N_2O-N) and zero gas (ultra pure N_2) according to the manufacturer's protocols and was re-calibrated twice per month. Calibration procedures are detailed in Appendix A2. The analyzer recorded N_2O-N concentrations on-line as ppm_V, and emission rates were estimated using the

flow rates from the odor control fans which pull gas from the headspace of the aeration and membrane basins. The gaseous mass balance calculation is detailed in Appendix A2, and information about the odor control blowers and fan curves is provided in Appendix A3. A mobile sampling unit was constructed for field sampling so the analyzer could be easily moved to different sampling locations. The sampling unit consisted of the analyzer (placed in a weather-proof, temperature-controlled housing) and a gas conditioning system. The gas conditioning system consisted of a thermo-electric gas cooler to remove water vapor from the sample gas, a coalescing filter, a pump to continuously draw the sample, and a rotameter to control the gas flow rate. Photos and description of the sampling unit are available in Figure A5. The gaseous analyzer was moved to three different sampling locations in the plant to determine the impact of sampling location and the odor control system since the configuration and operation of the plant made long-term, continuous sampling of a fully representative off-gas sample impossible. There are two main foul-air ducts (one for the membrane basins and one for the aeration basins) which converge in a single duct before entering the odor control trains. The first sampling point allowed for distinct sampling of the membrane basins, the second allowed for sampling of a fully representative gas sample of the membrane basins combined with the aeration basins (in conjunction with deliberate operation of only two odor control blowers), and the third investigated the impact of the odor control system (caustic/hypo chemical scrubbers and activated carbon beds) on emissions. This analysis is discussed at length in Appendix A4. Gaseous sample point locations are noted in Figure 3-2.

3.3.5 Analytical Methods

The plant's operational data were tracked on-line using the plant's control system and recorded in the PI historian database, and included pH, temperature, DO, air flow, and liquid flow on an

hourly basis. There were also two in-line nitrogen probes in the process, one measuring NH_4^+ and NO_3^- in zone 3 of aeration basin 1 and the other measuring NH_4^+ in the membrane effluent. This data (at high temporal resolution) allowed for the identification of diurnal patterns in the plant. King County Wastewater Treatment Division (WTD) staff also performed routine water quality testing, most often using autosamplers to collect 24-hour composite samples that were then analyzed following standard methods. Results from these tests were recorded in the HachWIMS reporting tool. A complete list of parameters tracked by the PI historian and HachWIMS reporting tool is available in Table A2. N_2O emission data were interpreted in the context of nitrogen removal using data from the HachWIMS reporting tool. 24-hour composite samples of TKN were sampled weekly and 24-hour composite samples of NH_4^+ were sampled three times per week. Samples from the influent, primary effluent (PE), and membrane effluent were used to calculate daily TKN and NH_4^+ removed throughout the activated sludge and membrane processes. Emission factors were then calculated by dividing daily N_2O-N emission estimates by nitrogen loading or removal. Nitrification efficiency was estimated as the percent of NH_4^+ removed between the PE and membrane effluent samples. Denitrification efficiency was estimated as the percent of NH_4^+ removed that did not remain as $NO_2^- + NO_3^-$ in the membrane effluent.

3.3.6 Correlation Analysis

Spearman rank correlation was performed on data from several process parameters at Brightwater. Correlation analysis was performed in Python 3.8.8 using Python Data Analysis Library (Pandas). The data was collected from the HachWIMS reporting tool, the PI historian database, and from aqueous probes placed throughout the process stream. Correlation analysis was performed at two temporal resolutions, with hourly data used to determine *diurnal*

correlations, and daily data (as well as hourly data converted to 24-hour averages) used to determine *non-diurnal* correlations. The non-diurnal correlations served to circumvent bias from the daily patterns that many parameters in WRFs exhibit.

3.3.7 Method Limitations

To comprehensively capture seasonal variations in N_2O emissions and determine a definitive annual emission estimate, monitoring would have had to continue for a full calendar year to capture the complete temperature and precipitation range of the plant. However, the monitoring period (October – March) was chosen because it captures the end of the dry season and most of the rainy season in Western Washington, and it preceded upcoming capital improvements that may impact N_2O emissions, thus offering a baseline for future comparison. It is unclear how seasonal variations in temperature and precipitation affect N_2O emissions. Warmer weather increases the specific growth rate of nitrifiers[88] which may increase emissions, however one study found that N_2O peaked during precipitation events at low temperatures[89]. The range of influent temperature during the monitoring period was 9.4 – 20 °C (49 – 67 °F), and the range of influent temperature for the previous year (the 5.5-month monitoring period and the preceding 6.5 months) was 8.5 – 20.8 °C (47-69 °F). The average annual rainfall at the site was 0.14 inches per day, and during the monitoring period it was 0.18 inches per day. The day with the most rainfall in the previous year was on December 21, 2020 (during the monitoring period), with 2.08 inches. The monitoring campaign was therefore reasonably representative of annual dry and wet weather conditions, albeit with a short measurement duration during the dry conditions.

Another limitation to our method was the regularity of testing for nitrogen concentrations in the plant. While our on-line N_2O analyzers captured N_2O data at extremely high resolution, testing

for nitrogen loading was completed in a lab, limiting the resolution of NH_4^+ data to three times per week and TKN data to once per week. This means that while there was very high resolution for N_2O mass emission data, the emission factors (the determination of which are a main objective of N_2O emission studies) were based on far fewer data points. This study included assumptions about factors such as gas flow in the odor control system and the interpolation of air flow rates, which are detailed in Appendices A3 and A4. Since industry standard methods and equipment were used, the uncertainty involved in this study is expected to be comparable to previous studies of this type.

3.4 RESULTS

3.4.1 N_2O Emissions

A significant diurnal variation in N_2O emissions was identified, with emission peaks positively correlated with several process parameters including PE flow, aeration basin (AB) air flow, and NH_4^+ and NO_3^- concentrations in the aeration basins (Figure 3-4). Correlation coefficients are listed in Table A3. N_2O-N mass emission rates calculated from the aqueous analyzer very closely tracked the rates calculated from the gaseous analyzer. During the period that the gaseous analyzer was sampling gaseous emissions from the plant (Figure 3-5), a 66% average difference between estimated emissions from the aqueous and gaseous analyzers was observed. Thus, an adjustment factor of 0.66 was applied to emission estimates from the aqueous analyzer. This adjusted aqueous estimate was used to determine the N_2O emission factors and is the metric reported throughout the paper. During the period that the gaseous analyzer was sampling only the emissions from the membrane basins, it was estimated that 39% of total plant emissions were from the membrane basins and 61% were from the aeration basins. By using the sampling point

downstream of the odor control scrubbers, it was determined that the odor control system did not significantly impact N_2O emissions. The average concentration reported by the first aqueous probe, representative of anoxic zone conditions, was 0.025 mg N_2O-N L^{-1}. The average concentration reported by the second probe, representative of aerated zone conditions, was 0.040 mg N_2O-N L^{-1}. However, most N_2O emissions were stripped from the aqueous phase in aerated zones even if they were generated in anoxic zones, and only 4% of emissions were attributed to anoxic zones. Additionally, the MLE process recycles mixed liquor from the aerobic to anoxic zones, thus some dissolved N_2O likely gets transported back to the anoxic zones.

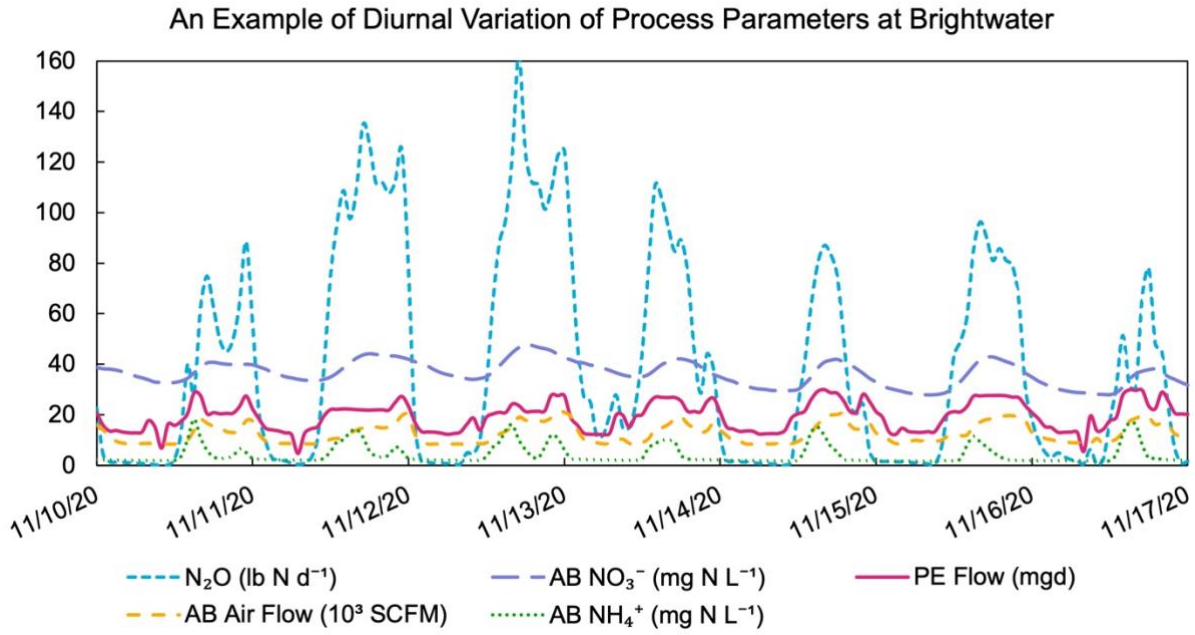

Figure 3-4. Process parameters demonstrating diurnal variation with N_2O. A representative 7-day period (November 10-17) was chosen to display data at high temporal resolution (hourly) to demonstrate diurnal variability.

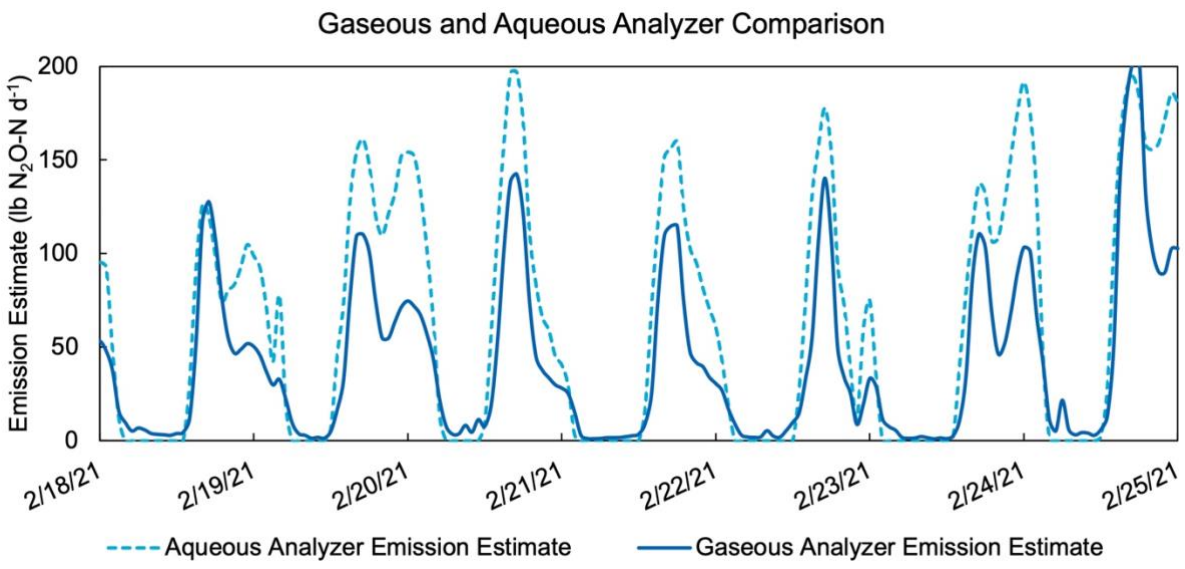

Figure 3-5. Discrepancy between aqueous and gaseous emission estimates while the gaseous analyzer sample was fully representative of both aeration and membrane basin emissions.

Since N_2O emission factor reporting has not been standardized, we report emission factors three different ways: based on influent nitrogen loading as TKN, TKN removal within the plant, and NH_4^+-N removal in the secondary processes. The average N_2O-N emission factor was 0.58% of influent TKN (standard deviation (SD) 0.33%), 0.60% of TKN removed (SD 0.34%), and 0.81% of NH_4^+-N removed (SD 0.47%), with an average daily emission of 46 lbs. N d^{-1} (SD 23 lbs. N d^{-1}) and 2.53 lbs. N $Mgal^{-1}$ (SD 1.6 lbs. N $Mgal^{-1}$). Extrapolating these emission factors to TKN loading data from 2019, an annual emission of 12.5 metric tons of N_2O per year was estimated. This equals 3700 metric tons of CO_2 equivalents per year. The different emission factors over the course of the monitoring period are displayed in Figure 3-6, and daily N_2O emissions are displayed in Figure 3-7.

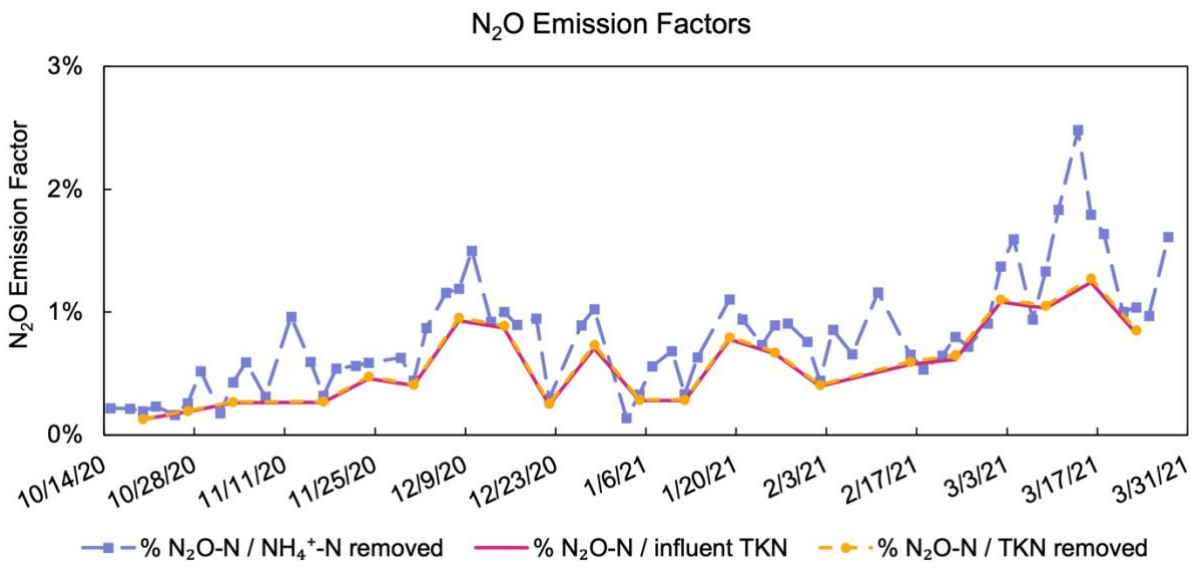

Figure 3-6. N_2O emission factors over the course of the monitoring period.

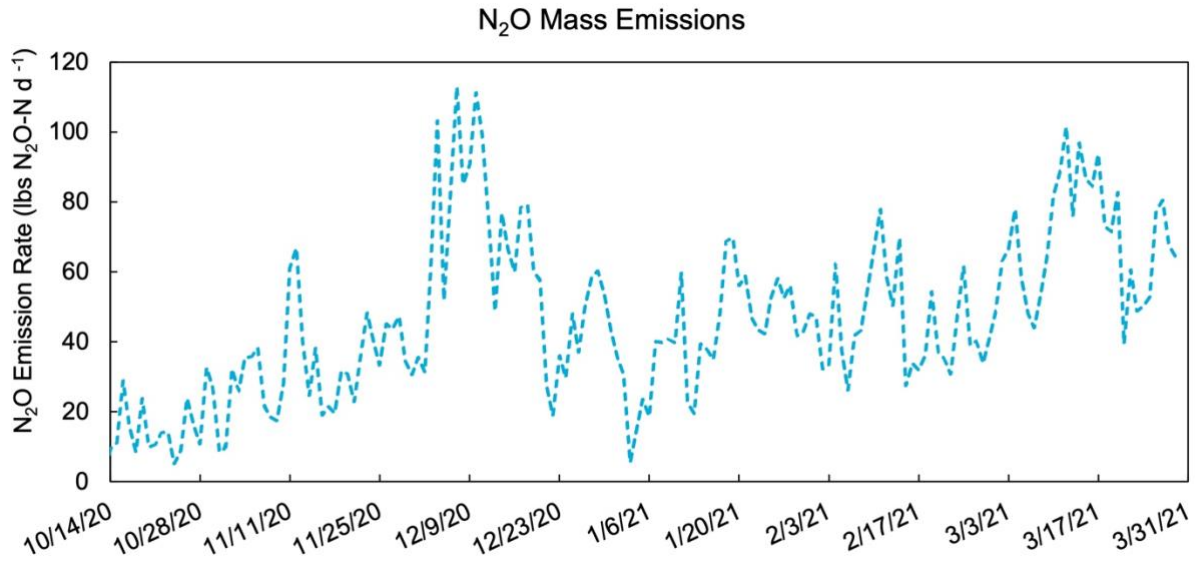

Figure 3-7. N_2O mass emissions over the course of the monitoring period.

3.4.2 Correlation Analysis

Spearman rank correlation was used on average daily data, and the correlation coefficients with an absolute value greater than 0.4 were determined to be correlated with N_2O emissions, and $p <$

0.05 was considered statistically significant. Process parameters demonstrating statistically significant correlation with N_2O are described in Table 3-2. Full correlation analysis results are summarized in Table A4.

Table 3-2. Process parameters demonstrating statistically significant correlation with N_2O emissions. Parameters demonstrated positive correlation with N_2O unless noted negative (-).

Sample Location	**Parameter**
Influent	pH
Primary Effluent	COD:N (-)
Aeration Basin	NH_4^+, NO_3^-, Nitrification Efficiency
Membrane Effluent	NH_4^+, NO_2^-+NO_3^-, pH (-)
Final Effluent	NO_2^-+NO_3^-

3.5 DISCUSSION

Brightwater's emission factor of 0.58% of influent TKN falls within the range of expected emission rates based on a monitoring survey of N_2O emissions from activated sludge processes in the US, with biological nitrogen removal (BNR) processes emitting 0.01 - 2.59% of influent TKN[10]. It falls below the IPCC emission factor of 1.6% for centralized, aerobic treatment plants, but within the reported range of .016 - 4.5%[90]. The median emission factor from a review of several MLE plants was 0.86% of the N-load[76], although factors as high as 4% of the N-load have been reported[86]. Brightwater's factor of 0.58% falls below this reported median.

3.5.1 Correlated Process Parameters

The relatively high standard deviations for the average emission factors demonstrate the high variability of N_2O emissions from the plant, which can also be observed in Figure 3-6. To

determine potential causes of this variability, it is of interest to investigate the results of the correlation analysis. Table 3-2 displays the process parameters that demonstrated statistically significant correlation with N_2O emissions, independent of diurnal variations in the plant.

The parameter that provides the most insight about N_2O production at Brightwater is the nitrification efficiency, which was estimated as the percent of PE TKN that was oxidized throughout the biological and membrane processes. The denitrification capacity of the plant was limited (with an average N removal efficiency of 30%), and no significant correlation between N_2O and denitrification efficiency was identified. Studies of BNR WRFs have often attributed major N_2O fluxes to nitrifier denitrification, but it is common that process configuration affects which pathway dominates emissions[76]. Brightwater's limited denitrification capability may have reduced the relevance of nitrifier denitrification to total plant emissions. Our results align with results from a pilot BNR MBR that found nitrification to be the major source of N_2O emissions[91]. While Brightwater's denitrification capacity was moderate (30%), nitrification was high, with the daily average efficiency ranging from 99.56% to 99.84% during the monitoring period. The nitrification efficiency correlated positively with N_2O emissions, and we conclude that these emissions can be attributed to the oxidation of NH_2OH that occurs during nitrification. However, if Brightwater were to develop more denitrification capacity in the future, the proportion of N_2O produced by denitrification may increase.

Correlation analysis between N_2O emissions and concentrations of nitrogen constituents throughout the plant revealed that influent and PE nitrogen loads were not significantly correlated with N_2O emissions. This indicates that conditions in the aeration and membrane basins were most relevant to elevated N_2O emissions, not simply high N-loading in general. Full results of the correlation analysis can be found in Appendix A4. Increased NO_2^- concentrations

have been widely linked to elevated N_2O emissions[7], however at Brightwater there is very little NO_2^- present. While the membrane and final effluent samples combine NO_2^- and NO_3^-, multiple grab samples revealed that the samples were on average 99% NO_3^-. Therefore, NO_2^- probably did not significantly affect N_2O emissions at Brightwater. The positive correlations between N_2O and NH_4^+ and NO_3^- concentrations in the aeration basin and effluent suggest that nitrification contributed the most to N_2O emissions.

pH has previously been positively correlated with N_2O because of nitrifiers' sensitivity to pH, with Nitrosomonas' optimal pH between approximately 7.0 and 8.0[92,93]. In our study, the range of influent pH was between 6.2 and 8.7, with an average of 7.4 (SD 0.25). Nitrifiers' pH sensitivity affects their nitrification capacity, although nitrification is inhibited both above and below their optimal range. In a study of NH_4^+ oxidation at different pH, oxidation rates at pH 7.0 were much higher than at pH 8.2 or 6.0[94]. Alkalinity is consumed during the nitrification process, which lowers pH. The theory of nitrification-driven emissions is supported by the positive correlation between N_2O emissions and influent pH, and the negative correlation with effluent pH (Table 3-2). Denitrification raises pH, so if the N_2O was from denitrification, a positive correlation with effluent pH would be expected. Our reported negative trend strengthens the conclusion that nitrification (not denitrification) was the major driver of N_2O emissions at the plant.

Another parameter that can influence N_2O emissions is the COD:N ratio, which averaged 5.4 at Brightwater. Increased N_2O emissions due to low COD:N ratio have been observed in wastewater treatment processes[87,95]. One study observed the same negative correlation in their MLE plant, and attributed it to the limitation of denitrification by lack of organic carbon availability[81]. Another MBR plant was operated at a COD:N ratio of 5 and reported that the

COD:N ratio indirectly increased pH and free ammonia concentration, inhibiting nitrifiers and promoting N_2O emissions because of stress on the nitrification pathway[91]. The denitrification process depends on NO_3^- produced from nitrification, so their simultaneous occurrence makes it difficult to distinguish which process produces more N_2O at a certain WRF. Additionally, N_2O measured in the aeration basin could be from the nitrification taking place or could be residual dissolved N_2O from denitrification in the anoxic basin. Thus, the positive correlation between the COD:N ratio and N_2O at Brightwater could be caused by either nitrification or denitrification, however our analysis still suggests that nitrification is the major source of N_2O emissions at the plant.

3.5.2 Analyzer Ease of Use

This study provided insight about gaseous and aqueous analyzer ease of use and the practicality of employing either analyzer at scale. The gaseous analyzer required significant infrastructure for use outdoors (Figure A5), was relatively cumbersome to get on-line, and had a few instances of freezing temperatures affecting sample collection. The gaseous analyzer has the capability to measure concentrations of 0-1000 ppm_V N_2O-N, and by choosing appropriate calibration gases the equipment was effective for the concentration range of the plant. The aqueous probes came from the manufacturer ready to install and had fewer obstacles during startup. This study used an aqueous probe with a measurement range of 0-1.5 mg N_2O-N L^{-1}, but at Brightwater the maximum concentration measured by either probe was 0.32 mg N_2O-N L^{-1}, so a probe with a range of 0-0.56 mg N_2O-N L^{-1} will be chosen for future studies. Once each analyzer was set up and installed, 24-hour on-line monitoring, calibration, and data download was achieved without major setbacks. Plant configuration and site-specific needs will ultimately determine which

analyzers are best suited for an emissions monitoring study. More detailed information about analyzer ease of use is available in Appendix A6.

3.5.3 Aqueous and Gaseous Monitoring Methodologies

Development of the aqueous and gaseous monitoring methodologies provided valuable insight about the feasibility of using these technologies at other plants. The aqueous method is more feasible for long-term N_2O monitoring at plants without fully covered processes. However, the gaseous analyzer proved crucial to our estimation of plant emissions by allowing the calculation of an adjustment factor. Aqueous probes can estimate plant emissions to a fair degree of reliability; however, the calculation that converts dissolved N_2O concentration (as measured by aqueous probes) to a mass emission rate relies on assumptions about gas exchange that stem from experiments in lab reactors, which are an imperfect representation of the complex fluid mechanics within full-scale treatment plants. Myers et al. (2021) determined that while the trend of N_2O emission estimates based on aqueous analyzers tracked well with gaseous measurements, the *magnitude* of N_2O emissions could not be accurately estimated without correction[78]. While our unadjusted aqueous estimate was on the same order of magnitude as the adjusted estimate, not applying the adjustment factor of 0.66 would have resulted in a nearly doubled emission, which would have significantly increased the plant's calculated carbon footprint. Additionally, determining an adjustment factor allowed our estimates to be highly process specific. While the calculation to convert dissolved N_2O to mass emissions relies on real-time temperatures and aeration rates, it does not account for downstream processes such as the membranes and membrane basins at Brightwater. A potentially significant source of N_2O in MBRs is from stripping due to agitation air to remove excessive biofilm from the membrane surfaces—a factor which the literature calculation does not account for. In fact, the finding that 39% of plant

emissions were from the membrane basins exemplifies the importance of accounting for downstream processes. Application of an adjustment factor could be beneficial for any plant that may emit N_2O from processes excluded from existing methodologies. For the majority of plants where gaseous sampling via a covered process is not possible, short-term monitoring using a floating hood and gaseous analyzer is recommended. If gaseous sampling via a covered process *is* possible, it is recommended that the dynamics of gas flow through the system are thoroughly understood, because even though Brightwater was fully covered, deliberate operation of specific foul air blowers was needed to achieve a fully representative sample.

3.6 CONCLUSION

After monitoring N_2O on-line for 5.5 months at a full-scale MBR, using both gaseous and aqueous methods, the main conclusions are:

- On average, 0.58% of influent TKN was emitted as N_2O-N—lower than the median emission factor of 0.86% from a review of MLE plants.
- The aqueous analyzer overestimated emissions. A factor of 0.66 was required to adjust the aqueous analyzer's value to match that of the gaseous analyzer, which we believe accurately measured emissions from the covered process.
- 39% of plant emissions were emitted in the membrane basins.
- Emissions were positively correlated with influent pH, NH_4^+ and NO_3^- in the aeration basins and effluent. They were negatively correlated with primary effluent COD:N ratio and effluent pH. Emissions were also correlated with nitrification efficiency, leading our speculation that nitrification was the major N_2O production pathway in the plant.

Chapter 4. SUSTAINABLE NITROGEN AND PHOSPHORUS REMOVAL: LIMITING NITROUS OXIDE EMISSIONS FROM A GRANULAR SLUDGE SEQUENCING BATCH REACTOR

4.1 ABSTRACT

Maximizing nutrient removal and minimizing greenhouse gas emissions are imperative for the future of wastewater treatment. A lab-scale sequencing batch reactor (SBR) was enriched with aerobic granular sludge (AGS) capable of phosphate removal and simultaneous nitrification-denitrification (SND). N_2O emissions were tracked at varying dissolved oxygen (DO) and nitrite (NO_2^-) concentrations, with >99% SND efficiency and 93%-100% phosphate removal efficiency. Higher DO and NO_2^- concentrations were associated with higher N_2O emissions. Emissions were minimized at a DO concentration of 1 mg L^{-1}, with an average emission factor of 0.18% of oxidized NH_3-N emitted as N_2O-N, which is lower than factors from many full-scale treatment plants[76] and similar to a Nereda® full-scale AGS SBR[96]. This challenges assertions that AGS emits more N_2O than conventional activated sludge. Molecular analyses revealed that the efficient SND was likely achieved with shortcut nitrogen removal facilitated by a low presence of nitrite oxidizing bacteria and a large population of denitrifying phosphate accumulating organisms, which far outnumbered denitrifying glycogen accumulating organisms. Implemented at full-scale, this technology has the potential to sufficiently remove nitrogen and phosphorus from wastewater while minimizing treatment plant greenhouse gas emissions.

4.2 INTRODUCTION

Nitrous oxide (N_2O) is a potent greenhouse gas with a Global Warming Potential approximately 300 times greater than an equivalent amount of carbon dioxide (CO_2) over a 100-year horizon[3]. This substantial warming potential makes N_2O a significant greenhouse gas that must be closely monitored and regulated in order to comprehensively address climate change[2]. Anthropogenic N_2O emissions account for approximately 40% of total emissions, which primarily originate from fertilizing agricultural soils, operating cattle feedlots, wastewater treatment, burning fossil fuels, and industrial processes like producing nitric acid[5]. Emissions from different wastewater treatment plants (WWTPs) are highly variable, with the IPCC potential emission factors for centralized, aerobic treatment plants ranging from 0.016% to 4.5% of influent nitrogen[6]. This indicates uncertainty about the contribution of WWTPs to total N_2O emissions, especially as nitrogen removal processes become mandated. Wastewater treatment systems are one of the few nitrogen cycling systems that are inherently engineered, meaning that they are a source of emissions that can be more readily controlled than other sources. N_2O is one of the main contributors to total greenhouse gas emissions from wastewater treatment systems (approximately 5 million metric tons of CO_2 equivalents per year in the US), meaning that minimizing plant emissions could significantly reduce their carbon footprint[5].

Additionally, nitrogen (as ammonia, nitrate, or nitrite) as well as phosphorus (as phosphate) in wastewater effluent contribute to eutrophication in receiving water bodies, which can lead to hypoxia and fish kills. In the US, nitrogen pollution is considered the most serious *coastal* pollution problem[18,19], and phosphorus is often the limiting (thus most important to control) nutrient in *freshwater* ecosystems, meaning minimizing concentrations of each in surface waters is essential to ecosystem health[97]. In recent years, WWTPs have begun exploring the use of

aerobic granular sludge (AGS) to meet heightened nitrogen and phosphorus removal requirements. AGS is a type of spherically-shaped biofilm that can minimize plant footprint and increase efficiency due to its fast settleability and dense microbial structure. Under aerated conditions, granules exhibit an oxygen penetration gradient, which allows simultaneous nitrification-denitrification (SND) and thus the potential for complete nitrogen removal. AGS can be enriched with phosphorus accumulating organisms (PAOs), which take phosphate from the bulk liquid under aerobic conditions, resulting in effluent with reduced phosphate levels[53]. PAOs most typically utilize oxygen for cell respiration, however they are capable of utilizing NO_3^-/NO_2^- as an electron acceptor in the absence of oxygen and are then termed denitrifying-PAO (DPAO), as both N and P are removed in the same process[51]. Glycogen accumulating organisms (GAO) also accumulate glycogen and polyhydroxyalcanoate (PHB) and can also denitrify under oxygen-limited conditions (DGAO)[98], but they cannot use phosphate for energy generation and therefore only contribute to N and C but not P removal. However, GAO compete with PAO for VFAs, so it is advantageous to select for a PAO dominated population to facilitate EBPR processes[99]. There are several laboratory studies measuring N_2O from granular sludge reactors, however operational parameters vary significantly from reactor to reactor, and it is of interest to investigate emissions from systems focusing specifically on nutrient removal. Aerobic granular sludge has three main N_2O emission pathways during wastewater treatment. During the first step of *nitrification* ammonia oxidizing bacteria (AOB) produce NH_2OH, which reacts with NO_2^- to form NO and N_2O. While this is usually a chemical oxidation reaction, recent research has shown that the reaction may proceed biologically by cytochrome P460 in N. *europaea* under anaerobic conditions[37] or mediated by the NH_2OH oxioreductase (HAO) enzyme under aerobic conditions[38]. Under anoxic conditions, AOB can also denitrify from NO_2^- to N_2O[80], which is

known as *nitrifier denitrification*. During *heterotrophic denitrification* (by organisms such as DPAOs and DGAOs), NO_2^- /NO_3^- are reduced to N_2 gas, with N_2O as one of the intermediates. There is evidence that GAO may emit more N_2O than GAO[61,62,100]. In a PAO-SND system, N_2O could be emitted via any of the three pathways. Recently, N_2O from a Nereda® full-scale granular sludge sequencing batch reactor in the Netherlands was measured, indicating the relevance of this continued research as granular sludge becomes more popular at full-scale[96].

In this study, a lab-scale sequencing batch reactor (SBR) was inoculated with AGS and operated for 329 days. Complete nitrification, denitrification, and phosphorus removal was achieved. Nutrient removal rates and N_2O emissions were tracked under varied dissolved oxygen (DO) and nitrite concentrations to determine how these process conditions impact N_2O emissions. Molecular techniques were employed to identify the microbial communities that dominated the system and to determine how they contributed to nutrient removal and N_2O emissions.

4.3 MATERIAL AND METHODS

4.3.1 Aerobic Granular Sludge Reactor

AGS was seeded from King County's pilot reactor at West Point Treatment Plant (Seattle, WA), which was enriched with phosphorus accumulating organisms (PAOs) and capable of SND during aeration. Granules were sampled from the mainstream SBR reactor as described by Figdore et al. (2018)[101]. A 3-L lab-scale reactor column was operated in anoxic-oxic sequencing batch reactor (SBR) cycles consisting of 5 minutes water filling, 20 minutes anaerobic idling, 5 minutes well-mixed anaerobic feeding, 60 minutes idling, 180 minutes aeration, 5 minutes settling, and 5 minutes decanting. The reactor was continuously mixed with N_2 gas during the anaerobic phase and air during the aerobic phase. pH was controlled at 7.5 with automatic dosing

of 1 M NaOH or 1 M HCl. Room temperature was controlled at 20°C. During the aeration phase, compressed air was added intermittently to control DO at 2.0 (± 0.2) mg O_2 L^{-1}. During the anaerobic phase, N_2 gas was added intermittently to keep DO at 0 mg O_2 L^{-1}. LabVIEW software (National Instruments, v.2014) was used for reactor instruments and controls. Two 10-L synthetic wastewater media were used, consisting of (A) 66.14 g $C_2H_3NaO_2$, 3.50 g KCl, 7.44 g K_2HPO_4, 2.96 g KH_2PO_4, and (B) 19.08 g NH_4Cl, 8.87 g $MgSO_4 \cdot 7H_2O$, and 100 ml "Vishniac and Santer" trace element solution[102]. The protocol for preparation of "Vishniac and Santer" solution is available in Appendix B1. During anaerobic feeding, 150 mL of each media was fed with 1250 mL deionized water, resulting in feed concentrations of 500 mg COD L^{-1}, 50 mg NH_4^+-N L^{-1}, and 20 mg PO_4^{3-}-P L^{-1}. With the settling time of 5 minutes and a decant height of 0.5 m, granules with settling velocity greater than 6 m hr^{-1} were retained in the reactor. The total decant volume was 1.5 L, corresponding with a volume exchange ratio of 50% each cycle. Each reactor cycle was 280 minutes long, resulting in 5.14 cycles per day, treating approximately 8 L of synthetic wastewater daily. A settled sludge bed volume of approximately 750 mL was controlled with weekly wasting, translating to a solids retention time (SRT) ranging from 65 to 95 days during the N_2O sampling period.

These process conditions served as the "baseline" for reactor operations and were varied according to the parameter being tested for N_2O emission response. To test the impact of DO during the aerobic phase, DO was controlled at either 2, 3, or 1 mg O_2 L^{-1}, with all other parameters maintaining baseline conditions. When DO was varied, the reactor was allowed to stabilize for approximately one week before measuring N_2O emissions, and the reactor was returned to DO 2 mg O_2 L^{-1} after triplicate sampling. For each test, the reactor was allowed to stabilize until nitrogen removal (ammonia oxidation and nitrate/nitrite reduction) was achieved,

with ammonium, nitrate, and nitrite concentrations nearing zero at the end of the aerobic phase. To test the impact of elevated nitrite concentrations, NO_2^- solutions were injected into the reactor at the beginning of the aerobic phase for reactor concentrations of 1 and 4 mg NO_2^--N L^{-1} and compared to emissions under baseline conditions (0 mg NO_2^--N L^{-1}).

4.3.2 N_2O Gas Analyzer

N_2O concentrations in the reactor's off-gas were measured on-line using a gas filter correlation (GFC) analyzer (Teledyne API T320). Gas in the reactor circulated at 2 liters per minute (LPM) using a diaphragm vacuum pump and aquarium stone at the bottom of the reactor column. This gas system was a closed loop, except for inputs from compressed air and N_2 and a one-way output for off-gas. When air or N_2 were added intermittently to maintain the DO setpoint, off-gas was analyzed by the GFC before exiting the system. The GFC's internal pump continuously sampled 0.892 LPM, so an inlet for sweep air was added, such that the GFC sampled ambient air when off-gas was not being emitted from the reactor. The reactor and analyzer setup is displayed in Figures B1-B3. The analyzer was calibrated according to the manufacturer's protocols. The baseline concentration of N_2O in ambient air is approximately 0.3 ppm, which the analyzer continuously sampled as sweep air, thus 0.3 was subtracted from every analyzer measurement. The emission factor calculation is available in Appendix B2.

4.3.3 Analytical Methods

Suspended and volatile solids (TSS and VSS) were analyzed weekly according to Standard Methods 2540D and 2540E[103]. Granule size distribution was tracked biweekly using test sieves between 212 and 2000 µm (ASTM E-11 Standard). Acetate concentrations at the end of the anaerobic idling period were periodically measured with the Dionex^{TM} ICS-5000$^+$ Capillary

HPIC™ System (Thermo Fischer Scientific). Nutrient concentrations in the reactor were sampled using cycle tests, in which grab samples were collected every 20 minutes during the 180 minute aerobic phase and analyzed for NH_3-N, PO_4^{3-}-P, NO_2^--N, and NO_3^--N. Cycle tests only consisted of data from the aerobic phase of the SBR cycle to avoid introducing oxygen into the system during anoxic phases and thus inadvertently encouraging the growth of heterotrophic bacteria. Ammonia (EPA Method 350.1)(ISO 7150), nitrite (EPA Method 254.1)(SM 4500-NO_2^-), nitrate (SM 4500-NO_3^-), and ortho-P (EPA Method 365.1)(SM 4500-P.E.) concentrations were measured using the Gallery™ Automated Photometric Analyzer (Thermo Fischer Scientific). Nitrate was measured indirectly by subtracting the nitrite concentration from the concentration of total oxidized nitrogen species.

4.3.4 Microbial Analyses

DNA extraction

Granules were sampled from the aerobic phase under baseline process conditions, transferred to 2 mL microtubes, and centrifuged at 15,000 rpm for 2 minutes in a Centrifuge 415D (Eppendorf, Germany). The supernatant was discarded, and the pellet was stored at -80°C. DNA was extracted from 95 – 105 mg of AGS using the DNeasy PowerBiofilm Kit (Qiagen, Germany) following the manufacturer's protocol with a few exceptions: a Bead Beater FastPrep®-24 Instrument (MP, USA) was used for the mechanical cell lysing step at 4 m s^{-1} for 20 s, and DNA samples were incubated with 200 µL of inhibitor removal solution (IRS) for 30 min. Initial DNA concentration and quality were examined spectrophotometrically by a NanoDrop 2000 (Thermo Fisher Scientific, Wilmington, DE).

16S rRNA gene sequencing

Extracted DNA was diluted with Ultrapure™ DNase/RNase-Free distilled water into the working concentration of 27 - 29 ng μL^{-1}. Samples were sequenced by MiSeq Systems (Illumina, sequencing lab: MRDNA, Texas). Each nucleotide sequence was filtered for quality, trimmed, merged, and analyzed using USEARCH software (Edgar 2010). After filtering for quality, an average of 4,405 reads were obtained for each sample. The taxonomic assignment of each nucleotide sequence was determined using the RDP Classifier v18[104]. The relative abundance of each taxon was calculated based on the number of reads belonging to that taxon per total number (ca. 4,405) of reads.

Quantitative polymerase chain reaction (qPCR)

DNA stock was further diluted with Ultrapure™ DNase/RNase-Free distilled water to a working concentration of 2 ng μL^{-1}. After dilution, the DNA working concentration was determined by Qubit™ dsDNA HS Assay kit (ThermoFisher Scientific, USA). The total qPCR reaction volume was 10 µL, consisting of 5 µL SensiFAST™ SYBR® No-ROX Kit 2X (BioLine, USA), 0.5 µL of each primer, and 4 µL DNA template. qPCR was performed with a Roche LightCycler 96 Instrument (Roche, Germany). qPCR reactions targeted the bacterial ammonia monooxygenase gene *amoA* (AOB), the bacterial nitrite oxidoreductase beta subunit gene *nxr*B (NOB), the 16S rRNA gene of *Candidatus* 'Accumulibacter phosphatis' (PAO), Competibacter (GAO), and the 16S rRNA gene of general bacteria (EUB). The qPCR thermal profiles started with 5 minutes heating at 94 ˚C, followed by 50 cycles of 94 ˚C for 10 seconds (s), 50-60 ˚C for 5-13 s, and 72 ˚C for 5-13 s. The complete qPCR protocol is available in Appendix B3, and information about the primers and annealing temperatures can be found in Table B4

Fluorescence in situ hybridization (FISH)

Granules were sampled from the aerobic phase under baseline process conditions and transferred to 2 mL microtubes and centrifuged at 15,000 rpm for 2 minutes in a Centrifuge 415D (Eppendorf, Germany). The supernatant was discarded, and the pellet was resuspended in 4% paraformaldehyde before incubating on ice for 120 minutes. The paraformaldehyde was washed off by centrifugation, removal of supernatant, and resuspension in 1 x PBS. The final resuspension was in an ethanol and PBS solution at 1.25:1 volumetric ratio and stored at -20 ºC. Granules were frozen in a tissue freezing medium at -20 ºC and cut into 20 µm slices using a cryostat (Thermo Scientific CryoStar NX50). Granule slices were adhered onto gelatin-coated microscopic glass slides with 8 wells. The granule slices were then dried at 46 ºC and dehydrated with subsequent (3 minutes each) 50%, 80%, and 98% ethanol concentrations. For each well, 10 µL of hybridization buffer solution was added, consisting of 5 M NaCl, 1 M Tris-HCl (pH 8.0), 35% (v/v) formamide, and 0.02% sodium dodecyl sulfate (SDS). Next, 1 µL of each probe mix (5 µM for Cy3/Cy5 and 8.3 µM for fluorescein-labelled probes) was added to each well. Table B7 lists the FISH probes used. The hybridization step took place in a humid chamber at 46 ºC overnight. Immediately after hybridization, slides were washed with a washing buffer (pre-heated to 48°C) consisting of 20 mM Tris-HCl (pH 8.0), 0.08 mM NaCl, 5 mM EDTA (pH 8.0) and 0.01% SDS. Washing was performed by first carefully flooding each well with washing buffer three times, then immersing the slide into the washing buffer for 15 minutes. Next, the slides were submerged in Milli-Q water for three minutes and air dried at room temperature. Antifade fluorescent mounting medium (20 mM Tris at pH 8.0, 0.5% N-propyl gallate, and 90% glycerol) was added to each well and covered with a cover slip. The complete FISH protocol is in Appendix B6. Slides were observed using a confocal microscope (Zeiss Axioskop 2 MOT)

fitted with a camera (Zeiss Axiocam 503 mono). Laser microscopy was performed using a Laser Scanning Microscope (LSM 5 Pascal version 4.2).

4.4 RESULTS

4.4.1 Reactor Performance

Under baseline conditions, the reactor consistently exhibited excellent simultaneous nitrification, denitrification, and phosphate removal. An average nitrification rate of 0.41 mg NH_3-N (g VSS L hr)$^{-1}$ (95% NH_3 oxidized) was achieved, and the average phosphate removal rate was 3.14 mg PO_4^{3-}-P (g VSS L hr)$^{-1}$ (97% of P present at the beginning of the aerobic phase removed). The average denitrification rate was high, with less than 0.1% of influent N remaining as nitrate or nitrite at the end of the aerobic phase. Since nitrification and denitrification took place simultaneously, with nitrate and nitrite being added and removed from the bulk liquid at the same time, it was not possible to measure specific denitrification rates in the reactor. However, SND efficiency, based on residual NO_2^- and NO_3^- remaining at the end of each cycle[105], was between 99% and 100% under baseline conditions and for each DO and NO_2^- test. 100% of COD (as acetic acid) was consistently consumed during the anaerobic phase (200 mg COD L^{-1} hr^{-1}), preventing COD breakthrough to the aerobic phase which can promote the growth of filamentous bacteria in the reactor. Reactor performance metrics are summarized in Table B8.

After initial stabilization (days 1-50), volatile suspended solids (VSS) increased from approximately 16 to 32 mg per mL of settled sludge. Granules exhibited the capability to rapidly increase in size under baseline reactor operation, with the percentage of granules measuring larger than 2000 μm increasing from 6% to 50% over the course of 73 days. Granule size

distribution over time is reported in Figure B7. The accumulation of large, dense granules allowed a high biomass to volume ratio (averaging 31 mg VSS mL^{-1}) in the reactor.

4.4.2 N_2O Emissions

Under long-term operation at DO 2 mg L^{-1} (baseline conditions) and normalized to an average reactor VSS of 23 grams, the N_2O emission rate averaged 0.52% (± 0.11%) of oxidized NH_3-N. Reported as a percent of influent NH_3-N emitted as N_2O-N, this rate equals 0.50% (± 0.10%).

N_2O Emissions at Varied DO Concentration

At different dissolved oxygen concentrations, nutrient removal and N_2O emission rates varied. While successful nitrogen and phosphorus removal was achieved at DO concentrations of 1, 2, and 3 mg O_2 L^{-1}, ammonia and phosphate removal rates and accumulation of NO_x in the middle of the aeration phase increased with increasing DO. At 1 mg O_2 L^{-1}, the average nitrification rate was 0.23 mg N (g VSS L hr)$^{-1}$, 83% NH_3-N removal was achieved, and phosphate removal rate was 2.81 mg P (g VSS L hr)$^{-1}$. At 2 mg O_2 L^{-1} these values were 0.41, 95%, and 3.14, respectively. At 3 mg O_2 L^{-1} the rates were 0.48 mg N (g VSS L hr)$^{-1}$, 99% NH_3-N removal, and 4.90 mg P (g VSS L hr)$^{-1}$. These rates are summarized in Table B8. The nutrient concentration profiles are displayed in Figure 4-1, with ammonia and phosphate removal rates increasing with increased DO, but accumulation of nitrate and nitrite also increasing with increased DO. N_2O emission rates at DO 1, 2, and 3 were 0.18% (± 0.06%), 0.52% (± 0.11%), and 1.65% (± 0.23%) of oxidized NH_3 respectively. This equals 9x greater emissions at DO 3 compared to DO 1. This positive emission trend with DO can be seen in Figure 4-2.

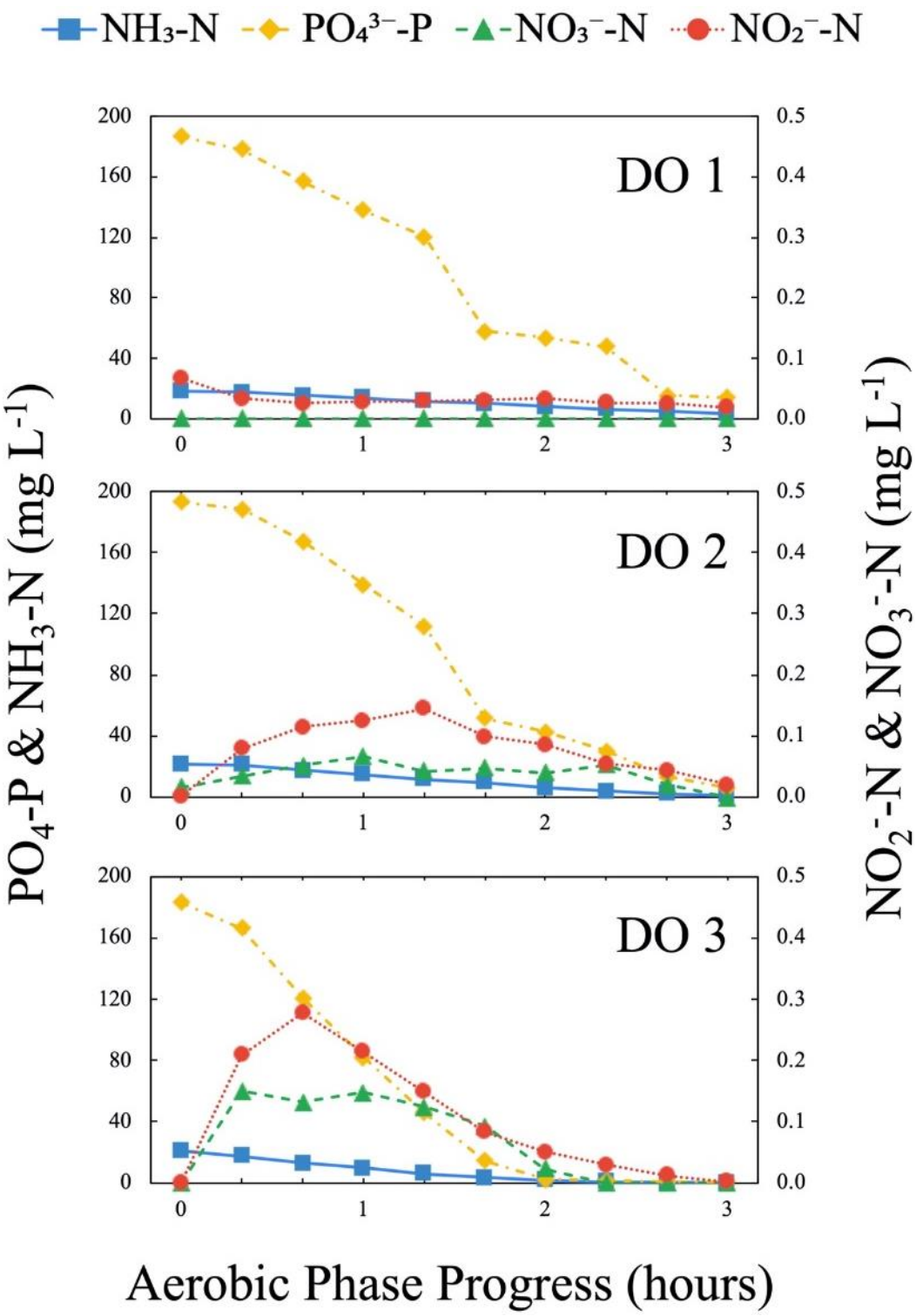

Figure 4-1. Aerobic phase nutrient concentration profiles at varied dissolved oxygen concentrations.

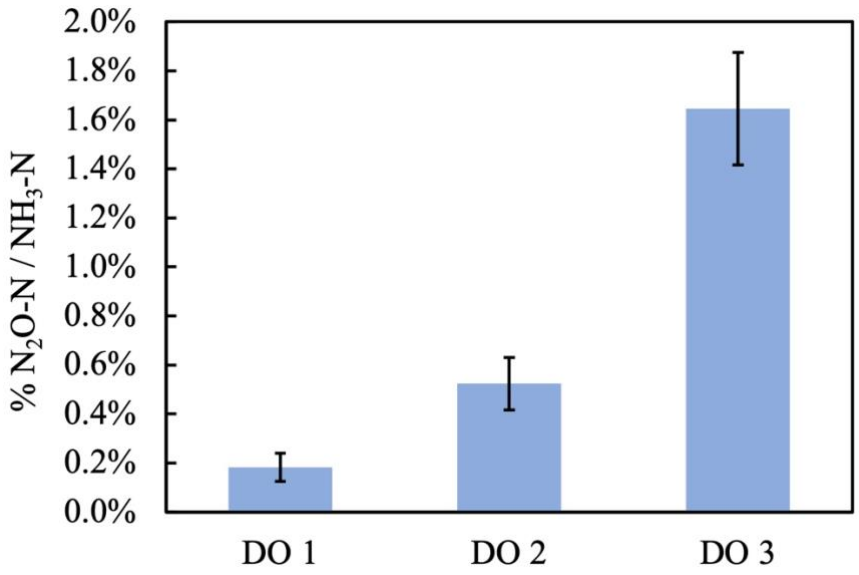

Figure 4-2. Percent of oxidized NH_3-N emitted as N_2O-N at dissolved oxygen concentrations of 1, 2, and 3 mg O_2 L^{-1}.

With Varied Nitrite Spike Concentrations

To test the impact of nitrite accumulation on N_2O emissions, nitrite spikes of differing concentrations were added to the reactor at the beginning of the aerobic phase. With nitrite spikes of 0, 1, and 4 mg N L^{-1}, the nitrification rates were 0.41, 0.34, and 0.26 mg N (g VSS L hr)$^{-1}$ respectively. The P-removal rates were 3.14, 3.35, and 3.20 mg P (g VSS L hr)$^{-1}$. These rates are summarized in Table B8. The nutrient concentration profiles can be seen in Figure 4-3. The N_2O-N emission factors increased as nitrite spike concentrations increased, from 0.52% with no nitrite spike to 0.68% at 1 mg NO_2^--N L^{-1} and 4.18% at 4 mg NO_2^--N L^{-1} (Figure 4-4). This amounts to 8x greater emissions at 4 mg NO_2^--N L^{-1} compared to baseline conditions with no nitrite spike.

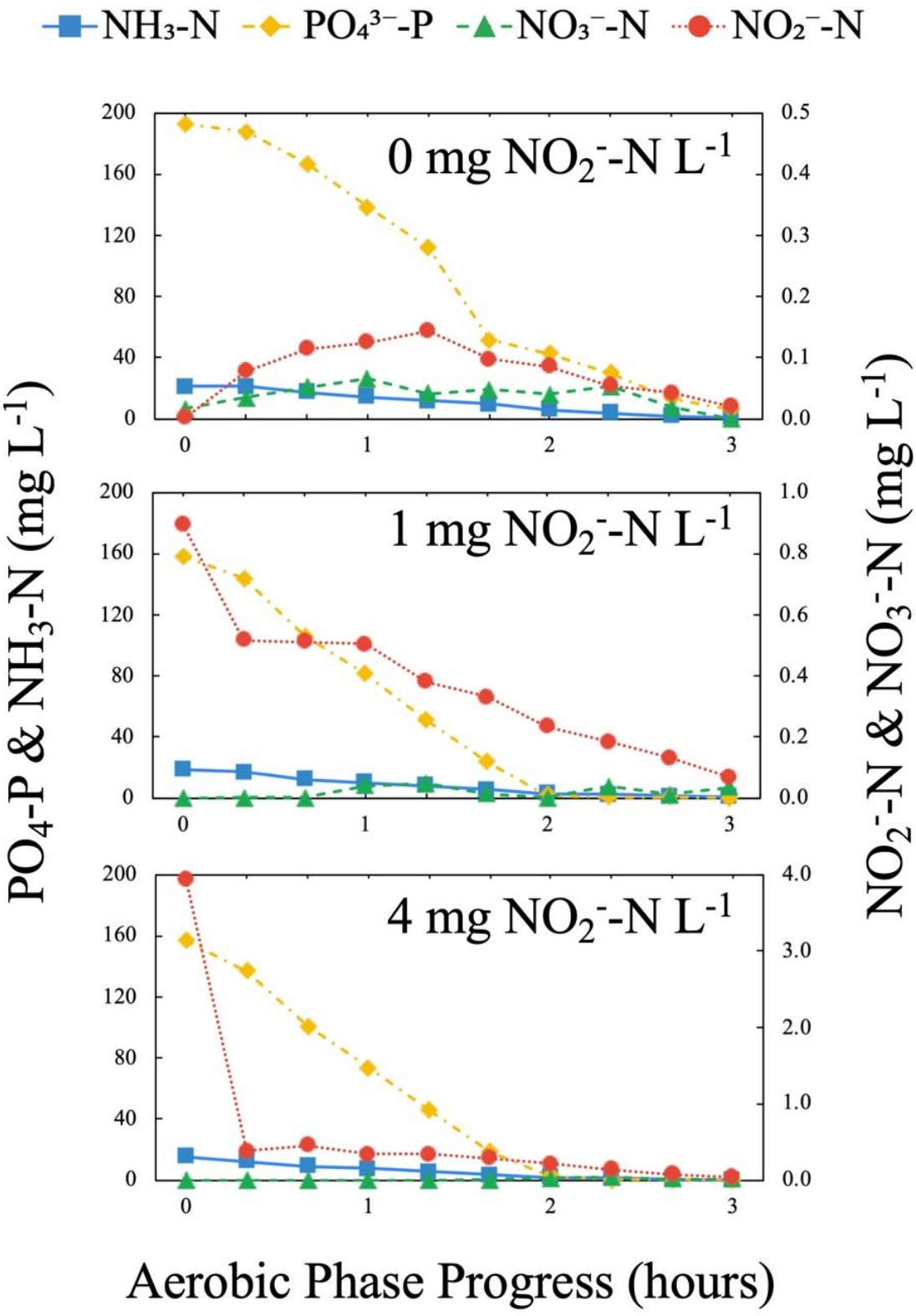

Figure 4-3. Aerobic phase nutrient concentration profiles for varied NO_2^- concentration spikes with DO controlled at 2 mg O_2 L^{-1}.

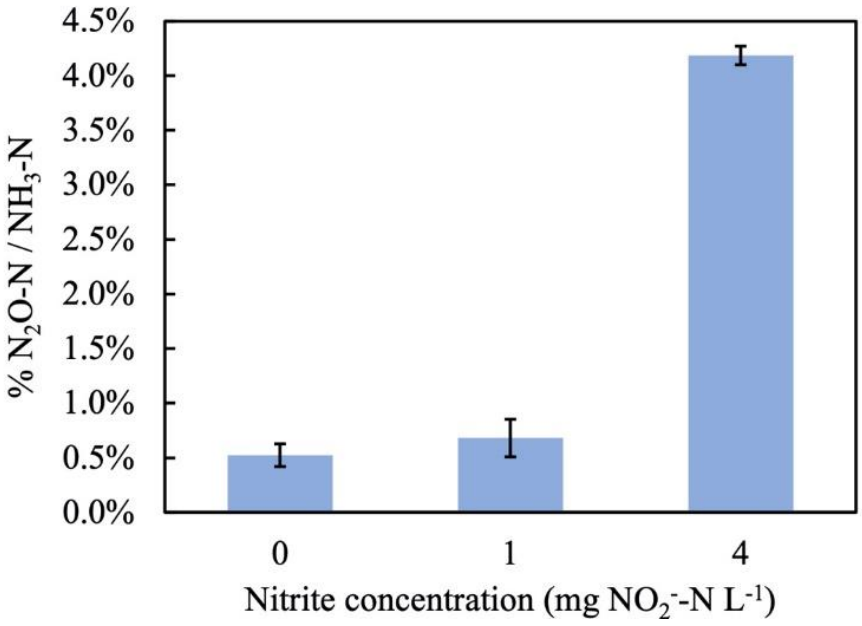

Figure 4-4. Percent of oxidized NH_3-N emitted as N_2O-N at differing NO_2^- concentrations at the beginning of the aerobic phase, with DO controlled at 2 mg O_2 L^{-1}.

4.4.3 Microbial Community

The genes selected to represent AOB, NOB, PAO, and GAO had an abundance of 7% (AOB), 5% (NOB), 14% (PAO), and 0.3% (GAO) of EUB. qPCR results are summarized in Figure 4-5.

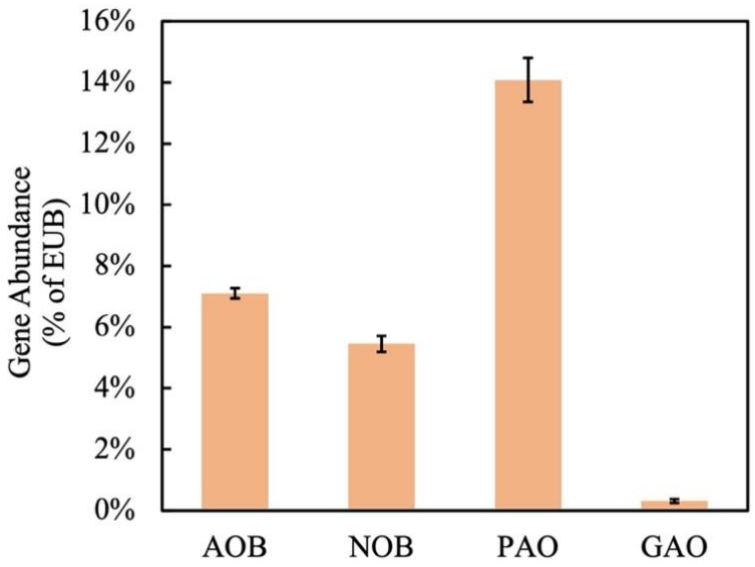

Figure 4-5. qPCR results for AGS under baseline conditions.

16S rRNA gene sequencing revealed that a few types of bacteria dominated the system. 16S data are available in Figure B4. A large proportion of the bacteria were unclassified *Rhodocyclales* (29.4%), which could potentially be denitrifying PAO[106,107]. *Nitrosomonas* (11.7%) were the dominant AOB, and the most prevalent denitrifier was *Pseudoxanthomonas* (11.9%)[108]. 7.3% were of the genus *Chryseobacterium*, which could potentially be capable of simultaneous heterotrophic nitrification and aerobic denitrification[109].

Two different stains were performed to investigate the spatial distribution of bacterial groups within the granules. Results can be seen in Figure 4-6, with color separated images in Figure B5.

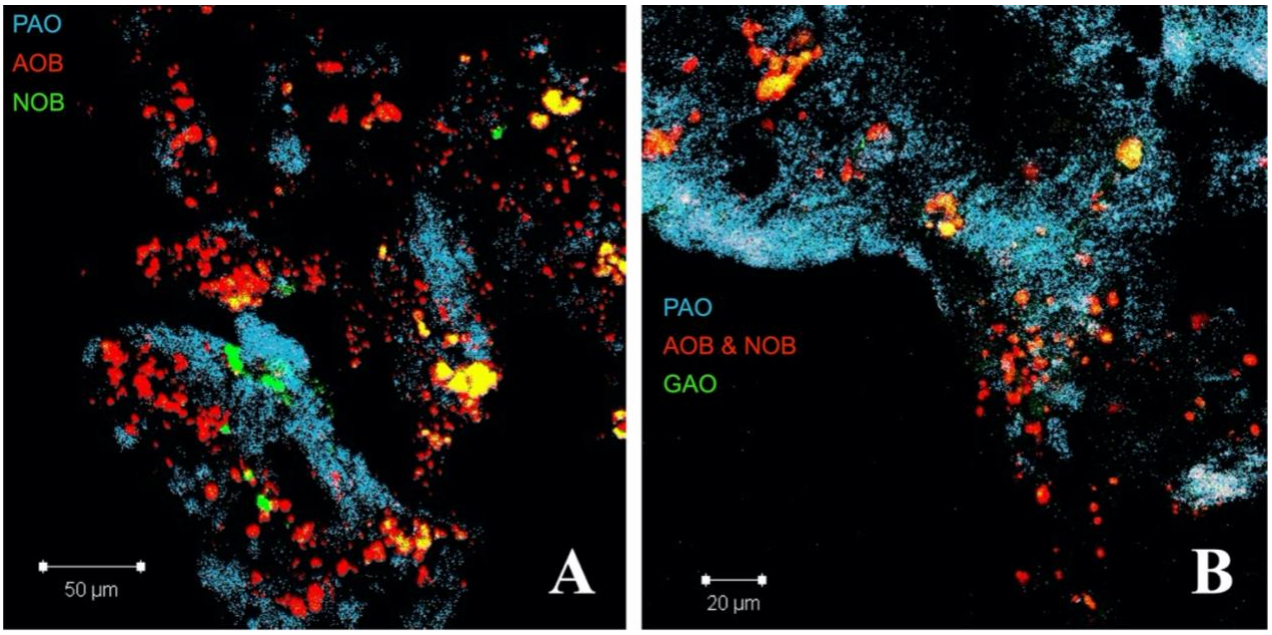

Figure 4-6. FISH imagery with PAO, AOB, and NOB displayed in A and PAO, AOB+NOB, and GAO in B.

4.5 DISCUSSION

4.5.1 Baseline N_2O Emissions

The average N_2O emission factor under baseline conditions (0.52% of oxidized NH_3-N) is in the range of reported emissions from laboratory reactors and full-scale treatment plants, which generally emit between 0% and 5% of influent nitrogen as N_2O[8]. However, our reported rate is low compared to many previous studies of AGS reactors, which report a wide range from 1%[110] to 22%[105]. It has previously been suggested that AGS may emit more N_2O than conventional activated sludge flocs because of incomplete denitrification to N_2O and not N_2 in the inner core of the granule[111]. In AGS aerobic bacteria are located on the oxygenated surface of granules, with nitrifiers at a depth of 70-100 µm, whereas denitrifiers dominate the anoxic inner core, growing as deep as at 800-900 µm into the granule interior[112–114]. While this spatial gradient can enable simultaneous nitrification-denitrification, it can also lead to elevated N_2O emissions

because there is no strict boundary between oxic and anoxic, which means the biofilm may not be conducive to distinct colonies of aerobic nitrifiers and anaerobic denitrifiers. Shi et al. (2011) reported an N_2O emission factor of 4.7% of nitrogen removed (emitted as N_2O-N) in their AGS reactor, which is higher than many emission factors from conventional activated sludge[115]. The only N_2O monitoring study of a full-scale AGS SBR reported an emission factor of 0.33% of influent total nitrogen from a Nereda® reactor in the Netherlands[96]. Our baseline emission factor (0.50% of influent nitrogen) is close to this reported full-scale emission factor. Our findings indicate that AGS can be implemented without greater N_2O emissions than other wastewater treatment technologies. To uncover the mechanisms that enabled this low-emission system, we investigated the reactor's response to varied process parameters and analyzed the microbial community that developed in the granules.

4.5.2 Emissions Response to Altered Process Conditions

In conventional activated sludge, low DO is generally associated with elevated N_2O emissions because of the introduction of the nitrifier denitrification pathway[116]. However, in our SND AGS we observed the opposite trend, with lower DO associated with lower emissions. In AGS systems with increased DO concentration, oxygen penetrates further into granules, which can lead to increased nitrification rates[117] and decreased denitrification rates[118]. In our reactor, nitrification rates and N_2O emissions increased with increased DO concentrations (Figures 4-1 and 4-2), thus the elevated N_2O could be attributed to higher activity of nitrifiers and the hydroxylamine oxidation pathway. However, the denitrification pathway can also be affected by altered DO concentration. While the simultaneous nature of nitrification and denitrification in our system made it cumbersome to directly measure denitrification rates in the reactor, the accumulation of nitrate and nitrite during the aerobic phase provides context about the nitrogen

removal dynamics. Accumulation of nitrate and nitrite during the aerobic phase of a SND reactor means that the denitrification rate is lagging behind the nitrification rate. This can be observed in Figure 4-1, DO 3, with some nitrite and nitrate accumulating in the middle of the aerobic phase before eventually being reduced. This accumulation of NO_x could be due to a heightened nitrification rate, which introduces an influx of electron acceptors and triggers an increased denitrification rate. Alternatively, NO_x accumulation could indicate that denitrification rate has decreased, so it is difficult to determine the activity of each pathway *in situ*. With the elevated nitrite spike tests, P-removal rates were relatively consistent, nitrification rate decreased, and N_2O emissions increased. The declining nitrification rates signify that nitrification was inhibited by elevated nitrite concentrations, and increased levels of N_2O were emitted because of increased nitrifier denitrification (NO_2^- reduction to N_2O)[74] or stress on denitrifiers, leading to incomplete denitrification and higher emission of N_2O[87]. At every DO concentration, NO_3^- and NO_2^- concentrations remained low (never exceeding 0.3 mg L^{-1}), so it is possible that efficient SND and the minimization of NO_2^- accumulation minimized N_2O emissions from our system.

Another explanation as to why lower DO was associated with lower emissions could be that maintaining lower DO requires less oxygen addition, thus the reactor experiences less gas stripping. Since the reactor was operated with a closed-loop gas system at atmospheric pressure, stripped gas only exited the system once additional oxygen was added to maintain DO. It is possible that some amount of gaseous N_2O circulated throughout the gas system and was eventually reduced by denitrifiers in the AGS. Future investigations using both aqueous and gaseous analyzers could explore this hypothesis.

4.5.3 Microbial Community

In PAO-SND AGS, N_2O may be emitted via any of the three main N_2O emission pathways (nitrification, heterotrophic denitrification, or nitrifier denitrification). Our reactor consistently had high rates of nitrification and denitrification, thus each pathway likely contributed some N_2O to total reactor emissions.

Nitrifiers

During the first step of nitrification ammonia oxidizing bacteria (AOB) produce NH_2OH, which reacts with NO_2^- to form NO and N_2O. Since our system was essentially fully-nitrifying, it is likely that this pathway contributed some N_2O to total emissions. A large population of nitrifiers was found with qPCR, with 7% of EUB identified as AOB (Figure 4-5). 16S revealed that the most prevalent AOB were *Nitrosomonas*, which are the most common AOB in conventional activated sludge[119]. FISH imagery (Figure 4-6A) revealed clusters of AOB without NOB nearby, signifying the presence of shortcut nitrogen removal (nitritation-denitritation), when AOB oxidize NH_3 to NO_2^- and denitrifiers immediately reduce this NO_2^- to NO, N_2O, and N_2, shortcutting the second step of nitrification usually completed by NOB. Shortcut nitrogen removal is attractive for wastewater treatment because compared to the complete nitrification-denitrification pathway, 25% less oxygen (and thus electricity) and 40% less carbon is needed[120]. It has been demonstrated that under carbon-limited conditions, shortcut nitrogen removal can have lower N_2O emissions than a conventional process, however the partial nitrification pathway may be more susceptible to shock loading conditions and accumulation of free ammonia[121], which can trigger N_2O production[122].

The qPCR primer used to identify NOB targeted the beta subunit of the *nxr*B gene (nitrite oxioreductase). This is the gene capable of oxidizing nitrite to nitrate, and is found in bacteria in many environmental systems[123] but this gene can also be operated in reverse and hence be indicative of heterotrophic denitrifiers. However, in our system *Nitrospira* and *Nitrobacter*, which are the NOB most frequently found in AGS systems[124], were not identified with 16S sequencing. The suppression of nitrite oxidizers has been utilized as a strategy to achieve full nitrogen removal via nitritation-denitritation (as opposed to complete nitrification-denitrification)[125], and it is possible that this suppression occurred in our system. While many NOB are obligate nitrifiers, some have mixotrophic capabilities[126]. Interpreting the 16S data, we suspect that *Chryseobacterium* (7.3% of classified bacteria) introduced the *nxr*B gene (5 % of EUB) to our system. *Chryseobacterium* have been identified in different types of environmental systems including swine wastewater treatment[127] and an EBPR SBR[128]. It has been suggested that certain *Chryseobacerium* species have a complete nitrification and denitrification pathway, with both nitrate and nitrite reductase[109]. However, this pathway remains speculative and further research on the organism is necessary to confirm this metabolism, but it is interesting to mention as a possible novel pathway. It is uncertain how active the nitrite oxidation pathway was in our system, since nitrate concentrations were consistently very low, and we suspect that the reactor had high levels of shortcut nitrogen removal (bypassing the need for nitrite oxidation).

Denitrifiers

Efficient SND and low concentrations of NO_x during the aerobic phase depended on a robust community of denitrifiers. With 14% of EUB quantified as PAO, we suggest that many of these organisms also performed denitrification. Under anaerobic conditions, PAO excrete intracellularly stored polyphosphate as orthophosphate (extracellularly) and use the gained

energy to accumulate polyhydroxyalkanoates (PHA) from volatile fatty acids (VFAs) in the bulk liquid. Under aerobic conditions, the stored PHA is metabolized, providing energy and carbon for cell growth. Intracellular polyphosphate is formed while removing orthophosphate from the bulk liquid[53]. PAO use oxygen as the terminal electron acceptor under oxygenated conditions, but can transition to using nitrate or nitrite as electron acceptor under oxygen-limited conditions, then termed denitrifying PAO (DPAO) with N and P removed in the same process[98]. Since the inner layers of granules do not have an abundant supply of O_2 to serve as electron acceptors, PAO found in these anoxic zones are likely DPAO. The metabolic plasticity of PAO can be observed in the FISH imagery (Figure 4-6B), with PAO growing throughout the granule, both at the oxygenated edge and into anoxic zones towards the granule core. The unclassified Rhodocyclales detected with 16S (29.4% of bacteria) were presumably PAO that could denitrify in oxygen-limited conditions[106,107]. Research has shown DPAO reactors may experience elevated N_2O emissions because of the inhibition of nitrous oxide reductase (*nos*Z) by nitrite that accumulates during denitrification[63], which could explain the significant N_2O response to nitrite spikes in our system.

GAO were investigated with molecular techniques because they compete with PAO for VFAs needed for growth and accumulate glycogen instead of phosphate, so they can be problematic for EBPR systems. Figure 4-6B demonstrates the distribution of PAO and GAO. The high PAO:GAO ratio (45.5) identified with qPCR is apparent in the imagery. Based on the COD consumed and P released during the reactor's anaerobic phase using the equation from López-Vázquez et al. (2007), the fraction of PAO (versus GAO) in the reactor was predicted to be approximately 80%[129]. The fraction observed with qPCR was approximately 98%. This very high ratio means that the EBPR capabilities of the system were very high, with PAO dominating

the system. GAO have also demonstrated denitrifying capabilities (DGAO) with similar mechanisms to DPAO[60]. It has been observed that DGAO can cause increased N_2O emissions[61,62,100], possibly because PHB consumption is the rate-limiting step for organisms growing on storage compounds[64]. However, it is also possible that the cited studies experienced elevated N_2O emissions solely from nitrite accumulation. Bassin et al. (2012) observed that DGAO were the main organisms responsible for the reduction of nitrate to nitrite in an AGS SBR[130], so low abundance of GAO may be because of the shortcut nitrogen removal pathway, in which nitrate levels remain low and a prominent DGAO community is not needed.

4.5.4 Mitigating Emissions

This system demonstrated that (spatially and temporally) efficient nitrogen and phosphorus removal is possible using a SND-PAO AGS SBR. Nitrite and dissolved oxygen concentration tests revealed that N_2O emissions can be minimized at low DO concentrations avoiding spikes of high nitrite concentrations. Low N_2O emissions at low DO is beneficial because the electricity needed by a WWTP is lower at lower DO setpoints, which could further reduce a plant's carbon footprint. Emissions were relatively low in this system, likely because of efficient SND and the presence of shortcut nitrogen removal aided by a robust community of DPAO. The factors that may have aided in the establishment of these communities include a long startup period with carefully ramped up feeding levels, a very long SRT (65-95 days), large granule size, and carefully controlled DO levels.

4.6 CONCLUSIONS

An aerobic granular sludge anoxic-oxic sequencing batch reactor achieved simultaneous nitrification, denitrification, and phosphate removal, and N_2O emissions were tracked in response to different DO and nitrite concentrations. The main findings were:

- N_2O emissions were minimized at DO 1, with 0.18% of oxidized NH_3-N emitted as N_2O-N. This emission factor is in the low range of reported values for wastewater treatment processes.
- N_2O emissions increased with increasing DO, with 9x greater emissions at DO 3 compared to DO 1.
- N_2O emissions increased with increased nitrite, with 8x greater emissions at 4 mg NO_2^--N L^{-1} compared to baseline conditions with no nitrite spike.
- Molecular analyses identified a microbial population capable of shortcut nitrogen removal performed by AOB and denitrifying PAO. The low levels of NOB and DGAO may have allowed the shortcut nitrogen removal pathway to dominate and enabled minimal N_2O emissions from the system.

Chapter 5. CONCLUSIONS

Climate change has become more and more apparent with events like extreme heat and flooding threatening people's lives and livelihoods. While there are several key industries that should be responsible for drastically reducing their GHG emissions, scientists and engineers must continue to investigate all areas of potential emissions mitigation, especially as insights from one industry may inform investigations across disciplines. As municipalities in the US manage tightening effluent discharge regulations and look forward to potential GHG emission regulations, investigating N_2O from wastewater treatment processes will be increasingly important.

5.1 KING COUNTY N_2O MONITORING

The 5.5-month N_2O monitoring campaign at Brightwater successfully quantified plant emissions and developed a methodology for N_2O monitoring at other King County WWTPs. To our knowledge, the study was the most comprehensive N_2O emissions monitoring of a full-scale, fully-covered MBR. This provides valuable information about emission factors, dynamics, and monitoring methodologies for other treatment plants looking to estimate or measure emissions. Key findings included an average emission factor of 0.58% of influent TKN emitted as N_2O-N, 39% of plant emissions exiting through the membrane basins, and correlation with many process parameters including nitrification efficiency. Additionally, insights about the practicality of employing aqueous and gaseous analyzers at full-scale were discussed.

After the campaign at Brightwater Treatment plant (Chapter 3), the N_2O analyzers were moved to King County's South Treatment Plant (Renton, Washington), a conventional activated sludge plant. Methods and lessons learned from Brightwater were implemented in emissions monitoring at South Plant, making progress toward the goal of eventually monitoring all of King County's

major WWTPs for N_2O emissions. It will be interesting to investigate how well the methodology from Brightwater transfers to other types of plants, and how emission factors vary from different plants in the same geographic region. Once completed, King County will have a precise understanding of the N_2O emissions from their wastewater treatment processes and will be able to determine how these emissions affect the county's carbon footprint goals.

Additionally, a second N_2O monitoring campaign at Brightwater will take place after implementation of a capital aeration basin optimization project. The project is planned to address issues including biological foaming and foam removal limitations in the aeration basins, limited SRT control, and limited aeration and DO control. The project will implement automated aeration/DO control via new actuated valves, and automated SRT control and improved foam control with a classifying selector. Aeration control will be implemented in two phases, with DO zone control at higher DO concentrations implemented first, followed by aeration control at lower DO concentrations to trial SND operation. Aeration control for SND will include two control modes, one for DO zone control and one for ammonium-based aeration control (ABAC). If successful, SND would allow nitrification and denitrification processes to occur in the same aerated reactor and will reduce caustic and aeration demands relative to current operations. As previously investigated, the current process only achieves approximately 30% denitrification efficiency, and introducing more denitrification introduces the potential for more N_2O from the denitrification pathway. However, studies have suggested that more uniform spatial DO profiles and the promotion of SND can mitigate N_2O emissions[10,131,132], so it is possible that the improvements at Brightwater may result in a smaller emission factor. Nonetheless, comparing emission values and relevant process parameters from each monitoring period (pre- and post-

aeration upgrades) will allow us to better understand N_2O emissions from nitrification, denitrification, and SND processes at full-scale.

5.2 EMISSIONS FROM AEROBIC GRANULAR SLUDGE

After operating the laboratory reactor for 11 months, many insights were gained about AGS, SBR reactors, and monitoring N_2O emissions at bench-scale. The reactor successfully achieved simultaneous nitrification, denitrification, and phosphate removal, and on-line monitoring of N_2O with an off-gas analyzer was achieved while closely controlling DO concentrations. The conclusions about positive N_2O emission trends in response to increased DO and NO_2^- concentrations are significant. These findings will build upon the literature understanding of how changing process parameters impact N_2O emissions in AGS. The insights about the generally low N_2O emissions (0.18% of NH_3-N emitted as N_2O-N at 1 mg O_2 L^{-1}) and subsequent molecular analyses serve to address high-level questions about how N_2O from WWTPs are minimized from a microbial population perspective.

These findings are relevant for municipalities considering implementing AGS at full-scale, as GHG emissions may be regulated in the future and wastewater treatment processes can impact local carbon neutrality goals. Recently, van Dijk et al. (2021) performed a study tracking N_2O emissions from a full-scale AGS SBR, indicating the continued relevance of research like the studies presented in this thesis. The findings were extremely promising for the future of AGS SBRs, since the reported N_2O emission levels were comparable to low-emitting conventional activated sludge plants and low compared to conventional SBR systems[96]. This indicates that it is possible to emit minimal amounts of N_2O while maximizing nutrient removal, all with a small plant footprint. This technology would especially be valuable in urban areas with limited space

availability. The results from the lab reactor (Chapter 4) aligned with these findings, with relatively low N_2O emissions compared to conventional activated sludge and previous studies of lab SBRs. However, it must be noted that some studies report high N_2O emissions from AGS[115] which conflict with the results obtained here. Nonetheless, the prospect that N_2O can be minimized while achieving high levels of nutrient removal is advantageous and indicates that in AGS SBR systems, nutrient removal and emissions mitigation may go hand in hand.

5.3 FUTURE WORK

Insights from this thesis demonstrate the relevance of continued research to better comprehend N_2O emissions from WWTPs. Potential future investigations include:

- Standardizing emissions monitoring methodologies at full-scale treatment plants, with updated protocols for various plant configurations and standardized emission factor reporting (e.g. emissions always reported as percent of influent TKN emitted as N_2O-N).
- Improving the methodology for the conversion of aqueous concentrations to predicted gaseous emission values. This would require more studies measuring N_2O in both the gaseous and aqueous phase, as well as investigation into the fluid mechanics and behavior of gases in the liquid vs. gas phase in full-scale plants.
- Further investigation into emissions from aerobic granular sludge at full-scale, as well as the impact of various process control parameters on emissions.
- Measuring emissions from other recently developed wastewater treatment technologies and processes, especially those designed for BNR.

- Considering impacts on carbon footprint when designing treatment processes and selecting treatment plant upgrades.

REFERENCES

1. *IPCC, 2013: Climate Change 2013: The Physical Science Basis. Contribution of Working Group I to the Fifth Assessment Report of the Intergovernmental Panel on Climate Change* [Stocker, T.F., D. Qin, G.-K. Plattner, M. Tignor, S.K. Allen, J. Boschung, A. Nauels, Y. Xia, V. Bex and P.M. Midgley (eds.)]. Cambridge University Press, Cambridge, United Kingdom and New York, NY, USA, 1535 pp.

2. IPCC, 2007: *Climate Change 2007: The Physical Science Basis. Contribution of Working Group I to the Fourth Assessment Report of the Intergovernmental Panel on Climate Change* [Solomon, S., D. Qin, M. Manning, Z. Chen, M. Marquis, K.B. Averyt, M. Tignor and H.L. Miller (eds.)]. Cambridge University Press, Cambridge, United Kingdom and New York, NY, USA, 996 pp.

3. IPCC, 2014: *Climate Change 2014: Mitigation of Climate Change. Contribution of Working Group III to the Fifth Assessment Report of the Intergovernmental Panel on Climate Change* [Edenhofer, O., R. Pichs-Madruga, Y. Sokona, E. Farahani, S. Kadner, K. Seyboth, A. Adler, I. Baum, S. Brunner, P. Eickemeier, B. Kriemann, J. Savolainen, S. Schlömer, C. von Stechow, T. Zwickel and J.C. Minx (eds.)]. Cambridge University Press, Cambridge, United Kingdom and New York, NY, USA. IPCC.

4. IPCC 2006, 2006 IPCC Guidelines for National Greenhouse Gas Inventories, Prepared by the National Greenhouse Gas Inventories Programme, Eggleston H.S., Buendia L., Miwa K., Ngara T. and Tanabe K. (eds). Published: IGES, Japan.

5. EPA, 2017. Inventory of U.S. Greenhouse Gas Emissions and Sinks: 1990-2017 -- Waste. (2017).

6. Nourmohammadi, D., Esmaeeli, M.-B., Akbarian, H. & Ghasemian, M. Nitrogen removal in a full-scale domestic wastewater treatment plant with activated sludge and trickling filter. *J. Environ. Public Heal.* **2013**, 504705 (2013).

7. Kampschreur, M. J., Temmink, H., Kleerebezem, R., Jetten, M. S. M. & van Loosdrecht, M. C. M. Nitrous oxide emission during wastewater treatment. *Water Res.* **43**, 4093–4103 (2009).

8. Vasilaki, V., Massara, T. M., Stanchev, P., Fatone, F. & Katsou, E. A decade of nitrous oxide (N_2O) monitoring in full-scale wastewater treatment processes: A critical review *Water Res.* 392–412 (2019). doi:10.1016/j.watres.2019.04.022

9. Daelman, M. R. J., van Voorthuizen, E. M., Van Dongen, L., Volcke, E. I. P. & Van Loosdrecht, M. C. M. Methane and nitrous oxide emissions from municipal wastewater treatment--results from a long-term study. *Water Sci. Technol.* **67**, 2350–2355 (2013).

10. Ahn, J. H. *et al.* N_2O Emissions from Activated Sludge Processes, 2008−2009: Results of a National Monitoring Survey in the United States. *Environ. Sci. Technol.* **44**, 4505–4511

(2010).

11. Bellandi, G. *et al.* Multi-point monitoring of nitrous oxide emissions in three full-scale conventional activated sludge tanks in Europe. *Water Sci. Technol.* **77**, 880–890 (2018).

12. IPCC 2019, 2019 Refinement to the 2006 IPCC Guidelines for National Greenhouse Gas Inventories, Calvo Buendia, E., Tanabe, K., Kranjc, A., Baasansuren, J., Fukuda, M., Ngarize, S., Osako, A., Pyrozhenko, Y., Shermanau, P. and Federici, S. (eds). Published: IPCC, Switzerland.

13. University of California Museum of Paleontology. Nitrogen - Understanding Global Change. (2018). Available at: https://ugc.berkeley.edu/background-content/nitrogen/.

14. EPA-MAIA - Nitrogen. Available at: https://web.archive.org/web/20030419211624/http://www.epa.gov:80/maia/html/nitrogen.html.

15. Galloway, J. N., Cowling, E. B., Seitzinger, S. P. & Socolow, R. H. Reactive Nitrogen: Too Much of a Good Thing? *https://doi.org/10.1579/0044-7447-31.2.60* **31**, 60–63 (2002).

16. Carpenter, S. R. *et al.* Nonpoint Pollution of Surface Waters with Phosphorus and Nitrogen. *Ecol. Appl.* **8**, 559–568 (1998).

17. Boyer, E. W., Goodale, C. L., Jaworski, N. A. & Howarth, R. W. Anthropogenic nitrogen sources and relationships to riverine nitrogen export in the northeastern U.S.A. *Biogeochemistry* **57**, 137–169 (2002).

18. Howarth, R. W. *et al.* Issues in ecology: Nutrient pollution of coastal rivers, bays, and seas. (2000).

19. Rabalais, N. N. Nitrogen in Aquatic Ecosystems. *Ambio A J. Hum. Environ.* **31**, (2002).

20. Lapointe, B. E. & O'Connell, J. Nutrient-enhanced growth of Cladophora prolifera in harrington sound, bermuda: Eutrophication of a confined, phosphorus-limited marine ecosystem. *Estuar. Coast. Shelf Sci.* **28**, 347–360 (1989).

21. Valiela, I. *et al.* Macroalgal blooms in shallow estuaries: Controls and ecophysiological and ecosystem consequences. *Limnol. Ocean.* **42**, 1105–1118 (1997).

22. Galloway, J. N. *et al.* The Nitrogen Cascade. *Bioscience* **53**, 341–356 (2003).

23. Seitzinger, S. P., Kroeze, C. & Styles, R. V. Global distribution of N_2O emissions from aquatic systems: natural emissions and anthropogenic effects. *Chemosph. - Glob. Chang. Sci.* **2**, 267–279 (2000).

24. Wolfe, A. H. & Patz, J. A. Reactive nitrogen and human health: acute and long-term implications. *Ambio* **31**, 120–125 (2002).

25. Aber, J. D. *et al.* Forest biogeochemistry and primary production altered by nitrogen saturation. *Water Air Soil Pollut.* **85**, 1665–1670 (1995).

26. Vitousek, P. M. *et al.* Human Alteration of the Global Nitrogen Cycle: Sources and Consequences. *Ecol. Appl.* **7**, 737–750 (1997).

27. Cowling, E. B., Erisman, J. W., Smeulders, S. M., Holman, S. C. & Nicholson, B. M. Optimizing air quality management in Europe and North America: Justification for integrated management of both oxidized and reduced forms of nitrogen. *Environ. Pollut.* **102**, 599–608 (1998).

28. Madigan, M. T., Bender, K. S., Buckley, D. H., Matthew Sattley, W. & Stahl, D. A. *Brock Biology of Microorganisms*. (Pearson, 2018).

29. Canfield, D. E., Glazer, A. N. & Falkowski, P. G. The evolution and future of Earth's nitrogen cycle. *Science (80-.).* **330**, 192–196 (2010).

30. Eady, R. R. Structure- function relationships of alternative nitrogenases. *Chem. Rev.* **96**, 3013–3030 (1996).

31. Zehr, J. P., Jenkins, B. D., Short, S. M. & Steward, G. F. Nitrogenase gene diversity and microbial community structure: a cross-system comparison. *Environ. Microbiol.* **5**, 539–554 (2003).

32. Bernard, S. M. & Habash, D. Z. The importance of cytosolic glutamine synthetase in nitrogen assimilation and recycling. *New Phytol.* **182**, 608–620 (2009).

33. Arp, D. J. & Stein, L. Y. Metabolism of inorganic N compounds by ammonia-oxidizing bacteria. *Crit. Rev. Biochem. Mol. Biol.* **38**, 471–495 (2003).

34. Hatzenpichler, R. Diversity, physiology, and niche differentiation of ammonia-oxidizing archaea. *Appl. Environ. Microbiol.* **78**, 7501–7510 (2012).

35. Leininger, S. *et al.* Archaea predominate among ammonia-oxidizing prokaryotes in soils. *Nature* **442**, 806–809 (2006).

36. Wuchter, C. *et al.* Archaeal nitrification in the ocean. *Proc. Natl. Acad. Sci. U. S. A.* **103**, 12317–12322 (2006).

37. Caranto, J. D., Vilbert, A. C. & Lancaster, K. M. Nitrosomonas europaea cytochrome P460 is a direct link between nitrification and nitrous oxide emission. *Proc. Natl. Acad. Sci.* **113**, 14704–14709 (2016).

38. White, C. J. & Lehnert, N. Is there a pathway for N_2O production from hydroxylamine oxidoreductase in ammonia-oxidizing bacteria? *Proc. Natl. Acad. Sci.* **113**, 14474–14476 (2016).

39. van Cleemput, O. Subsoils: chemo-and biological denitrification, N_2O and N_2 emissions. *Nutr. Cycl. Agroecosyst.* **52**, 187–194 (1998).

40. Daims, H., Lücker, S. & Wagner, M. A New Perspective on Microbes Formerly Known as Nitrite-Oxidizing Bacteria. *Trends Microbiol.* **24**, 699–712 (2016).

41. van Kessel, M. A. H. J. *et al.* Complete nitrification by a single microorganism. *Nature* **528**, 555–559 (2015).

42. Pjevac, P. *et al.* AmoA-Targeted Polymerase Chain Reaction Primers for the Specific Detection and Quantification of Comammox Nitrospira in the Environment. *Front. Microbiol.* **8**, 1508 (2017).

43. Delgado-Vela, J. Nitrogen and Sulfur Cycling During Wastewater Treatment. (2018).

44. Zumft, W. G. Cell biology and molecular basis of denitrification. *Microbiol. Mol. Biol. Rev.* **61**, 533–616 (1997).

45. Moreno-Vivián, C., Cabello, P., Mart\'\inez-Luque, M., Blasco, R. & Castillo, F. Prokaryotic nitrate reduction: molecular properties and functional distinction among bacterial nitrate reductases. *J. Bacteriol.* **181**, 6573–6584 (1999).

46. Einsle, O. *et al.* Structure of cytochrome c nitrite reductase. *Nature* **400**, 476–480 (1999).

47. Hino, T. *et al.* Structural basis of biological N_2O generation by bacterial nitric oxide reductase. *Science (80-.).* **330**, 1666–1670 (2010).

48. Zumft, W. G. & Kroneck, P. M. H. Respiratory transformation of nitrous oxide (N_2O) to dinitrogen by Bacteria and Archaea. *Adv. Microb. Physiol.* **52**, 107–227 (2007).

49. Wrage, N., Velthof, G. L., van Beusichem, M. L. & Oenema, O. Role of nitrifier denitrification in the production of nitrous oxide. *Soil Biol. Biochem.* **33**, 1723–1732 (2001).

50. Saito, T., Brdjanovic, D. & van Loosdrecht, M. C. M. Effect of nitrite on phosphate uptake by phosphate accumulating organisms. *Water Res.* **38**, 3760–3768 (2004).

51. Kerrn-Jespersen, J. P. & Henze, M. Biological phosphorus uptake under anoxic and aerobic conditions. *Water Res.* **27**, 617–624 (1993).

52. Kuba, T., Wachtmeister, A., Van Loosdrecht, M. C. M. & Heijnen, J. J. Effect of nitrate on phosphorus release in biological phosphorus removal systems. *Water Sci. Technol.* **30**, 263 (1994).

53. Satoh, H., Mino, T. & Matsuo, T. Uptake of organic substrates and accumulation of

polyhydroxyalkanoates linked with glycolysis of intracellular carbohydrates under anaerobic conditions in the biological excess phosphate removal processes. *Water Sci. Technol.* **26**, 933–942 (1992).

54. Gao, H. *et al.* Complete Nutrient Removal Coupled to Nitrous Oxide Production as a Bioenergy Source by Denitrifying Polyphosphate-Accumulating Organisms. *Environ. Sci. Technol.* **51**, 4531–4540 (2017).

55. Gao, H. *et al.* Genome-centric metagenomics resolves microbial diversity and prevalent truncated denitrification pathways in a denitrifying PAO-enriched bioprocess. *Water Res.* **155**, 275–287 (2019).

56. Miao, Z. *et al.* Effect of Free Nitrous Acid on Nitrous Oxide Production and Denitrifying Phosphorus Removal by Polyphosphorus-Accumulating Organisms in Wastewater Treatment. *Biomed Res. Int.* **2018**, 9192607 (2018).

57. Kuba, T., Murnleitner, E., van Loosdrecht, M. C. & Heijnen, J. J. A metabolic model for biological phosphorus removal by denitrifying organisms. *Biotechnol. Bioeng.* **52**, 685–695 (1996).

58. Lopez-Vazquez, C. M. *et al.* Modeling the PAO--GAO competition: Effects of carbon source, pH and temperature. *Water Res.* **43**, 450–462 (2009).

59. Crocetti, G. R., Banfield, J. F., Keller, J., Bond, P. L. & Blackall, L. L. Glycogen-accumulating organisms in laboratory-scale and full-scale wastewater treatment processes. *Microbiology* **148**, 3353–3364 (2002).

60. Oehmen, A., Carvalho, G., Lopez-Vazquez, C. M., van Loosdrecht, M. C. M. & Reis, M. A. M. Incorporating microbial ecology into the metabolic modelling of polyphosphate accumulating organisms and glycogen accumulating organisms. *Water Res.* **44**, 4992–5004 (2010).

61. Lemaire, R. *et al.* Identifying causes for N_2O accumulation in a lab-scale sequencing batch reactor performing simultaneous nitrification, denitrification and phosphorus removal. *J. Biotechnol.* **122**, 62–72 (2006).

62. Zeng, R. J., Lemaire, R., Yuan, Z. & Keller, J. Simultaneous nitrification, denitrification, and phosphorus removal in a lab-scale sequencing batch reactor. *Biotechnol. Bioeng.* **84**, 170–178 (2003).

63. Zeng, R. J., Yuan, Z. & Keller, J. Enrichment of denitrifying glycogen-accumulating organisms in anaerobic/anoxic activated sludge system. *Biotechnol. Bioeng.* **81**, 397–404 (2003).

64. JJ, B., K, D., MC, V. L. & JJ, H. Poly-beta-hydroxybutyrate metabolism in dynamically fed mixed microbial cultures. *Water Res.* **36**, 1167–1180 (2002).

65. Strous, M. *et al.* Missing lithotroph identified as new planctomycete. *Nature* **400**, 446–449 (1999).

66. Park, H., Rosenthal, A., Ramalingam, K., Fillos, J. & Chandran, K. Linking community profiles, gene expression and N-removal in anammox bioreactors treating municipal anaerobic digestion reject water. *Environ. Sci. Technol.* **44**, 6110–6116 (2010).

67. de Almeida, N. M. *et al.* Immunogold Localization of Key Metabolic Enzymes in the Anammoxosome and on the Tubule-Like Structures of Kuenenia stuttgartiensis. *J. Bacteriol.* **197**, 2432–2441 (2015).

68. van den Berg, E. M., Boleij, M., Kuenen, J. G., Kleerebezem, R. & van Loosdrecht, M. C. M. DNRA and Denitrification Coexist over a Broad Range of Acetate/N-NO3− Ratios, in a Chemostat Enrichment Culture. *Front. Microbiol.* **7**, 527 (2016).

69. Kraft, B. *et al.* Nitrogen cycling. The environmental controls that govern the end product of bacterial nitrate respiration. *Science (80-.).* **345**, 676–679 (2014).

70. Jia, M., Winkler, M. K. H. & Volcke, E. I. P. Elucidating the Competition between Heterotrophic Denitrification and DNRA Using the Resource-Ratio Theory. *Environ. Sci. Technol.* **54**, 13953–13962 (2020).

71. Van Niel, E. W. J., Arts, P. A. M., Wesselink, B. J., Robertson, L. A. & Kuenen, J. G. Competition between heterotrophic and autotrophic nitrifiers for ammonia in chemostat cultures. *FEMS Microbiol. Ecol.* **11**, 109–118 (1993).

72. Anderson, I. C., Poth, M., Homstead, J. & Burdige, D. A comparison of NO and N_2O production by the autotrophic nitrifier Nitrosomonas europaea and the heterotrophic nitrifier Alcaligenes faecalis. *Appl. Environ. Microbiol.* **59**, 3525–3533 (1993).

73. Bock, E., Schmidt, I., Stüven, R. & Zart, D. Nitrogen loss caused by denitrifying Nitrosomonas cells using ammonium or hydrogen as electron donors and nitrite as electron acceptor. *Arch. Microbiol.* **163**, 16–20 (1995).

74. Colliver, B. B. & Stephenson, T. Production of nitrogen oxide and dinitrogen oxide by autotrophic nitrifiers. *Biotechnol. Adv.* **18**, 219–232 (2000).

75. Kampschreur, M. J. *et al.* Effect of dynamic process conditions on nitrogen oxides emission from a nitrifying culture. *Environ. Sci. Technol.* **42**, 429–435 (2008).

76. Vasilaki, V., Massara, T. M., Stanchev, P., Fatone, F. & Katsou, E. A decade of nitrous oxide (N_2O) monitoring in full-scale wastewater treatment processes: A critical review. *Water Research* **161**, 392–412 (2019).

77. Baresel, C., Andersson, S., Yang, J. & Andersen, M. H. Comparison of nitrous oxide (N_2O) emissions calculations at a Swedish wastewater treatment plant based on water concentrations versus off-gas concentrations. *Adv. Clim. Chang. Res.* **7**, 185–191 (2016).

78. Myers, S., Mikola, A., Blomberg, K., Kuokkanen, A. & Rosso, D. Comparison of methods for nitrous oxide emission estimation in full-scale activated sludge. *Water Sci. Technol.* **83**, 641–651 (2021).

79. Jeff Foley; Zigou Yuan; Jurg Keller; Elena Senante; Kartik Chandran; John Willis; Anup Shah; Mark van Loosdrecht; Ellen van Voorthuizen. N_2O and CH_4 Emission from Wastewater Collection and Treatment Systems: State of the Science Report and Technical Report. *Water Intell. Online* **14**, (2015).

80. Poth, M. & Focht, D. D. 15N kinetic analysis of N_2O production by Nitrosomonas europaea: An examination of nitrifier denitrification. *Appl. Environ. Microbiol.* **49**, 1134–1141 (1985).

81. Spinelli, M. *et al.* Critical analyses of nitrous oxide emissions in a full scale activated sludge system treating low carbon-to-nitrogen ratio wastewater. *J. Clean. Prod.* **190**, 517–524 (2018).

82. Townsend-Small, A., Pataki, D. E., Tseng, L. Y., Tsai, C.-Y. & Rosso, D. Nitrous Oxide Emissions from Wastewater Treatment and Water Reclamation Plants in Southern California. *J. Environ. Qual.* **40**, 1542–1550 (2011).

83. Brightwater Treatment Process. *King County Department of Natural Resources and Parks Wastewater Treatment Division* (2018).

84. Aboobakar, A. *et al.* Nitrous oxide emissions and dissolved oxygen profiling in a full-scale nitrifying activated sludge treatment plant. *Water Res.* **47**, 524–534 (2013).

85. Sun, S. *et al.* Reduction and prediction of N_2O emission from an Anoxic/Oxic wastewater treatment plant upon DO control and model simulation. *Bioresour. Technol.* **244**, 800–809 (2017).

86. Foley, J., de Haas, D., Yuan, Z. & Lant, P. Nitrous oxide generation in full-scale biological nutrient removal wastewater treatment plants. *Water Res.* **44**, 831–844 (2010).

87. Schulthess, R. V & Gujer, W. Release of nitrous oxide (N_2O) from denitrifying activated sludge: Verification and application of a mathematical model. *Water Res.* **30**, 521–530 (1996).

88. Van Hulle, S. W. H. *et al.* Engineering aspects and practical application of autotrophic nitrogen removal from nitrogen rich streams. *Chemical Engineering Journal* **162**, 1–20 (2010).

89. Vasilaki, V., Volcke, E. I. P., Nandi, A. K., van Loosdrecht, M. C. M. & Katsou, E. Relating N_2O emissions during biological nitrogen removal with operating conditions

using multivariate statistical techniques. *Water Res.* **140**, 387–402 (2018).

90. Buendia, C. *et al. 2019 Refinement to the 2006 IPCC Guidelines for National Greenhouse Gas Inventories Task Force on National Greenhouse Gas Inventories*.

91. Mannina, G., Capodici, M., Cosenza, A., Di Trapani, D. & van Loosdrecht, M. C. M. Nitrous oxide emission in a University of Cape Town membrane bioreactor: The effect of carbon to nitrogen ratio. *J. Clean. Prod.* **149**, 180–190 (2017).

92. Hynes, R. K. & Knowles, R. Production of nitrous oxide by Nitrosomonas europaea: Effects of acetylene, pH, and oxygen. *Can. J. Microbiol.* **30**, 1397–1404 (1984).

93. Grady, C. P. L. & Lim, H. C. *Biological Wastewater Treatment*. (Marcel Dekker, 1980).

94. Princič, A., Mahne, I., Megušar, F., Paul, E. A. & Tiedje, J. M. Effects of pH and oxygen and ammonium concentrations on the community structure of nitrifying bacteria from wastewater. *Appl. Environ. Microbiol.* **64**, 3584–3590 (1998).

95. Chung, Y. C. & Chung, M. S. BNP test to evaluate the influence of C/N ratio on N_2O production in biological denitrification. in *Water Science and Technology* **42**, 23–27 (Int Water Assoc, 2000).

96. van Dijk, E. J. H., van Loosdrecht, M. C. M. & Pronk, M. Nitrous oxide emission from full-scale municipal aerobic granular sludge. *Water Res.* **198**, 117159 (2021).

97. Correll, D. Phosphorus: a rate limiting nutrient in surface waters. *Poult. Sci.* **78**, 674–682 (1999).

98. Oehmen, A., Carvalho, G., Freitas, F. & Reis, M. A. Assessing the abundance and activity of denitrifying polyphosphate accumulating organisms through molecular and chemical techniques. *Water Sci. Technol.* **61**, 2061–2068 (2010).

99. Winkler, M. K. H. *et al.* Selective sludge removal in a segregated aerobic granular biomass system as a strategy to control PAO–GAO competition at high temperatures. *Water Res.* **45**, 3291–3299 (2011).

100. Zeng, R. J., Yuan, Z. & Keller, J. Enrichment of denitrifying glycogen-accumulating organisms in anaerobic/anoxic activated sludge system. *Biotechnol. Bioeng.* **81**, 397–404 (2003).

101. Figdore, B. A., David Stensel, H. & Winkler, M. K. H. Bioaugmentation of sidestream nitrifying-denitrifying phosphorus-accumulating granules in a low-SRT activated sludge system at low temperature. *Water Res.* **135**, 241–250 (2018).

102. Vishniac, W. & Santer, M. The Thiobacilli. (1957).

103. APHA. Standard Methods for the Examination of Water and Wastewater. (2012).

104. Wang, Q., Garrity, G., Tiedje, J. & Cole, J. Naive Bayesian classifier for rapid assignment of rRNA sequences into the new bacterial taxonomy. *Appl. Environ. Microbiol.* **73**, 5261–5267 (2007).

105. Zhang, F. *et al.* Effect of operational modes on nitrogen removal and nitrous oxide emission in the process of simultaneous nitrification and denitrification. *Chem. Eng. J.* **280**, 549–557 (2015).

106. Wang, Z., Li, W., Li, H., Zheng, W. & Guo, F. Phylogenomics of Rhodocyclales and its distribution in wastewater treatment systems. *Sci. Reports 2020 101* **10**, 1–12 (2020).

107. Mehlig, L. *et al.* Biodiversity of Polyphosphate Accumulating Bacteria in Eight WWTPs with Different Modes of Operation. *J. Environ. Eng.* **139**, 1089–1098 (2013).

108. Finkmann, W., Altendorf, K., Stackebrandt, E. & Lipski, A. Characterization of N_2O-producing Xanthomonas-like isolates from biofilters as Stenotrophomonas nitritireducens sp. nov., Luteimonas mephitis gen. nov., sp. nov. and Pseudoxanthomonas broegbernensis gen. nov., sp. nov. *Int. J. Syst. Evol. Microbiol.* **50**, 273–282 (2000).

109. Kundu, P., Pramanik, A., Dasgupta, A., Mukherjee, S. & Mukherjee, J. Simultaneous Heterotrophic Nitrification and Aerobic Denitrification by Chryseobacterium sp. R31 Isolated from Abattoir Wastewater. *Biomed Res. Int.* **2014**, (2014).

110. Lochmatter, S., Maillard, J. & Holliger, C. Nitrogen Removal over Nitrite by Aeration Control in Aerobic Granular Sludge Sequencing Batch Reactors. *Int. J. Environ. Res. Public Heal. 2014, Vol. 11, Pages 6955-6978* **11**, 6955–6978 (2014).

111. Quan, X., Zhang, M., Lawlor, P. G., Yang, Z. & Zhan, X. Nitrous oxide emission and nutrient removal in aerobic granular sludge sequencing batch reactors. *Water Res.* **46**, 4981–4990 (2012).

112. Tay, T.-L., Ivanov, V., Yi, S., Zhuang, W.-Q. & Tay, J.-H. Presence of Anaerobic Bacteroides in Aerobically Grown Microbial Granules. *Microb. Ecol.* **44**, 278–285 (2002).

113. Adav, S. S., Lee, D. J., Show, K. Y. & Tay, J. H. Aerobic granular sludge: Recent advances. *Biotechnol. Adv.* **26**, 411–423 (2008).

114. Gao, D., Liu, L., Liang, H. & Wu, W.-M. Aerobic granular sludge: characterization, mechanism of granulation and application to wastewater treatment. *http://dx.doi.org/10.3109/07388551.2010.497961* **31**, 137–152 (2011).

115. Shi, Y.-J. *et al.* Aerobic granulation for nitrogen removal via nitrite in a sequencing batch reactor and the emission of nitrous oxide. *Bioresour. Technol.* **102**, 2536–2541 (2011).

116. Tallec, G., Garnier, J., Billen, G. & Gousailles, M. Nitrous oxide emissions from secondary activated sludge in nitrifying conditions of urban wastewater treatment plants:

Effect of oxygenation level. *Water Res.* **40**, 2972–2980 (2006).

117. Quoc, B. N. *et al.* Aerobic granular sludge: Impact of size distribution on nitrification capacity. *Water Res.* 116445 (2020).

118. Layer, M. *et al.* Limited simultaneous nitrification-denitrification (SND) in aerobic granular sludge systems treating municipal wastewater: Mechanisms and practical implications. *Water Res. X* **7**, 100048 (2020).

119. Daims, H. & Nielsen, P. *FISH Handbook for Biological Wastewater Treatmentnull*. (IWA Publishing, 2009).

120. Zhang, X., Zhang, D., He, Q., Ai, H. & Lu, P. Shortcut nitrification–denitrification in a sequencing batch reactor by controlling aeration duration based on hydrogen ion production rate online monitoring. *https://doi.org/10.1080/09593330.2013.871046* **35**, 1478–1483 (2014).

121. Hwang, S., Jang, K., Jang, H., Song, J. & Bae, W. Factors Affecting Nitrous Oxide Production: A Comparison of Biological Nitrogen Removal Processes with Partial and Complete Nitrification. *Biodegrad. 2006 171* **17**, 19–29 (2006).

122. Béline, F., Martinez, J., Chadwick, D., Guiziou, F. & Coste, C. M. Factors affecting Nitrogen Transformations and Related Nitrous Oxide Emissions from Aerobically Treated Piggery Slurry. *J. Agric. Eng. Res.* **73**, 235–243 (1999).

123. Daims, H., Lücker, S. & Wagner, M. A New Perspective on Microbes Formerly Known as Nitrite-Oxidizing Bacteria. *Trends Microbiol.* **24**, 699 (2016).

124. Winkler, M., Kleerebezem, R., Khunjar, W., de Bruin, B. & van Loosdrecht, M. Evaluating the solid retention time of bacteria in flocculent and granular sludge. *Water Res.* **46**, 4973–4980 (2012).

125. Paul Roots *et al.* Integrated shortcut nitrogen and biological phosphorus removal from mainstream wastewater: process operation and modeling. *Environ. Sci. Water Res. Technol.* **6**, 566–580 (2020).

126. Winkler, M.-K. H., Le, Q. H. & Volcke, E. I. P. Influence of Partial Denitrification and Mixotrophic Growth of NOB on Microbial Distribution in Aerobic Granular Sludge. *Environ. Sci. Technol.* **49**, 11003–11010 (2015).

127. Wang, N. *et al.* Enhanced sludge reduction during swine wastewater treatment by the dominant sludge-degrading strains Chryseobacterium sp. B4 and Serratia sp. H1. *Bioresour. Technol.* **330**, 124983 (2021).

128. Kämpfer, P., Dreyer, U., Neef, A., Dott, W. & Busse, H.-J. Chryseobacterium defluvii sp. nov., isolated from wastewater. *Int. J. Syst. Evol. Microbiol.* **53**, 93–97 (2003).

129. López-Vázquez, C. M., Hooijmans, C. M., Brdjanovic, D., Gijzen, H. J. & van

Loosdrecht, M. C. M. A practical method for quantification of phosphorus- and glycogen-accumulating organism populations in activated sludge systems. *Water Environ. Res.* **79**, 2487–2498 (2007).

130. Bassin, J. P., Kleerebezem, R., Dezotti, M. & van Loosdrecht, M. C. M. Simultaneous nitrogen and phosphate removal in aerobic granular sludge reactors operated at different temperatures. *Water Res.* **46**, 3805–3816 (2012).

131. Li, H. *et al.* N_2O generation and emission from two biological nitrogen removal plants in China. *New pub Balaban* **57**, 11800–11806 (2015).

132. Ribeiro, R. P. *et al.* The response of nitrous oxide emissions to different operating conditions in activated sludge wastewater treatment plants in Southeastern Brazil. *Water Sci. Technol.* **76**, 2337–2349 (2017).

APPENDIX A

Supplementary information for

Chapter 3:

Nitrous Oxide Emissions from a Full-Scale Membrane Bioreactor Treatment Plant Using Aqueous and Gaseous Monitoring Techniques

Number of pages: 21
Number of figures: 8
Number of tables: 4

Table of contents

A1. AQUEOUS ANALYZER: UNISENSE ENVIRONMENT A/S N_2O WASTEWATER SYSTEM

CALIBRATION

The aqueous N_2O analyzer was calibrated according to Unisense Environment A/S's procedure (Aarhus, Denmark). After initial calibration, the system was re-calibrated bimonthly. After installing the sensors, they were allowed to stabilize for at least 4 hours. First, a vessel was filled with 4 liters of tap water, with the tap water close to the temperature of the process water. The temperature of the tap water was measured (and recorded) and the sensor was placed in the bucket. After the sensor signal stabilized, the calibration was performed. This procedure was performed for each of the N_2O sensors.

Zero-point calibration: On the controller screen, check for a stable sensor signal. Press the grey lowest left "Operator" button (Password: 1234) to access the "Device menu." To begin calibration, follow the pathway: Calibration > N2O Sensor 1 > Two-point calibration. Press "OK" to enter the Reference input screen. Tap the blue number field to enter "0.000" and press "OK."

Stock solution calibration: Break the neck of the stock solution ampule. Immediately use the syringe and needle to slowly draw out 5 mL of the liquid. Inject the stock solution into the tap water bucket. Avoid allowing the stock solution to make contact with the air by injecting it underwater. Stir gently with the N_2O sensor. Right after the signal has stabilized, press the "OK" button. Tap the blue number field and enter "0.94." Enter the "Device menu" again. Access the "User level" to input the temperature of the tap water. For each sensor, enter the temperature of the water used for calibration and press "OK."

EMISSION CALCULATION

N_2O concentrations from the aqueous analyzer were converted to gaseous emission estimates following the protocol of Unisense Environment A/S.

First, the N_2O mass transfer coefficient was calculated based on aeration field size and air flow.

$$v_g \cong \frac{Q_A}{\text{Aeration field size}} \qquad \textbf{(1.1)}$$

Then, the N_2O mass transfer coefficient was calculated using the temperature compensated N_2O concentration in the aerated reactor and the calculated superficial gas velocity.

$$k_L a_{N_2O\ 20°C} = \left\{\frac{D_R}{D_L}\right\}^{-0.49} \times 34500 \times (v_g)^{0.86} \qquad \textbf{(1.2)}$$

$$k_L a_{N_2O\ 20°C} = \left\{\frac{D_R}{0.815\ \text{m}}\right\}^{-0.49} \times 34500 \times (v_g)^{0.86} \qquad \textbf{(1.3)}$$

$$k_L a_{N_2O\ T_{Process}} = k_L a_{N_2O\ 20°C} \times (1.024)^{(T_{Process} - 20°C)} \qquad \textbf{(1.4)}$$

Where v_g: superficial gas velocity $(m^3/m^2 s)$
Q_A: Total air flow for the aerated reactor (m^3/s)
D_R: Depth over the diffuser of the reactor (m)
D_L: Depth of the laboratory reactor (0.815 m)
$k_L a_{N_2O\ 20°C}$: N_2O mass transfer coefficient from lab experiments at 20°C (d^{-1})[1]
$k_L a_{N_2O\ T_{Process}}$: N_2O mass transfer coefficient corrected to $T_{Process}$ (d^{-1})
$T_{Process}$: Process temperature (°C)

With the temperature compensated N_2O mass transfer coefficient known, the N_2O emission rate per reactor volume (either aerated or non-aerated) could be calculated using equations 2 and 3[2].

$$\text{Aerated zones: } r_{N_2O,T_{Process}} = H_{N_2O,T_{Process}} \times S_{N_2O} \left[1 - e^{-\frac{k_L a_{N_2O}}{H_{N_2O}} \times \frac{v_R}{Q_A}}\right] \times \frac{Q_A}{V_R} \quad (\mathbf{2})$$

$$\text{Non-aerated zones: } r_{N_2O,T_{Process}} = k_L a^{\text{Non-aerated}}_{N_2O,\,T_{Process}} \left[S_{N_2O} - \frac{C_{N_2O,air}}{H_{N_2O,\,T_{Process}}}\right] \quad (\mathbf{3})$$

Where $r_{N_2O,T_{Process}}$: N_2O emission rate $(g-N\ N_2O/m^3\ d)$
$H_{N_2O,T_{Process}}$: Henry's constant (dimensionless)
S_{N_2O}: N_2O concentration $(g-N\ N_2O/m^3)$
Q_A: Total air flow through reactor per day (m^3/d)
V_R: Volume of aerated part of reactor (m^3)
$k_L a_{N_2O}$: N_2O mass transfer coefficient $(1/d)$
$C_{N_2O,air}$: N_2O concentration in air equilibrium $(g-N/m^3)$

The dimensionless Henry's constant is also dependent on process temperature, so the temperature correction is calculated using equations 4.1 - 4.2.

$$H_{N_2O,T_{Process}} = \frac{1}{k_H \bullet R \bullet (T_{Process}+273.15) \bullet 10^3 \frac{L}{m^3}} \quad (\mathbf{4.1})$$

$$k_H = k_H{}^{\theta} \times e\text{^}\left(\frac{-\Delta solnH}{R}\left(\frac{1}{T_{Process}+273.15} - \frac{1}{T^{\theta}+273.15}\right)\right) \quad (\mathbf{4.2})$$

---

[1] Foley, J., de Haas, D., Yuan, Z. & Lant, P. Nitrous oxide generation in full-scale biological nutrient removal wastewater treatment plants. *Water Res.* **44**, 831–844 (2010).

[2] Schulthess, R. V & Gujer, W. Release of nitrous oxide (N_2O) from denitrifying activated sludge: Verification and application of a mathematical model. *Water Res.* **30**, 521–530 (1996).

Where k_H^{θ}: Henry's constant at the standard temperature ($mol/L \bullet bar$)
T^{θ}: Standard temperature = 25℃
$T_{Process}$: Mixed liquor temperature (℃)
$-\Delta solnH/R$: The enthalpy of the solution (K)

From literature, the following constants are given:

k_H^{θ}	$\frac{-\Delta solnH}{R}$	$C_{N_2O,air}$	R	$k_L a$ Non − aerated $N_2O, T_{Process}$
($mol/L \bullet bar$)	(K)	($g-N/m^3$)	($m^3 \bullet bar/mol \bullet K$)	($1/d$)
0.0247	2675	.0003	8.314×10^{-5}	- 4

A2. GASEOUS ANALYZER: TELEDYNE AI GFC 7002T N_2O ANALYZER

CALIBRATION
This protocol is adapted from the Teledyne Operation Manual Model GFC 7002T / GFC 7002TU N_2O Analyzer Section 9 Calibration Procedures.

Calibration Preparations
The calibration procedures in this section assume that the range mode, analog range and units of measure have already been selected for the analyzer. If this has not been done, please do so before continuing.

- Delivering span and zero gases for the higher resolution the GFC 7002T / GFC 7002TU can be difficult. Attention must be paid to the quality of the gases, the level of contaminants in the gases as well as the history and conditioning of the gas delivery components.
- The analyzer must be continually operating with and adequate flow of sample gas, for 2 hours prior to performing a calibration (12 hours is recommended for the initial calibration).
- DO NOT calibrate the analyzer if it has been turned off or if no sample gas has been flow though it within the last 2 hours.
- After this stabilization period is complete and just prior to performing the initial calibration, force the instrument to perform an auto-reference measurement.

Required Equipment, Supplies, and Expendables
Calibration of the GFC7002T / GFC7002TU Analyzer requires specific equipment and supplies. These include, but are not limited to, the following:

- Gas lines to and from the analyzer should be PTFE or FEP Teflon, glass, or stainless steel only. Zero-air source which must be synthetic air, ultra-zero air or nitrogen (N_2). A zero air generator like a T-API M701 should not be used.

- Span gas source (defined below).
- A recording device such as a strip-chart recorder and/or data logger (optional). Data recording device should be capable of bi-polar operation so that negative readings can be recorded.
- For electronic documentation, the internal data acquisition system can be used.

Zero Air

Zero air or zero calibration gas is defined as a gas that is similar in chemical composition to the measured medium but without the gas to be measured by the analyzer.

For the GFC7002T/GFC7002TU zero air should contain less than 25 ppb of N_2O and other major interfering gases such as water vapor. It should have a dew point of -5°C or less.

If your application is not a measurement in ambient air, the zero calibration gas should be matched to the composition of the gas being measured. Pure nitrogen (N_2) can be used as a zero gas for applications where N_2O is measured in nitrogen.

Span Gas

Span Gas is a gas specifically mixed to match the chemical composition of the type of gas being measured at near full scale of the desired measurement range. It is recommended that the span gas used have a concentration equal to 80-90% of the full measurement range.

If Span Gas is sourced directly from a calibrated, pressurized tank, the gas mixture should be N_2O mixed with Zero Air or N_2 at the required ratio.

For oxygen measurements using the optional O_2 sensor, we recommend a reference gas of 21% O_2 in N2.

- For quick checks, ambient air can be used at an assumed concentration of 20.8%.
- Generally, O_2 concentration in dry, ambient air varies by less than 1%. 9.1.1.3.

Calibration Gas Standards and Traceability

All equipment used to produce calibration gases should be verified against standards of the National Institute for Standards and Technology (NIST). To ensure NIST traceability, we recommend to acquire cylinders of working gas that are certified to be traceable to NIST Standard Reference Materials (SRM). These are available from a variety of commercial sources.

Note*:* It is generally a good idea to use 80% of the reporting range for that channel for the span point calibration.

For instance, if the reporting range of the instrument is set for 50.0 PPM, the proper span gas would be 40.0 PPM.

Data Recording Devices

A strip chart recorder, data acquisition system or digital data acquisition system should be used to record data from the serial or analog outputs of the GFC7002T / GFC7002TU.

- If analog readings are used, the response of the recording system should be checked against a NIST traceable voltage source or meter.
- Data recording devices should be capable of bi-polar operation so that negative readings can be recorded.
- For electronic data recording, the GFC7002T / GFC7002TU provides an internal data acquisition system (DAS). APICOM, a remote control program, is also provided as a convenient and powerful tool for data handling, download, storage, quick check and plotting.

Manual Calibration

Note: *Impact on Readings or Data Zero/Span Calibration Checks Vs. Zero/Span Calibration:* Pressing the ENTR button during the following procedure resets the stored values for OFFSET and SLOPE and alters the instrument's Calibration.

This should ONLY BE DONE during an actual calibration of the GFC7002T / GFC7002TU.

NEVER press the ENTR button if you are only checking calibration. If you wish to perform a calibration CHECK, do not press ENTR.

Setup For Basic Calibration Checks And Calibration

Step One: Connect the Sources of Zero Air and Span Gas as shown below

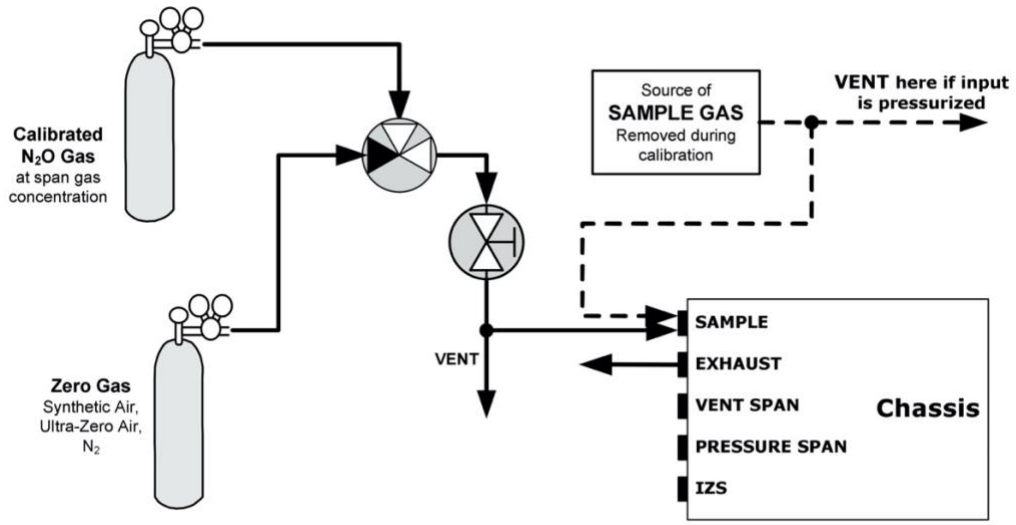

Figure A1. Pneumatic connections using bottled span gas

Performing a Basic Manual Calibration Check

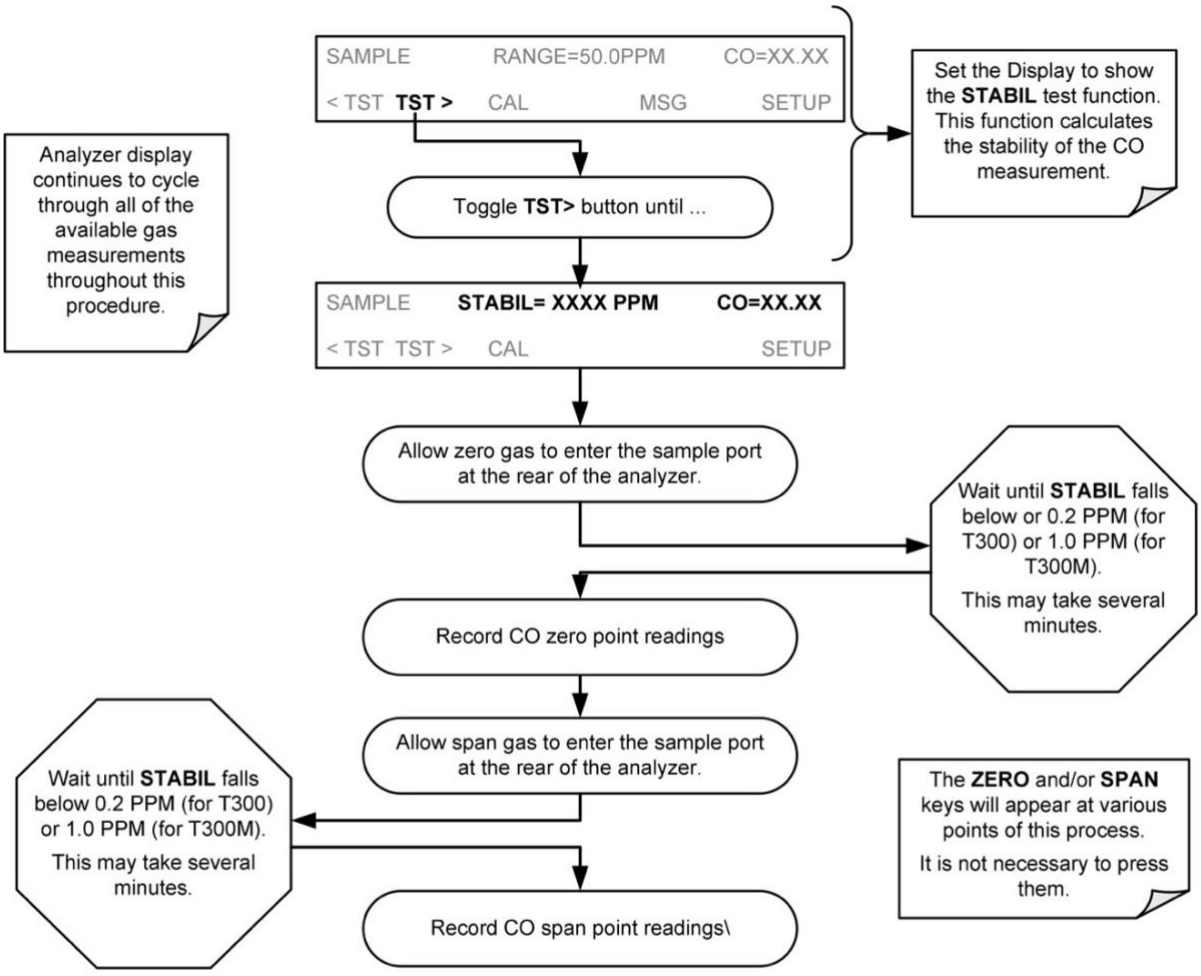

Note: The above screen(s) show CO concentration displayed. Your instrument will indicate and display N_2O concentration.

Figure A2. Performing a basic manual calibration check

The following section describes the basic method for manually calibrating the GFC7002T / GFC7002TU.

If the analyzer's reporting range is set for the AUTO range mode, a step will appear for selecting which range is to be calibrated (LOW or HIGH). Each of these two ranges MUST be calibrated separately.

Note: *Impact on Readings or Data*

If the ZERO or SPAN buttons are not displayed during zero or span calibration, the measured concentration value during this time is out of the range allowed for a reliable calibration.

Setting the Expected Span Gas Concentration

Note: When setting expected concentration values, consider impurities in your span gas. The expected N_2O span gas concentration should be 80% of the reporting range of the instrument.

The default factory setting is 40 ppm. To set the span gas concentration, press:

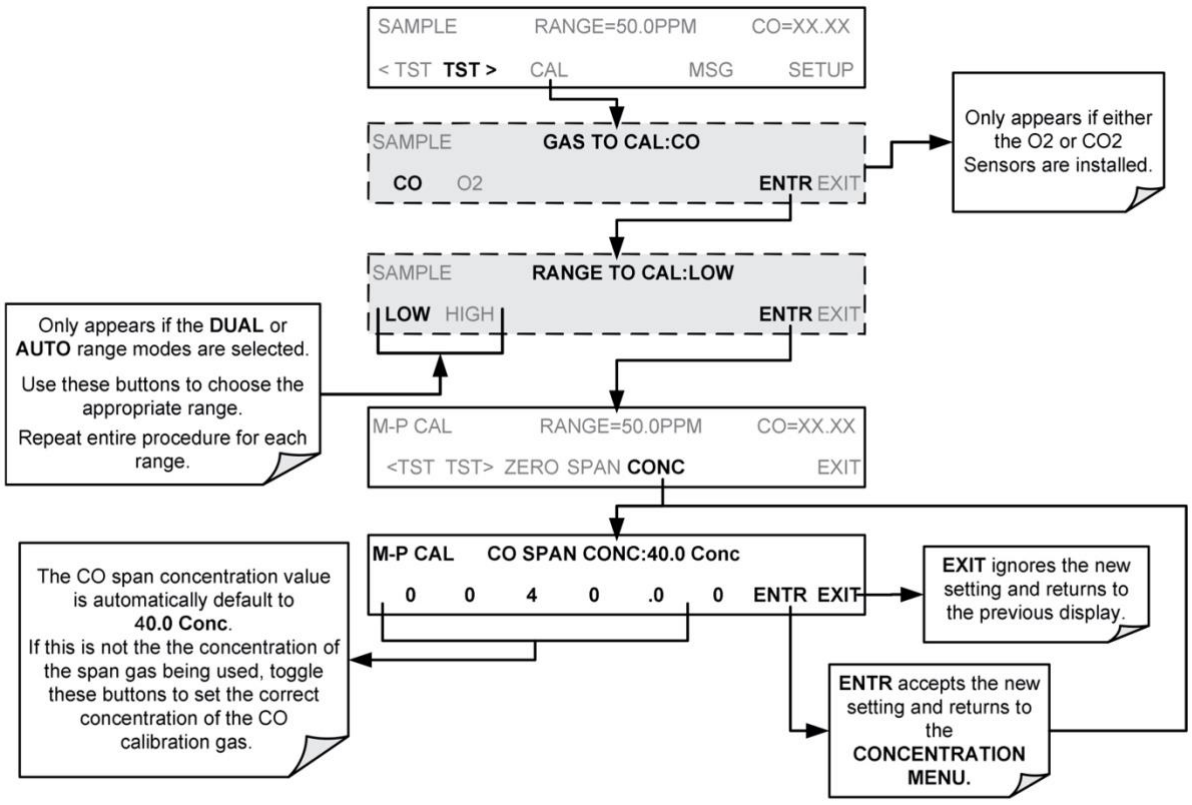

Note: The above screen(s) show CO concentration displayed. Your instrument will indicate and display N_2O concentration.

Figure A3. Setting the expected span gas concentration

Zero/Span Point Calibration Procedure

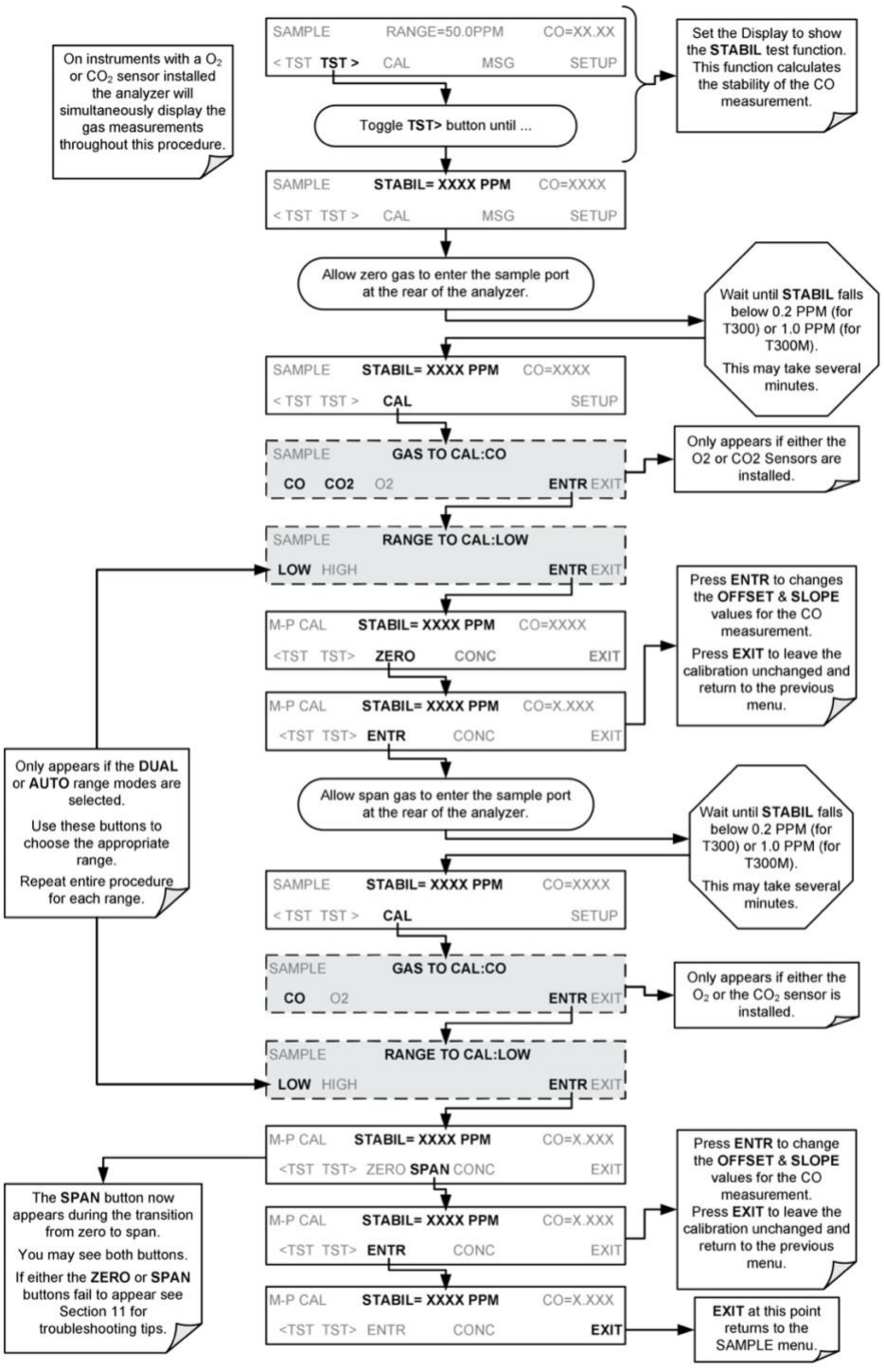

Note: The above screen(s) show CO concentration displayed. Your instrument will indicate and display N_2O concentration.

Figure A4. Zero/span point calibration procedure

EMISSION CALCULATION

The gaseous mass balance calculation depended on PPM_V concentrations recorded by the gaseous analyzer, concepts from the ideal gas law, and the foul air flow rate. Gaseous N_2O data was recorded by the Teledyne AI GFC 7002T N_2O Analyzer. APIcom software was used to configure and acquire data from the analyzer. The configuration collected averaged N_2O (PPM_V) data every 10 minutes. After acquiring data with the APIcom software, a pivot table was used to calculate hourly average N_2O concentrations. With N_2O concentration (PPM_V) and foul air flow (SCFM), the following equations were used to find N_2O mass flow:

$$Q_{N_2O,V} = \left(\frac{C_{N_2O}}{10^6}\right) \bullet Q_{\text{Foul Air}} \qquad \textbf{(1.1)}$$

$$\rho_{N_2O,std} = \left(\frac{P_{std}}{\left(\frac{R}{MW_{N_2O}}\right) \bullet T_{std}}\right) \qquad \textbf{(1.2)}$$

$$Q_{N_2O,M} = Q_{N_2O,V} \bullet \rho_{N_2O,std} \qquad \textbf{(1.3)}$$

$$Q_{N-N_2O,M} = Q_{N_2O,M} \bullet \left(\frac{MW_N}{MW_{N_2O}}\right) \bullet \left(\frac{24h}{d}\right) \qquad \textbf{(1.4)}$$

Where

$Q_{N_2O,V}$: Volumetric flow of N_2O (SCFM)
C_{N_2O}: N_2O concentration reported by Teledyne analyzer (PPM_V)
$Q_{\text{Foul Air}}$: Total foul air flow from membrane and aeration basins (SCFM)
$\rho_{N_2O,std}$: Density of N_2O at standard pressure and temperature (lbm/ft^3)
P_{std}: Standard pressure (14.69 psi)
T_{std}: Standard temperature (60 °F)
R: Universal gas constant ($10.73\ psi_a \bullet ft^3/lb \bullet mol \bullet °R$)
MW_{N_2O}: Molecular weight of N_2O ($44.013\ lb/lb-mol$)
$Q_{N_2O,M}$: Mass flow of N_2O (lb/hr)
$Q_{N-N_2O,M}$: Mass flow of $N-N_2O$ ($lb\ N-N_2O/d$)
MW_N: Molecular weight of N_2 ($28.013\ lb/lb-mol$)

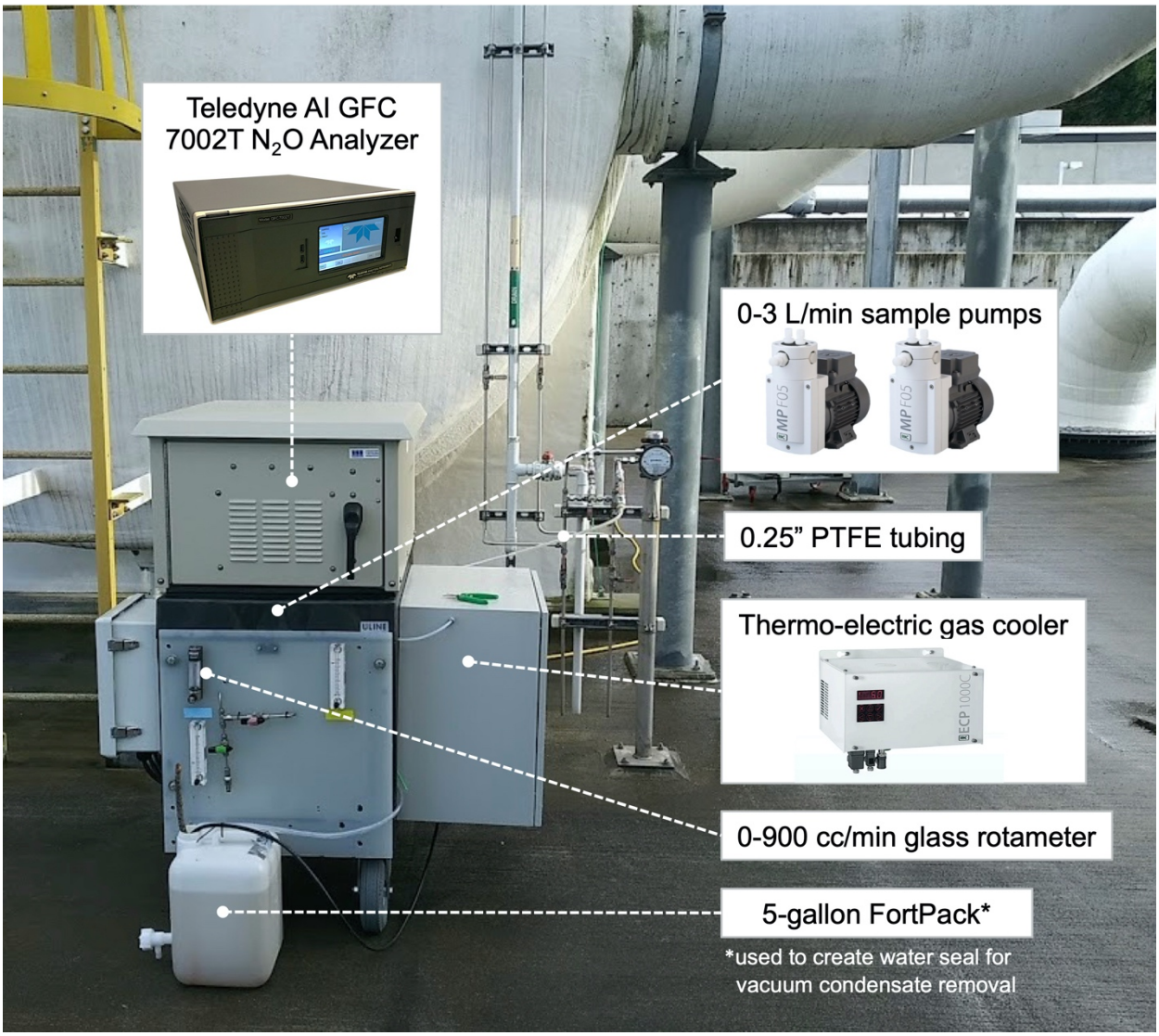

Figure A5. Gaseous N_2O field sampling unit.

A3. FAN PERFORMANCE CURVES AND FLOW RATE CALCULATION

To complete the emission estimate using N_2O concentration data collected by the gaseous analyzer, the gas flow rate through the odor control system was determined using data from the odor control blowers. At Brightwater, the gas flow rate through the odor control blowers is not measured in situ and needs to be interpolated based on the blower inlet damper position and blower differential pressure reported to the PI historian. This damper position is reported as a percentage between 60 and 100, relating to the blower inlet damper *percent open*. A differential pressure is also reported for each blower, which refers to the pressure difference introduced by the blower. The site-specific fan performance curves, reported with the submittal data from plant construction, report volumetric flow rate and static pressure values based on damper position (Figure A6). These curves were used to derive the gas flow rate from the blower data. The fan performance curves were only reported for damper positions in increments of 5%, thus a lookup table was created based on points on the curves and linear interpolation between these points. Each blower's damper position and differential pressure was then plugged into the lookup table to determine the corresponding gas flow rate, which was used in the N_2O mass balance for the gaseous analyzer. The fan performance curves were verified in field tests using a hotwire anemometer (Extech Instruments SDL350).

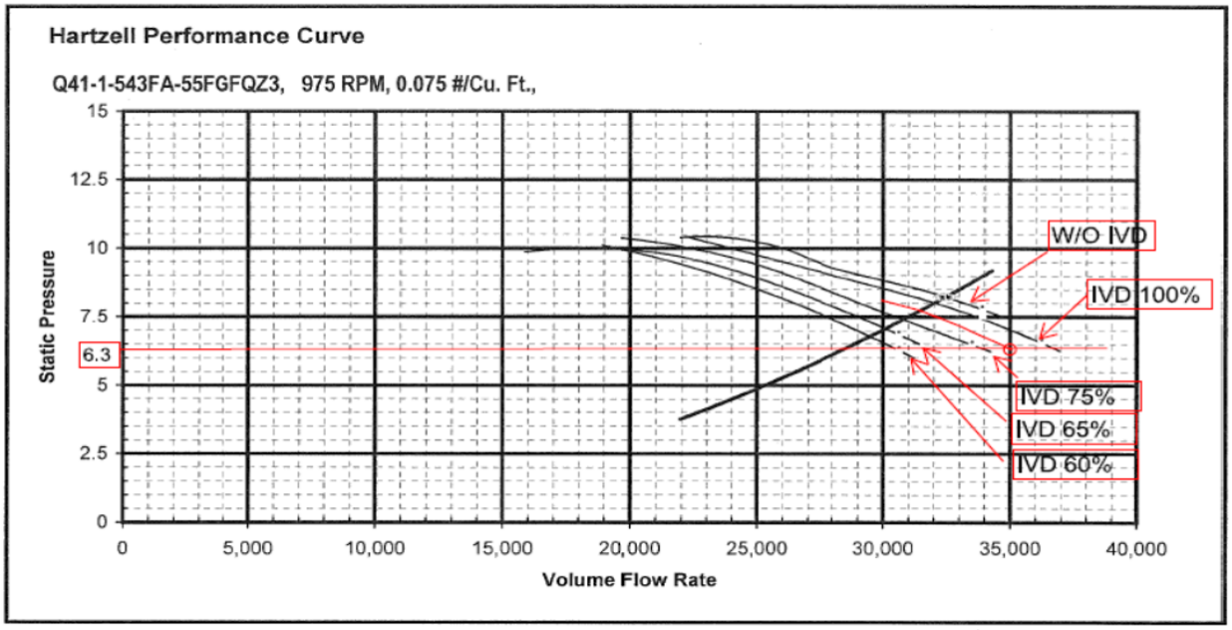

Figure A6. Performance curves for Brightwater odor control blowers. Static pressure is reported in inches water column (in wc). Volume flow rate is reported in standard cubic feet per minute (SCFM). IVD stands for Inlet Vane Damper and is reported as percent open.

A4. IMPACT OF ODOR CONTROL SYSTEM ON N_2O EMISSIONS

To determine the impact of the odor control system on N_2O emissions, the gaseous analyzer was placed in different sampling locations and data was analyzed in conjunction with data from the aqueous N_2O analyzer and blower operation records. The odor control system at Brightwater consists of four blowers that draw off-gas from the aeration basins and membrane basins through ducting and chemical (caustic/hypo) scrubbers and activated carbon (four bed, virgin activated) before it is emitted. This analysis served to answer two questions about the impact of the odor control system on N_2O emissions: (1) Does the odor control system (scrubbers and activated carbon) impact N_2O emissions leaving the plant? (2) How does blower operation and gas sampling location impact the gaseous analyzer's emission estimates?

To answer these questions, unique gas "flow regimes" were identified based on blower operation and gas sampling locations. Figure A7 shows a simplified representation of the odor control system. Gaseous analyzer sample locations are labeled as "N" (North), "S" (South), and "D" (Downstream), and the four odor control blowers are labeled 1-4.

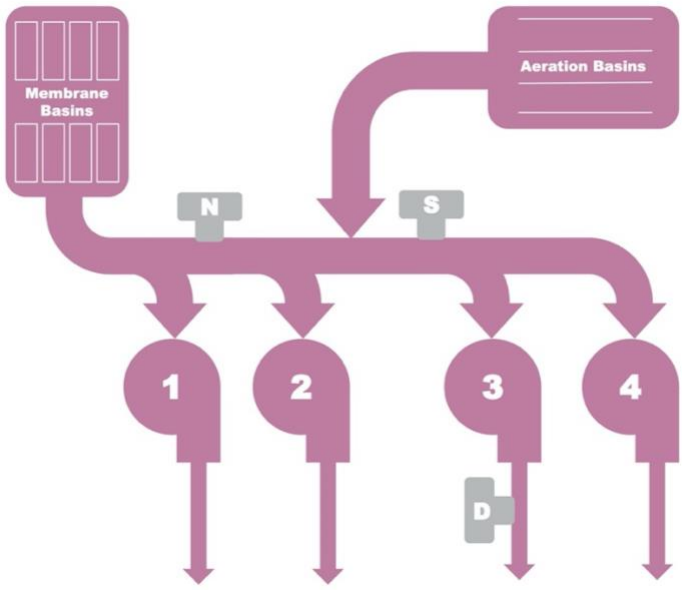

Figure A7. Brightwater treatment plant odor control system. Gaseous analyzer sample locations are labeled as "N" (North), "S" (South), and "D" (Downstream). The four odor control blowers are labeled 1-4.

At Brightwater, the four odor control blowers are rarely all operated simultaneously, and plant operators determine which blowers are needed depending on process conditions at the plant. Blower operation data were reported to the PI historian and downloaded for this analysis. Unique flow regimes were identified based on the combination of which odor control blowers were operating and the gas analyzer sample location. To distinguish the different configurations, a binary naming system was employed, with the first four digits describing the operation of

blowers 1-4, and the letter describing the sampling location of the gaseous analyzer. For example, 0011S is the configuration in which blowers 3 and 4 are on, and the gas analyzer is sampling from the "South" sampling location.

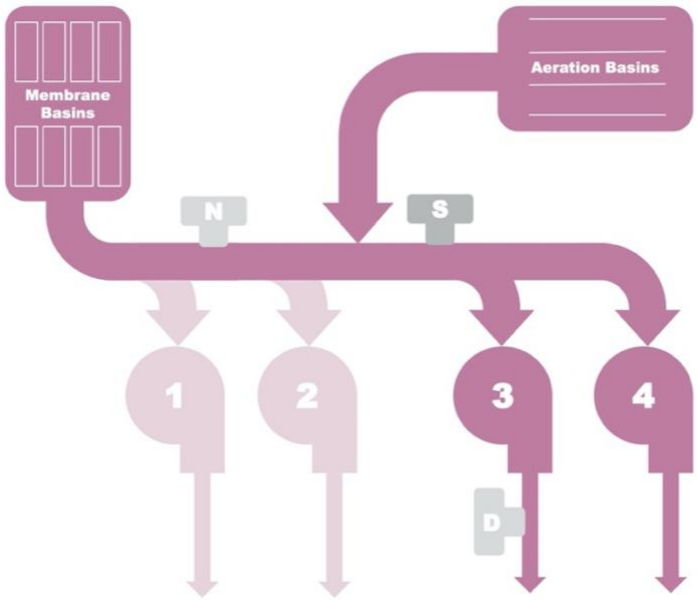

Figure A8. Configuration 0011S. Blowers 1 and 2 are off, and blowers 3 and 4 are on. The gaseous analyzer is located at the South sampling port.

To compare N_2O data under the different flow regimes, analysis was performed in Microsoft Excel using pivot tables to organize data from different time periods based on flow regime configuration. First, a configuration label was created for each hour of the monitoring campaign, based which blowers were operational and where the gaseous analyzer was located at any given time. This data was displayed with the hourly N_2O emission estimates from the gaseous analyzer. Next, pivot tables were used to calculate average N_2O emissions under each regime. On its own, these averages do not say much about the effect of different flow regimes on N_2O emissions because each average is from different time periods with different process conditions affecting emission rates, thus they cannot be compared to each other as-is. However, since the aqueous N_2O analyzer continuously measured N_2O emissions from the aeration trains, and these emission estimates are not affected by odor control blower operation, this data could be used as a "baseline" to normalize the gaseous data. In the same pivot table, hourly N_2O emission estimates from the aqueous analyzer were averaged for each regime. Now average emission estimates from both analyzers, from identical sampling periods, could be compared. Gaseous emission values were divided by aqueous emission values for a "gaseous / aqueous" percentage. For example, 66% for 0011S means that under the 0011S flow regime, the gaseous analyzer only estimates 66% of the emissions that the aqueous analyzer estimates. The complete result of this analysis is displayed in Table A1.

Table A1. Brightwater odor control system flow regime analysis. Configurations are labeled by which odor control blowers are in operation and where the gaseous analyzer is located. Under each unique configuration, the gaseous analyzer samples off-gas with a different amount of mixing from the different basins, resulting in gaseous emission values that represent emissions from different areas of the entire system. The aqueous analyzer always stayed in the same position in aeration basin 1, thus the aqueous emission values always represent emissions from the same area of the system.

Configuration	**Aqueous Emission Value [lb N_2O-N d^{-1}]**	**Gaseous Emission Value [lb N_2O-N d^{-1}]**	**Gaseous / Aqueous [%]**	**Duration [days]**
0011S	67	44	66%	23
0111D	64	50	78%	15
0111N	55	14	26%	15
0111S	91	78	86%	39
1011S	49	52	106%	27
1111S	103	139	134%	15

To answer question (1) regarding the impact of the odor control system on impact N_2O emissions leaving the plant, configurations 0111S and 0111D were compared. The only difference between these configurations is the location of the gaseous analyzer, either at the south sampling port or the downstream sampling port. Since the operation of blowers 2-4 remained consistent between these configurations, the impact of location upstream or downstream of scrubbers, and thus the impact of these treatments on emissions, could be determined. The normalized gaseous / aqueous percentages were 86% and 78% respectively. Although these values differ by 8%, this was determined to be within the range of measurement accuracy. Thus, it was determined that the odor control system did not significantly impact N_2O emissions.

Question (2) was addressed with configuration 0011S. Theoretically, under this configuration (displayed in Figure A8), all of the off-gas from both the membrane and aeration basins is measured by the gaseous analyzer (in the South sampling position). This is not the case with the other configurations, in which some off-gas may be emitted upstream of the analyzer measurement location. The normalized gaseous / aqueous percentage for 0011S was 66%, meaning that 66% of the emissions estimated by the aqueous analyzer were reported by the gaseous analyzer. This is meaningful because 0011S can be estimated as measuring “all emissions” in a mixed state. The aqueous analyzer should theoretically be able to predict N_2O mass emissions to a high degree of precision, however the calculation that converts dissolved N_2O concentrations to gaseous emissions relies on a number of assumptions, and it is expected that the emissions estimated by the aqueous analyzer would require some amount of scaling. Since there was both aqueous and gaseous data collection at Brightwater, the period of 0011S

data collection is especially valuable for determining the magnitude of scaling required to make the aqueous emission value as accurate as possible. With the result of 66% from the analysis, multiplying the aqueous value by 0.66 makes the gaseous and aqueous emissions equal.

Thus, a multiplier of 0.66 was applied to all of the data collected by the aqueous analyzer as our best estimate of the "true emissions" from the plant, since the aqueous analyzer was always in the same position and its readings were not affected by changes in odor control blower operation.

The data from 0111N may be assumed to measure only the emissions from the membrane basins, since under this flow regime off-gas from the membrane basins would pass under the North sampling point before mixing with off-gas from the aeration basins, and measured airflow to the membrane basins was always greater than measured airflow to the aeration basins. With this information, we can estimate what percentage of total emissions are being emitted from the membrane and aeration basins respectively. After adjusting the 55 lbs N_2O-N d^{-1} by 0.66, 39% of emissions can be attributed to the membrane basins and accordingly, 61% can be attributed to the aeration basins. This data is available in Table A1, and the calculation is as follows:

0011S gas sampling location (fully representative gas sample)

$$\frac{\text{Gaseous emission value}_{\,2/18/20\,-2/25/20}}{\text{Aqueous emission value}_{\,2/18/20\,-2/25/20}} = \frac{44\ [\text{lb}\ N_2O - \text{N}\ d^{-1}]}{67\ [\text{lb}\ N_2O - \text{N}\ d^{-1}]} = 0.66$$

Thus, the aqueous emission value overestimates emissions. To adjust the aqueous emission value to match the results of the fully representative gas sample, multiply by 0.66.

0111N gas sampling location (membrane basins only gas sample)

$$\begin{aligned}\text{Adjusted aqeous emission value}_{\,2/18/20\,-2/25/20} &= \text{Aqueous emission value}_{\,12/22/21\,-1/6/21} \times 0.66\\ &= 55\ [\text{lb}\ N_2O - \text{N}\ d^{-1}] \times 0.66\\ &= 36\ [\text{lb}\ N_2O - \text{N}\ d^{-1}]\end{aligned}$$

$$\frac{\text{Gaseous emission value}_{\,12/22/21\,-1/6/21}}{\text{Adjusted aqueous emission value}_{\,2/18/20\,-2/25/20}} = \frac{14\ [\text{lb}\ N_2O - \text{N}\ d^{-1}]}{36\ [\text{lb}\ N_2O - \text{N}\ d^{-1}]} = 0.44$$

Thus, the proportion of total emissions from *membranes only* is 0.39. This means 39% of emissions are from the membrane basins and 56% are from the aeration basins based on this period of data.

It is not surprising that the gaseous analyzer in other configurations over-estimated emissions, since the gaseous calculation relies on the assumption that the gas being sampled is well-mixed, and that the measured N_2O concentration can be multiplied by the volume gas flow through the odor control system to estimate the mass N_2O emitted. However, knowing that the aeration basins emit more N_2O than the membrane basins, any configuration that sampled aeration basin-off gas before it was well-mixed with membrane-basin off-gas would over-estimate emissions.

A5. CORRELATION ANALYSES

Table A2. Process parameters tracked at Brightwater (correlation analysis variables).

Data Source	Sample Location					
	Influent	**Primary Effluent**	**Mixed Liquor Feed**	**Aeration Basin**	**Membrane Effluent**	**Final Effluent**
HachWIMS	TKN, NH_3, NO_2+NO_3	TSS, BOD, COD, Alk, TKN, NH_3, NO_2+NO_3	SCOD, COD, NH_3		TKN, BOD, COD, Alk, NH_3, NO_2+NO_3	TKN, NH_3, NO_2+NO_3, Flow
PI Historian	pH, Temp			Basins 1-3: Flow, Air flow, DO (zones 1-4), TSS	pH, NH_4^+	Flow
Aqueous Probes				N_2O, Temp, NH_4^+, NO_3		

For Spearman rank correlation, the rule of thumb is that a coefficient with an absolute value between less than 0.4 has “very weak” or “weak” correlation, a coefficient between 0.4 and 0.6 has “moderate” correlation, a coefficient between 0.6 and 0.8 has “strong” correlation, and between 0.8 and 1.0 has “very strong” correlation. Variables with correlation coefficients greater than 0.4 and with p-values less than 0.05 were determined to have significant correlation with N_2O emissions.

Table A3. Correlation analysis results for hourly process parameter data. Each parameter's correlation coefficient with N_2O emissions is listed, and asterisks represent p-value range. P-values less than 0.1, 0.05, and 0.01 are displayed with 1-3 asterisks respectively.

Sample Location	**Parameter**	**Correlation With N_2O Emissions**
Influent	pH	0.11***
	Temperature (°F)	-0.04***
Aeration Basin 1	NH_4^+ (mg N L^{-1}) (YSI probe)	0.48***
	NO_3^- (mg N L^{-1}) (YSI probe)	0.64***
	Zone 1 Temperature (°C)	-0.18***
	Zone 2 Temperature (°C)	-0.2***
	Flow (mgd)	0.65***
	Air Flow (SCFM)	0.7***
	Zone 1 DO (mg L^{-1})	0.03**
	Zone 2 DO (mg L^{-1})	-0.59***
	Zone 3 DO (mg L^{-1})	-0.24***
	Zone 4 DO (mg L^{-1})	0.07***
	Zone 4 TSS (mg L^{-1})	0.01
Aeration Basin 2	NH_4^+ (mg N L^{-1}) (Hach probe)	0.55***
	Flow (mgd)	0.65***
	Air Flow (SCFM)	0.73***
	Zone 1 DO (mg L^{-1})	0
	Zone 2 DO (mg L^{-1})	-0.61***
	Zone 3 DO (mg L^{-1})	-0.6***
	Zone 4 DO (mg L^{-1})	-0.14***
	Zone 4 TSS (mg L^{-1})	-0.01
Aeration Basin 3	Flow (mgd)	0.65***
	Air Flow (SCFM)	0.68***
	Zone 1 DO (mg L^{-1})	-0.57***
	Zone 2 DO (mg L^{-1})	-0.65***
	Zone 3 DO (mg L^{-1})	-0.35***
	Zone 4 DO (mg L^{-1})	0.18***
	Zone 4 TSS (mg L^{-1})	0.05***
	Solids Return Flow (GPM)	0.51***
Membrane Effluent	pH	-0.48***
	NH_4^+ (mg N L^{-1}) (Hach probe)	0.22***
Final Effluent	Flow (mgd)	0.66***

Table A4. Correlation analysis results for daily process parameter data. Each parameter's correlation coefficient with N_2O emission is listed, and asterisks represent p-value range. P-values less than 0.1, 0.05, and 0.01 are displayed with 1-3 asterisks respectively.

Sample Location	**Parameter**	**Correlation with N_2O Emissions**
Influent	TKN (mg L^{-1})	0.23
	NH_4^+ (mg N L^{-1})	0.12
	NO_3^- + NO_2^- (mg N L^{-1})	0.2
	pH	0.55***
	Temperature (°F)	-0.31***
Primary Effluent	TSS (mg L^{-1})	0.02
	BOD (mg L^{-1})	0.05
	COD (mg L^{-1})	-0.02
	Alkalinity (mg L^{-1})	0.32**
	TKN (mg N L^{-1})	0.4*
	NH_4^+ (mg N L^{-1})	0.33***
	NO_3^- + NO_2^- (mg N L^{-1})	-0.11
	COD:N	-0.48***
	Daily Flow Variance (mgd)	0.23***
Aeration Basin 1	Zone 1 Temperature (°C)	-0.28***
	Zone 2 Temperature (°C)	-0.24***
	NH_4^+ (mg N L^{-1}) (YSI probe)	0.59***
	NO_3^- (mg N L^{-1})	0.49***
	Flow (mgd)	0
	Air Flow (SCFM)	0.12
	Zone 1 DO (mg L^{-1})	0.4***
	Zone 2 DO (mg L^{-1})	0.33***
	Zone 3 DO (mg L^{-1})	0.01
	Zone 4 DO (mg L^{-1})	0.01
	Zone 4 TSS (mg L^{-1})	0.07
Aeration Basin 2	NH_4^+ (mg N L^{-1}) (Hach probe)	0.01
	Flow (mgd)	-0.04
	Air Flow (SCFM)	0.34***
	Zone 1 DO (mg L^{-1})	0.11
	Zone 2 DO (mg L^{-1})	0.19**
	Zone 3 DO (mg L^{-1})	0.03
	Zone 4 DO (mg L^{-1})	0.08
	Zone 4 TSS (mg L^{-1})	-0.12

Aeration Basin 3	Flow (mgd)	0.07
	Air Flow (SCFM)	0.12
	Zone 1 DO (mg L^{-1})	-0.2***
	Zone 2 DO (mg L^{-1})	-0.06
	Zone 3 DO (mg L^{-1})	0.23***
	Zone 4 DO (mg L^{-1})	0.4***
	Zone 4 TSS (mg L^{-1})	-0.03
	Solids Return Flow (GPM)	0.21***
Mixed Liquor Feed	SCOD (mg L^{-1})	0.18
	COD (mg L^{-1})	0.21
	NH_4^+ (mg N L^{-1})	-0.35**
Membrane Effluent	BOD (mg L^{-1})	0.03
	COD (mg L^{-1})	-0.06
	Alkalinity (mg L^{-1})	-0.37***
	NH_4^+ (mg N L^{-1})	-0.01
	NO_3^- + NO_2^- (mg N L^{-1})	0.52***
	TKN (mg N L^{-1})	0
	pH	-0.45***
	NH_4^+ (mg N L^{-1})	0.46***
Final Effluent	TKN (mg N L^{-1})	-0.01
	NO_3^- + NO_2^- (mg N L^{-1})	0.48**
	Flow (mgd)	-0.26***
Misc.	Precipitation (in.)	-0.16**
	Nitrification rate (mg N L^{-1} d^{-1})	0.4*
	Nitrification efficiency (%)	0.45**
	Denitrification rate (mg N L^{-1} d^{-1})	0.09
	Denitrification efficiency (%)	-0.17

A6. ANALYZER EASE OF USE

GASEOUS ANALYZER

Setup and installation: The gaseous analyzer required significant infrastructure to turn it into a mobile field instrument for measuring aeration off-gas (Figure A3). Similar to other analyzers of its type, the analyzer itself is designed to be a bench-top laboratory unit operated in a conditioned space. Therefore, the analyzer was placed into a NEMA 3R enclosure with cooling fans, a heater, and thermostats to keep it within its operating temperature range. Since aeration off-gas can be humid and dirty, the sampling train consisted of a cooler to cool the sample, a coalescing filter to remove liquid droplets and particulates, a glass rotameter to measure flow, and an adjustable diaphragm pump to provide a constant flow rate. Sample lines and valves were Teflon or stainless steel. The cooler also had to be mounted in a NEMA 3R enclosure with fans. All equipment was mounted to a plastic roller cart with pneumatic tires and foam cushioning blocks under the analyzer enclosure to handle bumps. The system operated unattended 24 hours a day and largely without issues except for a few periods of freezing weather causing the gas sample line to accumulate with condensate.

Calibration: The gaseous analyzer required specialty zero and span gases to be produced by an industrial gas company. Very small gas cylinders (type A3) were selected for ease of transport; these provided more than a 6-month supply of calibration gas. The cylinders were transported on a cylinder rack mounted to a handcart. Several span gas mixtures were created and ultimately not used since the foul air N_2O concentration was not known prior to ordering the gases. The two-point calibration procedure took 30-60 minutes. Drift was negligible between calibrations every two weeks at the measurement range used. Startup assistance from the manufacturer would be recommended by the authors.

Data download: The N_2O analyzer had internal data storage which was accessed in the field via an ethernet cable and laptop computer; data was transferred as easy-to-use CSV files.

AQUEOUS ANALYZER

Setup and installation: The aqueous analyzer came ready to install outdoors from the manufacturer and is a simple pole-mount type. Extra-length cords were purchased to span long distances in the aeration basins. Since probes have a 4-6-month life, annual replacement costs impact the overall cost of ownership.

Calibration: Calibration of the aqueous probes was generally straightforward and required manufacturer calibration kit, a few buckets and a thermometer. Calibration took 30-60 minutes for each probe. The only calibration difficulties encountered were entrapped air bubbles in two of the probes; these were resolved using manufacturer's recommendations. Calibration kits from the manufacturer are a significant portion of the cost of ownership.

Data download: While the analyzer has the capability to be integrated into a plant control system and can even automatically calculate emission rates if provided continuous aeration air flow rates, a simple USB memory stick data download was used for this measurement effort. Post processing was accomplished with the manufacturer's provided software.

APPENDIX B

Supplementary information for

Chapter 4:

Sustainable Nitrogen and Phosphorus Removal: Limiting Nitrous Oxide Emissions From a Granular Sludge Sequencing Batch Reactor

Number of pages: 16
Number of figures: 7
Number of tables: 8

Table of contents

B1. PREPARATION OF VISHNIAC AND SANTER SOLUTION[3]

Table B1. Vishniac and Santer solution components

Step	Compound	Mass
1	$EDTA•H_2•Na_22H_2O$	100 g
2	$FeSO_4•7H_2O$	9.98 g
3	$ZnSO_4•7H_2O$	4.40 g
4	CaCl2•2H2O	16.36 g
5	$MnCl_2•4H_2O$ / $MnSO_4•H_2O$	10.12 g / 8.64 g
6	$Na_2MoO_4•2H_2O$	4.36 g
7	$CuSO_4•5H_2O$ / $CuCl_2•2H_2O$	3.14 g / 2.14 g
8	$CoSO_4•7H_2O$ / $CoCl_2•6H_2O$	3.22 g / 2.79 g

1. Dissolve completely* the EDTA in 1L of distilled water, setting the pH to 6.0 with KOH pellets (approximately 8.21 g at room temperature).
2. Dissolve completely* the $FeSO_4.7H_2O$.
3. Set the pH to 6.0 with KOH pellets (approximately 5.48 g at room temperature).
4. Add the remaining compounds, always dissolving each compound completely* before adding the next.
5. Set the pH to 4.0 with KOH pellets (approximately 10.04 g at room temperature).
6. Adjust the volume to 2L with distilled water.

*****If the next compound is added before everything has been dissolved, the process must be restarted from the beginning because of complex building. The temperature can be raised to speed up dissolution.

[3] Vishniac, W.; Santer, M. The Thiobacilli. **1957**.

B2. N_2O EMISSION CALCULATION

$$Emission\ Factor\ [\%] = \frac{\sum_i^k [C_{N_2O,sample} - C_{N_2O,sweep}] \cdot \frac{28013.48}{24.21 \cdot 10^6} \cdot Q_{sample} \cdot VSS_{normalized}}{(NH_{3\,i} - NH_{3\,j})(VSS_{reactor})(V_{liquid})}$$

Where i = beginning of the aerobic phase

j = end of the aerobic phase

k = end of the anaerobic phase

$C_{N_2O,sample}$ = concentration of N_2O (ppm_V)

$C_{N_2O,sweep}$ = concentration of N_2O in sweep air (0.3 ppm_V)

28013.48 = mg N_2O-N per mol N_2O

24.21 = ideal gas law conversion

10^6 = ppm conversion

Q_{sample} = sample flow rate into N_2O analyzer (0.892 liters per minute)

$VSS_{normalized}$ = average reactor VSS (23 grams)

$NH_{3\,i}$ = ammonia concentration at beginning of aerobic phase (mg NH_3-N L^{-1})

$NH_{3\,j}$ = ammonia concentration at end of the aerobic phase (mg NH_3-N L^{-1})

$VSS_{reactor}$ = reactor VSS on the day of the test (grams)

V_{liquid} = volume of liquid in reactor (liters)

B3. QUANTITATIVE POLYMERASE CHAIN REACTION (qPCR) PROTOCOL[4]

1. Clean the bench and all supplies using 70% ethanol.
2. On ice, thaw DNA samples and the plasmid needed for the standard.
3. Quantify the amount of DNA in wastewater treatment samples using the Qubit™ dsDNA HS Assay kit (ThermoFisher Scientific, USA).
4. Quantify amount of DNA of plasmid for the standard (s ng/µL).
5. Dilute DNA samples with RNAse & DNAse free water to a concentration of 1 ng/µL. Pipet mix and vortex the tubes.
6. Use the following equation to calculate copies of plasmid per µL for the standard:

$$x = \frac{6.023 \times 10^{23} \left(\frac{\text{copies}}{\text{mol}}\right) \times \text{concentration of target DNA} \left(\frac{\text{g}}{\mu\text{L}}\right)}{\text{TMW}\left(\frac{\text{g}}{\text{mol}}\right)}$$

   a) Sequence the plasmid insert to confirm the size of the target in bases. Calculate the amount (i.e., percentage) of insert DNA in the plasmid (e.g., for a 3,000 bp vector, a 123 bp DNA fragment is 3.9% of total DNA) and multiply it by the obtained concentration to determine the DNA concentration of the target (insert).

      For DPAO II, the base of the DNA fragment is 321 bp (check the base online), and the used vector is 3969 bp.

      So here, x concentration of target DNA = s ng/µL *321/ (321+3969)

   b) Calculate the Target Molecular Weight (TMW) by multiplying the number of base pairs of the target DNA by the average molecular weight of double strand DNA (dsDNA, 660 Daltons per base pair)

      For DPAO II, TMW = 321*660

7. Clean bench again and re-sterilize supplies.
8. Dilute the target DNA in a ladder from 10^8 copies to 10 copies using 2 µL of DNA and 18 µL of sterile dH_2O. Vortex each dilution and spin down briefly before making the next dilution.
9. Thaw the MasterMix: FastStart Essential DNA Green Master (REF 06402712001).
10. Prepare the qPCR reaction. For each reaction, the total volume is 10 µL.

---

[4] Protocol developed by Ting Xie (2018)

Table B2. qPCR reaction components

MasterMix	5 µL
Forward primer	0.5 µL
Reverse primer	0.5 µL
Template DNA	1 µL
H_2O	3 µL

Calculate and prepare the required MasterMix, primers and H_2O in one tube for aliquots. The addition order is H_2O => MasterMix => primers. Vortex the tube.

For example, if there are 8 standards and 6 samples (two reactions for each, and one negative control for all the reactions):

Table B3. Example qPCR reaction components

Reagent	**Each reaction**	**29 reactions**	**Multiply by a factor of 1.2 for pipetting**
H_2O	3 µL	87 µL	104.4 µL
MasterMix	5 µL	145 µL	174 µL
Forward primer	0.5 µL	14.5 µL	17.4 µL
Reverse primer	0.5 µL	14.5 µL	17.4 µL

11. Change gloves; wipe the tube rack with ethanol. Put the tubes for qPCR in the rack.
12. Pipet 9 µL of the mixture of MasterMix, primers and H_2O into each tube. Inject slowly to avoid separation.
13. Add 1 µL of diluted standard into each tube from high to low (10^8 to 10).
14. Add 1 µL of diluted DNA sample into each tube.
15. Vortex each dilution and spin down.
16. Input qPCR conditions and set up the qPCR reactions in Light Cycler 3 software. Carefully place the tubes into the qPCR instrument and start. Transfer the setting file to the instrument and start qPCR.

Table B4. Primers used for qPCR.

Target	Primer	Sequence	Amplicon length	Annealing temp. (°C)	Reference
Bacterial *amo*A gene (AOB)	amoA-1F amoA-2R	GGGGTTTCTACTGGTGGT CCCCTCKGSAAAGCCTTCTTC	491	60	Rotthauwe et al. 1997
Nitrite oxioreductase beta subunit *nxr*B gene (NOB)	nxrB169F nxrB638R	TACATGTGGTGGAACA CGGTTCTGGTCRATCA	485	57	Pester et al. 2014
16S rRNA PAO	PAO651f PAO846r	CTGGAGTTTGGCAGAGGG GTTAGCTACGGCACTAAAAGG	195	50	Fukushima et al. 2007
Competibacter (GAO)	GAO-Gbf GAO-Gbr	GAGTGGGCTAGAGGATCGTG TTCCCCRGATGTCAAGGCC	164	55	Fukushima et al. 2010
16S rRNA general bacteria (EUB)	515F-Y 926-R	GTGYCAGCMGCCGCGGTAA CCGYCAATTYMTTTRAGTTT	371	56	Parada et al. 2016

B4. FLUORESCENCE *IN SITU* HYBRIDIZATION (FISH) ANALYSIS PROTOCOL

Method is developed in Bremen/Munich[5]

PRINCIPLE:

FISH analysis is an ideal method for selective detection of a particular organism (Bacteria, fungi, or protozoa) in a mixture with others, using their specific 16S rRNA sequence. During hybridization the cells are exposed to elevated temperatures, detergents, and osmotic gradients. Thus, fixation of the cells is essential to maintain the morphological integrity of the cells. Fixation of cells with glutaraldehyde results in considerable autofluorescence of the specimen. Autofluorescence is minimized by fixation in freshly prepared (no older than 24h) 4% paraformaldehyde solution in PBS. In contrast with gram-negative, paraformaldehyde-fixed cells of gram-positive bacteria often have less permeability for the FISH probes. In this case, probe penetration can be enhanced by a Lysozyme/EDTA treatment of paraformaldehyde-fixed cells prior to hybridization by fixation in an ethanol series or by short fixation in an ethanol/paraformaldehyde mixture. In some cases, probe penetration can be enhanced by increasing the SDS concentration to 1%.

After fixation, the cells are immobilized on a microscopic slide and used for hybridization with 16S rDNA probes. To avoid non-specific binding of the rDNA probes, the hybridization is done at stringent conditions (46 °C, 0- 65% formamide) and specimens are washed with a washing buffer (48 °C). The target organisms can be detected by the characteristic fluorescence.

MATERIALS:

Fixation of cells:

- PBS (3x); 390 mM NaCl in 30 mM phosphate buffer (pH 7.2)
    - Dissolve 0.49 g KH2PO4 in 80 ml, add 2.3 g NaCl and adjust pH to 7.2. Adjust the volume to 100 ml.
- PBS (1x); 130 mM NaCl in 10 mM Phosphate buffer (pH 7.2)
    - Take 33 ml of PBS (3x) and adjust the volume to 100 ml with distilled water.
- 4% Paraformaldehyde in PBS
    - See below for preparation (note: paraformaldehyde is very toxic, use gloves)
- 98% Ethanol at -20°C
- 50%, 80% and 98% ethanol

[5] Pernthaler, J.; Glöckner, F. O.; Schönhuber, W.; Amann, R. Fluorescence in Situ Hybridization (FISH) with RRNA-Targeted Oligonucleotide Probes. *Methods Microbiol.* **2001**, *30*, 207–226. https://doi.org/10.1016/S0580-9517(01)30046-6.

- MilliQ at 4°C
- 1 M NaOH
    - Dissolve 4 g of NaOH in 80 ml distilled water, adjust the volume to 100 ml
- 1 M HCl

Hybridization:

- 10% KOH in 95% ethanol
    - Dissolve 10 g KOH in 95% ethanol.
- 0.1% gelatin solution in 0.01% chromium potassium sulfate dodecahydrate
    - Dissolve 0.1 g gelatin and 0.01 g chromium potassium sulfate dodecahydrate in 100 ml milliQ.
- 5 M NaCl
    - Dissolve 29.2 g NaCl in 80 ml milliQ and adjust the volume to 100 ml.
- 1 M Tris/HCl (pH 8.0)
    - Dissolve 12.1 g Tris base and adjust the pH to 8.0 with HCl. Adjust the volume to 100 ml.
- Formamide
    - Use formamide only in the fume hood and while wearing gloves.
- 0.5 M Na_2EDTA (pH 8.0)
    - Dissolve 18.1 g Na_2EDTA in 80 ml, adjust to pH 8.0 and adjust volume to 100 ml.
- 10% (v/v) SDS
    - Dissolve 2 g of sodiumdodecylsulfate in 20 ml of milliQ.

PROCEDURE:

Preparation of the fixative:

Caution 1: Paraformaldehyde is very toxic, use gloves.

Caution 2: Use only freshly prepared fixative (less than 24 h old), or recently thawed from a -20°C freezer.

- Heat 6.5 ml milliQ to 60°C (normally it is sufficient to warm it under hot tap water).
- Add 0.4 g paraformaldehyde.
- Add one drop of 1 M NaOH and shake vigorously until the solution has nearly clarified (1-2 min.)
- Remove the solution from the heat source and add 3.3 ml of 3x PBS.
- Adjust the pH to 7.2 with HCl (one drop 1 M HCl).
- Filter the solution through a 0.2 µm membrane filter.
- Keep the solution on ice until used.

Fixation of cells:

Note 1: Flocs, granules, aggregates, etc. should be dispersed by syringing, pottering or short sonification.

Note 2: Not all types of cells will pellet by centrifugation. This can be checked by filtration of the sample through a 0.2 μm membrane filter.

Note 3: Cells grown under extreme conditions (high pH, high salinity) may need the fixation buffer (PBS) to be adjusted correspondingly.

Note 4: Probe-conferred fluorescence is determined by the rRNA content of the fixed cells, which in turn depends on the growth rate of the original cells. Therefore, the procedure should be performed with rapidly growing cells.

Note 5: If FISH is performed on gram-positive cells, cells should be fixed in ethanol only by adding 1.2 volumes of 96% ethanol to 1 volume of cell suspension.

- Harvest cells by centrifugation or filtration.
- Wash and resuspend cells in 1x PBS or another appropriate washing buffer (see above). Be sure to disrupt the pellet cautiously to avoid large aggregates during FISH analysis.
- Add three volumes of fixative to one volume of suspension, keep on ice for 1-3 h.
- Wash and resuspend cells in 1x PBS.
- Add 1.25 volume 98 % ethanol (-20°C) to one volume of cell suspension. The suspension should have an appropriate cell density (108 -109 cells per ml). If not, dilute or concentrate.
- Store samples at -20°C. At this temperature, the sample is maintained for several months.

Pretreatment of the microscope slides:

Note 1: We use Teflon coated microscope slides. The hydrophobic coating separates 6 wells, preventing the mixing of probes in adjacent wells.

GELATIN COATING:

- Clean slides in warm detergent or KOH/ethanol solution for one hour, rinse carefully with milliQ, and dry.
- Coat clean slides with gelatin by spreading 10 μl of heated (70°C) 0.1 % gelatin / 0.01% chromium potassium sulfate dodecahydrate solution in each well (use Eppendorf-tip).
- Take off the coating (use Eppendorf-tip) and dry the slides. Alternatively, the slides can be coated with a Poly L-Lysin coating:
    - Clean the slides with 1% HCl / 70 % ethanol
    - Allow a diluted poly L-Lysin solution (0.01%) to come to room temperature (100 ml in Coplin jars)
    - Place slides in the Coplin jars for 5 min
    - Drain slides, dry 1 h at 60°C or overnight at room temperature in vertical position

IMMOBILIZATION OF CELL ON MICROSCOPE SLIDES:

- Spread 10 µl (2-15 µl) cell suspension in each well of a gelatin coated Teflon/glass microscope slide.
- Dry at 46°C for 10 min.
- Dehydrate cells by successive passage through 50, 80 and 98% ethanol (3 min each).
- Dry slides at room temperature (4 min), or under an air line if necessary.

If FISH is performed on gram-positive cells (always ethanol fixed cells) the next steps (printed in italic) are required:

- *Put 10 µl of mutanolysin (FLUKA 5000 U/ml in 0.1 M K3PO4 at pH 6.8) on each well at room temperature. Incubate about 30 minutes for newly fixed samples, for old cells 15 minutes is sufficient. Use only ethanol fixed cells.*
- *Wash afterwards with distilled water and repeat the dehydration steps by successive passage through 50, 80 and 98% ethanol (3 min each).*
- *Label slides with pencil (is not washed off).*
- *Store slides at -20°C.*

PROBE HANDLING:

- Probes arrive freeze-dried (lyophilized). Sterile milliQ is added for a final probe concentration of 100 pmol/µl. Shake at maximum speed in the thermostatic (23°C) Eppendorf shaker to dissolve (10 min).
- Prepare the working solution for a final concentration of 5 pmol/µl for CY3/5 and 8.3 pmol/µl for FLUOS. To mix multiple probes into a master mix, ensure that probes are spun down and vortexed to ensure complete mixing.
- Store probe stocks and working solutions at -20°C.
- Before the hybridization, thaw and store probes on ice.

HYBRIDIZATION:

Note 1: Oligonucleotide probes are degraded with exposure to light, so always keep probes (and probe-treated slides) out of the light when handling.

- Prepare hybridization buffer (see below) and keep at room temperature.
- Thaw oligonucleotide probes (working solutions).
- Prepare a hybridization tube by folding a tissue, putting it into a 50 ml Falcon tube, and pouring the rest of the hybridization buffer onto the tissue.
- Pipet 10 µl hybridization buffer in each well with cells.
- Add 1 µl of probe stock solution (final concentration 5 pmol/µl for CY3 and CY5-labeled probes and 8.3 pmol/µl for FLUOS labeled probes) without scratching the Teflon and gelatin coating.

- Immediately transfer the slide into the hybridization tube and incubate for 1.5 h at 46°C. Incubation can be done for several hours, or overnight.
- In the meantime, prepare the washing buffer (see below) and preheat this buffer in a water bath (48°C).

The next step should be performed rapidly:

- Rinse the hybridization with the washing buffer from the slide, avoiding mixing of probe from one well to another. If every well has the same probes, rinsing can be done by slowly flooding the slide with 1000 µl of washing buffer using a pipet. After flooding, the buffer / probe mixture can be retracted and discarded. Repeat this flooding 3 times. During this step, many cells can be lost, so being gentle is imperative.
- Transfer slide into the remaining washing buffer, and incubate 10-20 min at 48°C.
- Remove washing buffer by rinsing with milliQ water and drying the slides.
- Embed wells with Vectashield. This amplifies fluorescence and prevents fading. Very little Vectashield is needed (approximately one drop). Put a cover slip on the slide and seal into place using quick-dry nail polish.
- Specimens can now be analyzed with a fluorescence microscope.

PREPARATION OF HYBRIDIZATION BUFFER FOR IN SITU HYBRIDIZATION AT 46°C:

Pipet into a 2 ml Eppendorf:
•5 M NaCl (360 µl)
•1 M Tris/HCl (pH 8.0) (40 µl)
•Add formamide and milliQ according to Table B5.
•10% (w/v) SDS (4 µl)

PREPARATION OF WASHING BUFFER FOR WASHING AT 48°C FOR 20 MIN:

Pipet in a 50 ml Falcon tube and mix:
•Tris/HCl (pH 8.0) (1 ml)
•Add 5 M NaCl and 0.5 M EDTA (pH 8.0) according to Table B6.
•Fill Falcon tube up to 50 ml with milliQ
•Add 50 µl of 10% (w/v) SDS
•Preheat the washing buffer at 48°C prior to use.

Table B5. Formamide concentration table

Formamide % (v/v)	**Formamide (µl)**	**MilliQ (µl)**
0	0	1600
5	100	1500
10	200	1400
15	300	1300
20	400	1200
25	500	1100
30	600	1000
35	700	900
40	800	800
45	900	700
50	1000	600
55	1100	500
60	1200	400
65	1300	300

Table B6. Formamide in hybridization buffer concentration table

Formamide in hybridization buffer % (v/v)	**[NaCl] (mM)**	**5 M NaCl (µl)**	**0.5 M EDTA (µl)**
0	0.9	9000	
5	0.636	6300	
10	0.45	4500	
15	0.318	3180	
20	0.225	2250	500
25	0.159	1590	500
30	0.112	1120	500
35	0.08	800	500
40	0.056	560	500
45	0.04	400	500
50	0.028	280	500
55	0.02	200	500
60	0.008	80	500
70	0.000	0	350

Table B7. Oligonucleotide probes used for FISH

Probe	Sequence	Target	Fluorescent dyes
NSO190	CGATCCCCTGCTTTTCTCC	AOB	Cyanine 3
NSO1225	CGCCATTGTATTACGTGTGA		Cyanine 3
Ntspa 662	GGAATTCCGCGCTCCTCT	NOB	Fluorescein, Cyanine 3
Nit 1035	CCTGTGCTCCATGCTCCG		Fluorescein, Cyanine 3
PAO 462	CCGTCATCTACWCAGGGTATTAAC	PAO	Cyanine 5
PAO 651	CCCTCTGCCAAACTCCAG		Cyanine 5
PAO 846	GTTAGCTACGGACTAAAAGG		Cyanine 5
GAO Q989	TTCCCCGGATGTCAAGGC	GAO	Fluorescein
GAO Q431	TCCCCGCCTAAAGGGCTT		Fluorescein

Table B8. Reactor performance; nutrient removal and N_2O emission rates

Reactor Conditions	Nitrification Rate mg NH_3-N (g VSS L hr)$^{-1}$	Phosphate Removal Rate mg PO_4^{3-}-P (g VSS L hr)$^{-1}$	SND Efficiency[6] (%)	N_2O emission % NH_3-N emitted as N_2O-N
1 mg O_2 L^{-1}	0.23 (±0.01)	2.81 (±0.10)	99.9 (±0.06)	0.18 (±0.06)
2 mg O_2 L^{-1}	0.41 (±0.004)	3.14 (±0.16)	99.9 (±0.02)	0.52 (±0.11)
3 mg O_2 L^{-1}	0.48 (±0.02)	4.90 (±0.15)	100.0 (±0.01)	1.65 (±0.23)
0 mg NO_2^- L^{-1}	0.41 (±0.004)	3.14 (±0.16)	99.9 (±0.02)	0.52 (±0.11)
1 mg NO_2^- L^{-1}	0.34 (±0.01)	3.35 (±0.08)	99.7 (±0.28)	0.68 (±0.17)
4 mg NO_2^- L^{-1}	0.26 (±0.01)	3.20 (±0.16)	99.8 (±0.19)	4.16 (±0.08)

[6] Zhang, F.; Li, P.; Chen, M.; Wu, J.; Zhu, N.; Wu, P.; Chiang, P.; Hu, Z. Effect of Operational Modes on Nitrogen Removal and Nitrous Oxide Emission in the Process of Simultaneous Nitrification and Denitrification. *Chem. Eng. J.* **2015**, *280*, 549–557. https://doi.org/10.1016/J.CEJ.2015.06.016.

Figure B1. Lab-scale sequencing batch reactor with gaseous N_2O analyzer

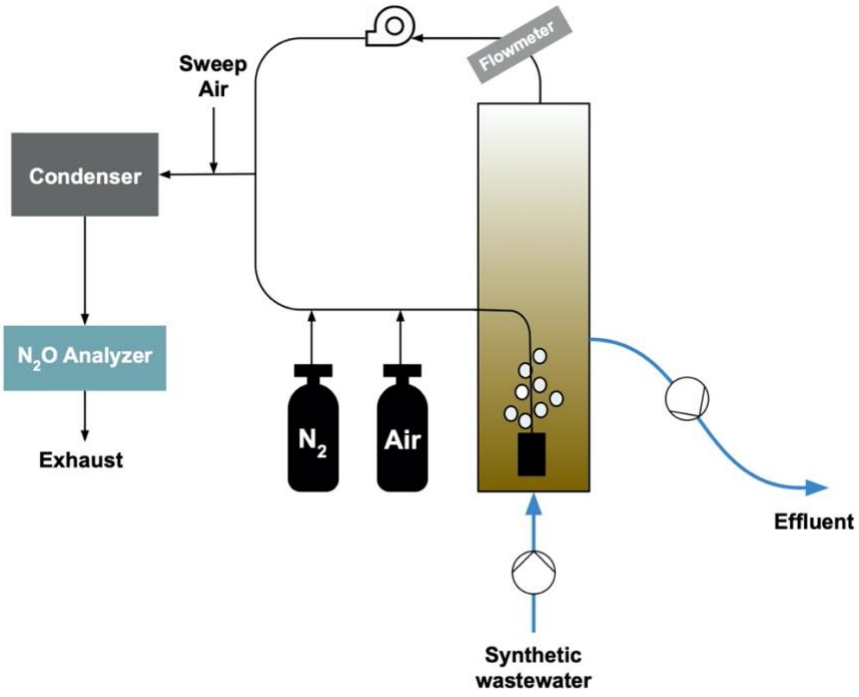

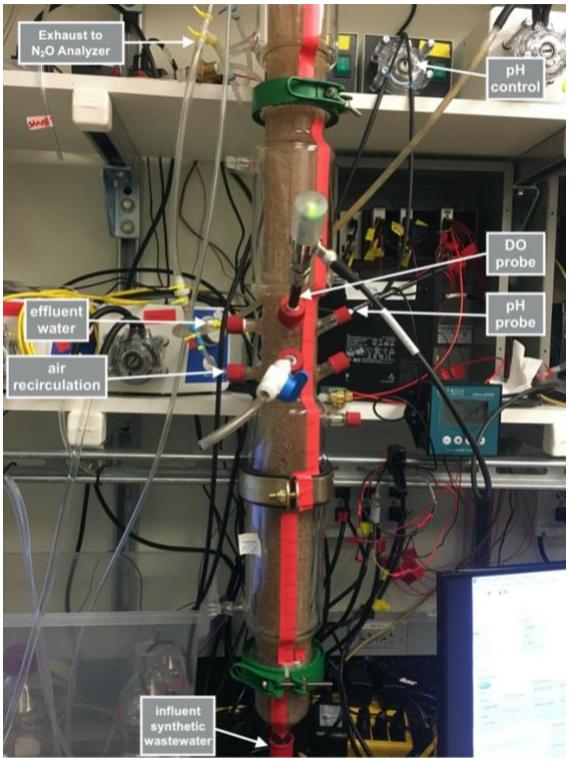

Figure B2. Image of lab reactor (some reactor components are not shown)

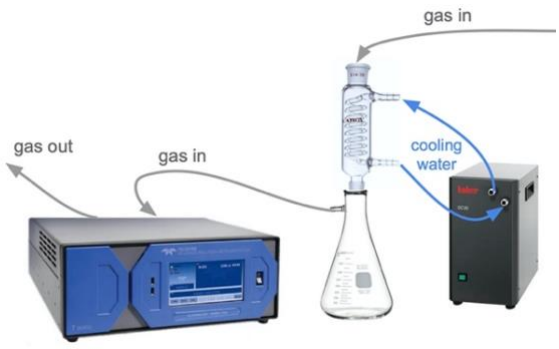

Figure B3. N_2O analyzer and condenser setup

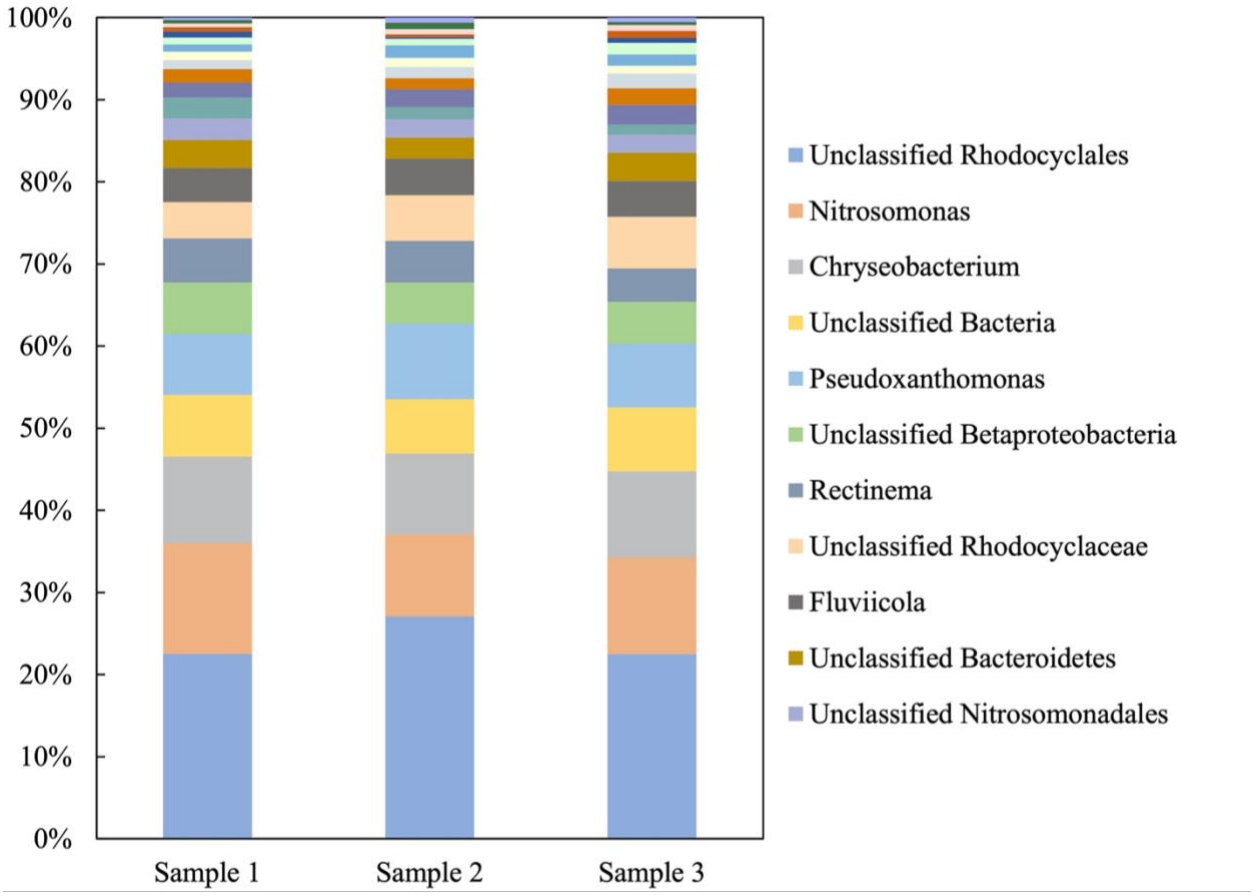

Figure B4. 16S rRNA sequencing data from AGS under baseline conditions

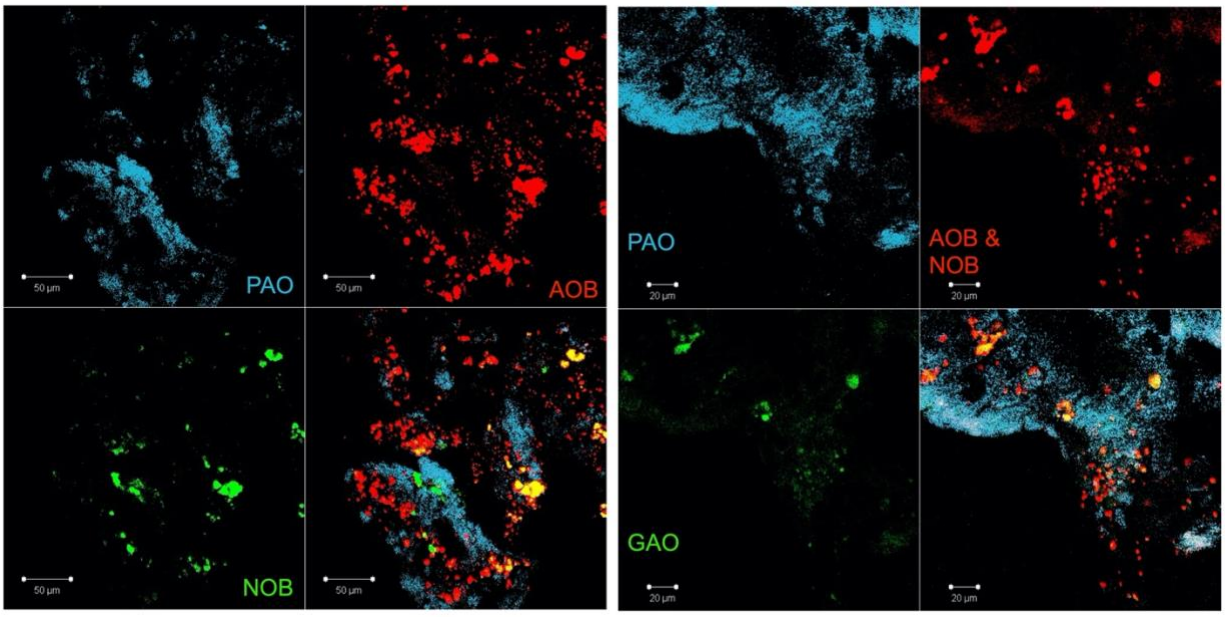

Figure B5. Color separated FISH images

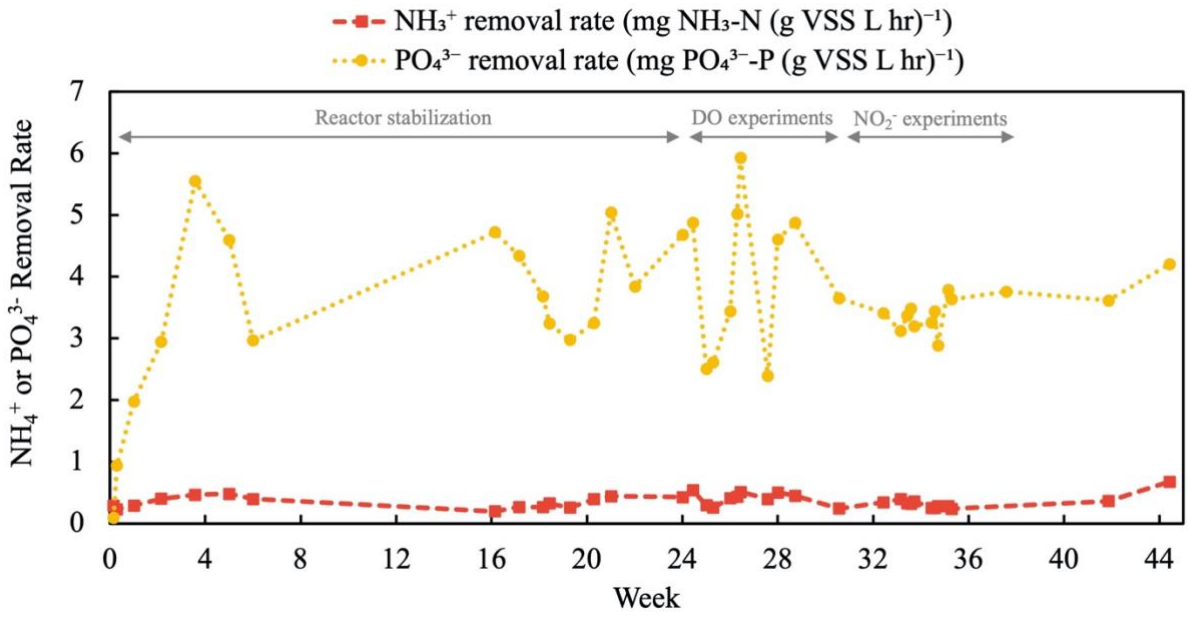

Figure B6. Reactor performance; ammonia and phosphate removal rates over reactor lifetime

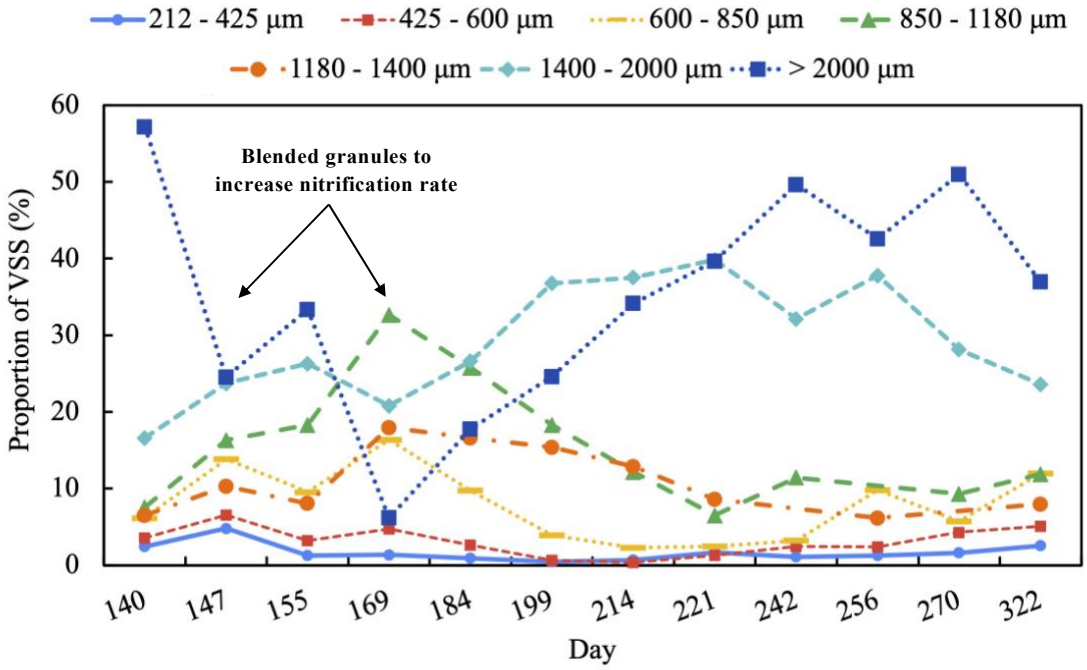

Figure B7. Granule size distribution over time